Electronic Supplementary Material (ESI) for Chemical Communications.
This journal is © The Royal Society of Chemistry 2019

Supplementary Information

Trisulfides over Disulfides: Highly Selective Synthetic Strategies, Anti-proliferative Activities and Sustained H_2S Release Profiles

Debojit Bhattacherjee,[ab] Abu Sufian,‡[a] Sulendar K. Mahato, ‡[a] Samiyara Begum, ‡[a] Kaustav Banerjee,[a] Sharmistha De,[a] Hemant Kumar Srivastava,*[a] Krishna P. Bhabak*[ab]

[a]Department of Chemistry, Indian Institute of Technology Guwahati, Guwahati-781039, Assam, India.
[b]Centre for the Environment, Indian Institute of Technology Guwahati, Guwahati-781039, Assam, India
‡Authors contributed equally

Author contribution
K.P.B. designed the project and supervised the research work and data analysis. D.B. optimized the experimental condition, synthesized most of the trisulfides and carried out cellular as well as spectroscopic studies. A.S. and S.K.M. synthesized disulfides and characterized. K.B. and S.D. carried out HPLC purifications and assisted in analyzing data. S.B. and H.K.S. carried out computational studies. The manuscript was prepared by K.P.B., H.K.S. and D.B.

Content

Experimental Section

Materials and Methods

Thin layer chromatographic (TLC) analyses were carried out on pre-coated silica gel on aluminium sheets. All the solvents used for chromatographic separations were distilled before use. Melting point of the synthesized compounds was recorded in a Büchi B540 melting point apparatus and the values are uncorrected. The NMR spectra were recorded with a Bruker Ascend^{TM} 400 and 600 spectrometer or Varian Mercury plus 400 MHz NMR Spectrometer. Chemical shifts are cited with respect to Me_4Si as internal standard. High resolution mass spectra (HR-MS) and GC-MS were obtained using an Agilent 6520 Accurate-Mass Quadrupole Time-of-Flight (Q-TOF) LC/MS spectrometer and PerkinElmer Clarus 680 GC/600C MS, respectively. CHNS analysis was performed by using Thermo Finnigan CHNS (O) Analyzer (Model: FLASH EA 1112 series). Cells were cultured under purified air class II bio-safety cabinet (Thermo Fisher). Finally, cells were incubated in CO_2 incubator (Eppendorf, Galaxy CO-170S). Cell viability assay was performed using Multiskan GO microplate reader (Thermo Fisher). Cellular morphology was visualized and imaged under Bio-Rad ZOE™ fluorescent cell imager microscope. The fluorescent sensor of H_2S (compound **8**) was synthesized following the reported method.[1]

Synthesis of Bunte salts

Bunte salts were prepared following the literature method with minor modifications.[2] To a stirred solution of sodium thiosulfate pentahydrate ($Na_2S_2O_3.5H_2O$) (1.77 mmol, 1.3 equiv) in 30% of ethanol-water mixture (5.0 ml), was added the corresponding halide precursor (1.36 mmol, 1.0 equiv) and stirred at room temperature for 4-5h. Progress of the reaction was monitored by TLC study. Upon completion of the reaction, ethanol component was removed under reduced pressure and the residue was used for the next step in general without any further purification.

The crude Bunte salt could also be purified using neutral alumina column chromatographic method with ethyl acetate and methanol as eluents. The Bunte salt corresponding to benzyl bromide was purified by the above method and was used in the optimization reactions of trisulfide and disulfide compounds.

Table S1. Optimization processes for **3a** in organic solvents.

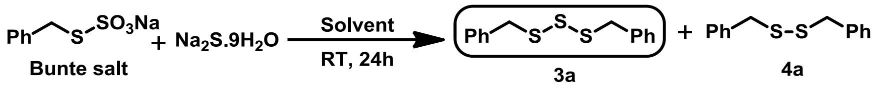

entry	Na_2S	solvent	temp (°C)	time (h)	Yield of **3a** (%)[a]	Yield of **4a** (%)[a]
1	0.5	MeOH	RT	24	9	63
2	0.5	EtOH	RT	24	21	60
3	0.5	Dioxane	RT	24	0	73
4	0.5	ACN	RT	24	30	40
5	0.5	DMSO	RT	24	8	65

[a]Calculated from the peak intensities of -S-CH_2- group in ^{1}H NMR spectra of product mixture.

General synthetic method for trisulfides 3a-3u

To a stirred solution of the crude Bunte salt (1.36 mmol, 1.0 equiv, considering 100% conversion of halides to Bunte salts) in water (20 ml), was added an aqueous solution (25 ml) of sodium sulfide nonahydrate (0.68 mmol, 0.5 equiv) at 0 °C in a drop-wise manner and the mixture was stirred at that temperature for the required duration. A white colored suspension appeared upon completion of the addition of sodium sulfide. The progress of the reaction was monitored by TLC study. Upon the completion of the reaction, the mixture was diluted with ethyl acetate and washed with brine solution. The combined organic layer was dried over anhydrous sodium sulfate and the solvent was evaporated under reduced pressure to afford crude trisulfides.

Compound 3a: Benzyl bromide (0.25 g, 1.36 mmol) was used to yield the trisulfide as white amorphous solid. Reaction time: 8h, Yield: (0.16 g, 77 %); M.P: 44 - 46 ºC; R_f = 0.5 (100 % petroleum ether). ^{1}H-NMR ($CDCl_3$, 400 MHz,): δ (ppm): 4.02 (s, 2H), 7.33 - 7.25 (m, 5H); ^{13}C-NMR ($CDCl_3$, 100 MHz): δ (ppm): 43.1, 127.6, 128.6, 129.4, 136.5. ESI-MS: *m/z* calcd for $C_{14}H_{14}S_3$ $[M+H]^+$: 279.0330; observed $[M+H]^+$: 279.0589.

Compound 3b:[3] Allyl bromide (1.00 g, 8.46 mmol) was used to yield the trisulfide as a yellow liquid. Reaction time: 5h, Yield (0.40 g, 50 %); R_f = 0.9 (100 % petroleum ether). ^{1}H-NMR ($CDCl_3$, 600 MHz) δ (ppm): 3.50 - 3.51 (d, 2H, *J* = 6.0 Hz), 5.20 - 5.25 (m, 2H), 5.85 - 5.91 (m, 1H). ^{13}C-NMR ($CDCl_3$, 150 MHz) δ (ppm): 41.6, 119.1, 132.7.

Compound 3c:[4] 5-Bromopent-1-ene (0.50 gm, 3.35 mmol) was used to yield the trisulfide as a yellow liquid. Reaction time: 12h, Yield (0.10 g, 24 %); R_f = 0.8 (100 % petroleum ether). ^{1}H-NMR ($CDCl_3$, 400 MHz) δ (ppm): 1.82 – 1.89 (m, 2H), 2.16 – 2.21 (m, 2H), 2.86 – 2.90 (t, 2H, *J* = 8.0 Hz) 4.98 - 5.08 (m, 2H), 5.74 - 5.85 (m, 1H). ^{13}C-NMR ($CDCl_3$, 100 MHz) δ (ppm): 27.2, 31.4, 37.3, 114.3, 136.6.

Compound 3d: *n*-Propyl bromide (0.50 g, 4.06 mmol) was used to yield the trisulfide as liquid product. Reaction time: 6h, Yield (0.23 g, 62 %); R_f = 0.8 (100 % petroleum ether). ^{1}H-NMR ($CDCl_3$, 400 MHz) δ (ppm): 1.00 - 1.04 (t, 3H, *J* = 8.0 Hz), 1.74 - 1.83 (m, 2H), 2.84 - 2.87 (t, 4H, *J* = 8.0 Hz). ^{13}C-NMR ($CDCl_3$, 100 MHz) δ (ppm): 13.3, 22.3, 41.0. ESI-MS: *m/z* calcd for $C_6H_{14}S_3$ $[M+H]^+$: 183.0330; observed $[M+H]^+$: 183.1127.

Compound 3e: *n*-Butyl bromide (5.08 g, 49.8 mmol) was used to yield the trisulfide as liquid product. Reaction time: 6h, Yield (1.57 g, 44 %); R_f = 0.7 (100 % petroleum ether). ^{1}H-NMR ($CDCl_3$, 400 MHz) δ (ppm): 0.92 - 0.96 (t, 3H, *J* = 8.0 Hz), 1.41 - 1.47 (m, 2H), 1.69 - 1.76 (m, 2H), 2.86 - 2.90 (t, 3H, *J* = 8.0 Hz). ^{13}C-NMR ($CDCl_3$, 100 MHz) δ (ppm): 13.6, 21.7, 30.9, 38.6. ESI-MS: *m/z* calcd for $C_8H_{18}S_3$ $[M+H]^+$: 211.0643; observed $[M+H]^+$: 211.1322.

Compound 3f: 4-Methylbenzyl bromide (0.25 g, 1.36 mmol) was used to yield the trisulfide as white amorphous solid. Reaction time: 3h, Yield: (0.16 g, 78 %); M.P: 61 - 63 ºC; R_f = 0.5 (100 % petroleum ether). ^{1}H-NMR ($CDCl_3$, 400 MHz): δ (ppm): 2.33 (s, 3H), 4.01 (s, 2H), 7.13 - 7.14 (d, 2H, *J* = 4.0 Hz), 7.19 - 7.21 (d, 2H, *J* = 4.0 Hz) ppm. ^{13}C-NMR ($CDCl_3$, 150 MHz): δ (ppm): 21.2, 42.9, 129.3, 129.3, 133.4, 137.3. ESI-MS: *m/z* calcd for $C_{16}H_{18}S_3$ $[M+K]^+$: 345.0202; observed $[M+K]^+$: 345.0171.

Compound 3g: 4-Isopropylbenzyl bromide (0.28 g, 1.36 mmol) was used to yield the trisulfide as viscous liquid. Reaction time: 3h, Yield: (0.15 g, 59 %); R_f = 0.5 (100 % petroleum ether). ^{1}H-NMR ($CDCl_3$, 600 MHz): δ (ppm): 1.22- 1.23 (d, 3H, *J* = 6.0 Hz), 2.86 - 2.90 (m, 1H) 4.01 (s, 2H), 7.17 - 7.18 (d, 2H, *J* = 6.0 Hz), 7.22 - 7.24 (d, 2H, *J* = 12.0 Hz); ^{13}C-NMR ($CDCl_3$, 100 MHz): δ (ppm): 23.9, 33.8. 43.0, 126.7, 129.4, 133.8, 148.3. ESI-MS: *m/z* calcd for $C_{20}H_{26}S_3$ $[M+NH_4]^+$: 380.1534; observed $[M+NH_4]^+$: 380.1540.

Compound 3h: 4-*tert*-Butylbenzyl chloride (0.25 g, 1.36 mmol) was used to yield the trisulfide as semi solid product. Reaction time: 3h, Yield: (0.15 g, 49 %); R_f = 0.5 (100 % petroleum ether). ^{1}H-NMR ($CDCl_3$, 600 MHz): δ (ppm): 1.30 (s, 9H), 4.01 (s, 2H), 7.23 - 7.25 (d, 2H, *J* = 12.0 Hz), 7.33 - 7.35 (d, 2H, *J* = 12.0 Hz). ^{13}C-NMR ($CDCl_3$, 150 MHz): δ (ppm): 31.3, 34.5, 42.9, 125.4, 125.6, 129.1, 133.4, 150.6. ESI-MS: *m/z* calcd for $C_{22}H_{30}S_3$ $[M+NH_4]^+$: 408.1848; observed $[M+NH_4]^+$: 408.1831.

Compound 3i: 4-Flurobenzyl bromide (0.26 g, 1.36 mmol) was used to yield the trisulfide as white amorphous solid. Reaction time: 3h, Yield: (0.18 g, 86 %); M.P: 63 - 65 ºC; R_f = 0.5 (100 % petroleum ether).^{1}H-NMR ($CDCl_3$, 400 MHz) δ (ppm): 4.00 (s, 2H), 6.98 - 7.03 (t, 2H, *J* = 12.0 Hz), 7.24 - 7.28 (m, 2H). ^{13}C-NMR ($CDCl_3$, 100 MHz) δ (ppm): 42.2, 115.4, 115.6, 131.0, 131.1, 132.2, 132.3, 161.1, 163.5. ESI-MS: *m/z* calcd for $C_{14}H_{12}F_2S_3$ $[M]^+$: 314.0069; observed: 314.0790. Anal. calcd for $C_{16}H_{12}F_6S_3$: C, 53.48, H, 3.85, S, 30.59. Found, C, 53.51, H, 3.78, S, 30.16.

Compound 3j: 4-Chlorobenzyl chloride (0.22 g, 1.36 mmol) was used to yield the trisulfide as off-white amorphous solid. Reaction time: 4h, Yield: (0.22 g, 69 %); M.P: 82 - 84 ºC; R_f = 0.5 (100 % petroleum ether). ^{1}H-NMR ($CDCl_3$, 600 MHz) δ (ppm): 3.98 (s, 2H), 7.22 - 7.24 (d, 2H, *J* = 12.0 Hz), 7.29 - 7.30 (d, 2H, *J* = 6.0 Hz). ^{13}C-NMR ($CDCl_3$, 150 MHz) δ (ppm): 42.2, 128.7, 130.7, 133.5, 134.9. Anal. calcd for $C_{14}H_{12}C_{l2}S_3$: C, 48.41; H, 3.48; S, 27.69. Found, C, 48.43, H, 3.70, S, 27.78.

Compound 3k: 4-Bromobenzyl bromide (0.34 g, 1.36 mmol) was used to yield the trisulfide as white amorphous solid. Reaction time: 4h, Yield: (0.15 g, 47 %); M.P: 70 – 72 ºC; R_f = 0.5 (100 % petroleum ether). ^{1}H-NMR ($CDCl_3$, 400 MHz) δ (ppm): 3.96 (s, 2H), 7.16 - 7.18 (d, 2H, *J* = 8.0 Hz), 7.44 - 7.46 (d, 2H, *J* = 8.0 Hz). ^{13}C-NMR ($CDCl_3$, 100 MHz) δ (ppm): 42.3, 121.6, 131.1, 131.7, 135.5. Anal. calcd for $C_{14}H_{12}Br_2S_3$: C, 38.55; H, 2.77; S, 22.05. Found, C, 38.38, H, 2.25, S, 22.44.

Compound 3l: 4-Trifluromethyl benzyl bromide (0.26 g, 1.36 mmol) was used to yield the trisulfide as viscous liquid. Reaction time: 4h, Yield: (0.24 g, 97 %); R_f = 0.5 (100 % petroleum ether).^{1}H-NMR ($CDCl_3$, 600 MHz) δ (ppm) : 4.04 (s, 2H), 7.40 - 7.41 (d, 2H, *J* = 6.0 Hz), 7.58 - 7.59 (d, 2H, *J* = 6.0 Hz). ^{13}C-NMR ($CDCl_3$, 150 MHz) δ (ppm): 42.2, 121.3-126.8 (q, *J* = 270.0 Hz), 125.5-125.6 (q, *J* = 10.5 Hz), 129.5-130.1 (q, *J* = 96.0 Hz), 129.7, 140.5. Anal. calcd for $C_{16}H_{12}F_6S_3$: C, 46.37, H, 2.92, F, 27.50, S, 23.21. Found, C, 46.03, H, 3.33, S, 22.45.

Compound 3m: 2-Nitrobenzyl bromide (0.10 g, 1.36 mmol) was used to afford the trisulfide as white amorphous solid with along with some disulfide. The crude product was purified by silica gel column chromatography to afford the pure trisulfide as white amorphous solid. Reaction time: 2h, Isolated yield: (0.05 g, 54%); M.P:105-107 ºC; R_f = 0.5 (10 % ethyl acetate in petroleum ether). ^{1}H-NMR ($CDCl_3$, 400 MHz) δ (ppm): 4.32 (s, 2H), 7.38 - 7.40 (d, 1H, *J* = 8.0 Hz), 7.46 - 7.50 (t, 1H, *J* = 8.0 Hz), 7.56 - 7.60 (t, 1H, *J* = 8.0 Hz), 8.07 - 8.09 (d, 1H, *J* = 8.0 Hz). ^{13}C-NMR ($CDCl_3$, 150 MHz) δ (ppm): 40.8, 125.8, 128.9, 132.5, 133.0, 133.4, 133.4, 147.7. ESI-MS: *m/z* calcd for $C_{14}H_{12}N_2O_4S_3$; observed: $[M+Na]^+$: 390.9851; observed $[M+Na]^+$: 390.9850.

Compound 3n: 2-Methylbenzyl bromide (0.25 g, 1.36 mmol) was used to yield the trisulfide as white amorphous solid. Reaction time: 6h, Yield: (0.16 g, 77 %); M.P: 38 - 40 ºC; R_f = 0.7 (100 % petroleum ether 60 - 80). ¹H-NMR ($CDCl_3$, 600 MHz): δ (ppm): 2.39 (s, 6H), 4.07 (s, 2H), 7.15 - 7.23 (m, 4H). ¹³C-NMR ($CDCl_3$, 150 MHz): δ (ppm): 19.2, 41.1, 126.0, 128.0, 130.6, 130.6, 134.0, 137.0. ESI-MS: *m/z* calcd for $C_{16}H_{18}S_3$ $[M+H]^+$: 307.0643; observed $[M+H]^+$: 307.0676.

Compound 3o: 3-Nitrobenzyl bromide (0.28 g, 1.36 mmol) was used to yield the trisulfide as white amorphous solid. Reaction time: 3h, Yield: (0.27 g, 91 %); M.P: 110 - 112 ºC; R_f = 0.5 (10 % ethyl acetate in petroleum ether).¹H-NMR ($CDCl_3$, 400 MHz) δ (ppm): 4.09 (s, 2H), 7.50 - 7.54 (t, 1H, *J* = 8.0 Hz), 7.61 - 7.63 (d, 1H, *J* = 8.0 Hz), 8.14 - 8.17 (d, 2H, *J* = 12.0 Hz). ¹³C-NMR ($CDCl_3$, 100 MHz) δ (ppm): 41.8, 122.7, 124.3, 129.6, 135.5, 138.5, 148.4. ESI-MS: *m/z* calcd for $C_{14}H_{12}N_2O_4S_3$ $[M+Na]^+$: 390.9851; observed $[M+Na]^+$: 390.9820.

Compound 3p: 3-Chlorobenzyl chloride (0.22 g, 1.36 mmol) was used to yield the trisulfide as white amorphous solid. Reaction time: 3h,Yield: (0.18 g, 73 %); M.P: 43 - 45 ºC; R_f = 0.5 (100 % petroleum ether).¹H-NMR ($CDCl_3$, 400 MHz) δ (ppm): 3.97 (2H, s), 7.18 - 7.19 (m, 1H), 7.25 - 7.26 (d, 2H, *J* = 4.0 Hz), 7.30 (s, 1H). ¹³C-NMR ($CDCl_3$, 100 MHz) δ (ppm): 42.4, 127.6, 127.8, 129.5, 129.8, 134.4, 138.5. ESI-MS: *m/z* calcd for $C_{14}H_{12}Cl_2S_3$ $[M+Na]^+$: 368.9370; observed $[M+Na]^+$: 368.4329.

Compound 3q: 3-Bromobenzyl bromide (0.34 g, 1.36 mmol) was used to yield the trisulfide as white amorphous solid. Reaction time: 3h, Yield: (0.24 g, 79 %); M.P: 57 - 59 ºC; R_f = 0.5 (100 % petroleum ether).¹H-NMR ($CDCl_3$, 400 MHz) δ (ppm): 3.96 (s, 2H), 7.17 - 7.24 (m, 2H), 7.40 - 7.42 (d, 1H, *J* = 8.0 Hz), 7.46 (s, 1H). ¹³C-NMR ($CDCl_3$, 100 MHz) δ (ppm): 42.4, 122.6, 128.1, 130.2, 130.7, 132.4, 138.8. ESI-MS: *m/z* calcd for $C_{14}H_{12}Br_2S_3$ $[M+K]^+$: 472.8099; observed $[M+K]^+$: 472.4377.

Compound 3r: 3,5-Dimethylbenzyl bromide (0.25 g, 1.36 mmol) was used to yield the trisulfide as white amorphous solid. Reaction time: 3h, Yield: (0.18 g, 79 %); M.P: 69 - 71 ºC; R_f = 0.5 (100 % petroleum ether 60-80). ¹H-NMR ($CDCl_3$, 400 MHz): δ (ppm): 2.30 (s, 6H), 3.98 (s, 2H), 6.90 (s, 1H). 6.93 (s, 2H). ¹³C-NMR ($CDCl_3$, 100 MHz): δ (ppm): 21.2, 43.3, 127.2, 129.3, 136.3, 138.2. ESI-MS: *m/z* calcd for $C_{18}H_{22}S_3$ $[M+NH_4]^+$: 352.1222; observed $[M+NH_4]^+$: 352.1238.

Compound 3s: 3,5-Di-*tert*-butylbenzyl bromide (0.38 g, 1.36 mmol) was used to yield the trisulfide as transparent viscous liquid. Reaction time: 24h, Yield: (0.22 g, 72 %); R_f = 0.5 (100 % petroleum ether). ¹H-NMR ($CDCl_3$, 600 MHz): δ (ppm): 1.32 (s, 18H), 4.06 (s, 2H), 7.15 (s, 2H), 7.33 (s, 1H). ¹³C-NMR ($CDCl_3$, 150 MHz): δ (ppm): 31.4, 34.8, 44.2, 121.6, 123.6, 135.4, 151.0. ESI-MS: *m/z* calcd for $C_{30}H_{46}S_3$ $[M+NH_4]^+$: 520.3106, observed $[M+NH_4]^+$: 520.3097.

Compound 3t: 2,4-Dichlorobenzyl chloride (0.28 g, 1.36 mmol) was used to yield the trisulfide as white amorphous solid. Reaction time: 4h, Yield: (0.26 g, 89 %); M.P: 84 - 86 ºC; R_f = 0.5 (100 % petroleum ether). ¹H-NMR ($CDCl_3$, 400 MHz) δ (ppm): 4.09 (s, 2H), 7.20 - 7.25 (m, 2H), 7.40 (s, 1H). ¹³C-NMR ($CDCl_3$, 150 MHz) δ (ppm): 39.7, 127.0, 129.6, 132.3, 132.8, 134.2, 134.9.

Compound 3u: 2-(Chloromethyl)naphthalene (0.30 g, 1.36 mmol) was used to yield the trisulfide as white solid. Reaction time: 4h, Yield: (0.25 g, 96 %); M.P: 118 – 121 ºC; R_f = 0.5 (100 % petroleum ether). ¹H-NMR ($CDCl_3$, 400 MHz) δ (ppm): 4.17 (s,. 2H), 7.40 - 7.47 (m, 4H), 7.47 - 7.45 (m, 2H), 7.70 (s, 1H), 7.79 (s, 4H). ¹³C-NMR ($CDCl_3$, 100 MHz) δ (ppm): 43.5, 126.0, 126.3, 127.2, 127.7, 127.8, 128.3, 128.5, 132.7, 133.3, 133.9. ESI-MS: *m/z* calcd for $C_{22}H_{18}S_3$ $[M+NH_4]^+$: 396.0909; observed $[M+NH_4]^+$: 396.0873.

Bulk-scale synthesis of a representative trisulfide 3f: To validate our method for a large scale synthesis of trisulfides, a representative trisulfide **3f** was synthesized using the method as shown above. The Bunte salt was prepared using 4-Methyl benzyl bromide (5.00 g, 27.00 mmol) and $Na_2S_2O_3.5H_2O$ (8.70 g, 35.12 mmol) in 30% ethanol-water system (50 ml) at room temperature for 5h. The crude Bunte salt was reacted with $Na_2S.9H_2O$ (3.24 g, 13.5 mmol) in water (150 ml) at 0 °C for 5h. After the usual work-up the crude trisulfide **3f** was obtained (3.24 g, 82%). Purity of the crude product was analysed by ¹H-NMR and reverse-phase analytical HPLC method (Figure S98).

Synthesis of unsymmetrical trisulfide 3v: To an aqueous solution (16 ml) of the column purified Bunte salts **6** and **7** (0.37 mmol) corresponding to 4-Methylbenzyl bromide and 4-Isopropylbenzyl bromide, respectively was added an aqueous solution (16.0 ml) of sodium sulfide nonahydrate (0.37 mmol) in a drop-wise manner at 0 °C and the mixture was stirred for 5h at that temperature. The progress of the reaction was monitored by TLC study. Upon the completion, the reaction mixture was diluted with ethyl acetate and washed with brine solution. The combined organic layer was dried over anhydrous sodium sulfate and the solvent was evaporated under reduced pressure to afford crude trisulfide mixture containing symmetrical and unsymmetrical trisulfides (**3f**, **3g**

and **3v**) at reasonably good yields. The crude mixture was then analyzed by a reverse-phase C-18 column in an analytical HPLC system to identify the trisulfides present in the mixture (Figure S94).

Table S2. Optimization of reaction condition for the selective synthesis of disulfide **4a**.

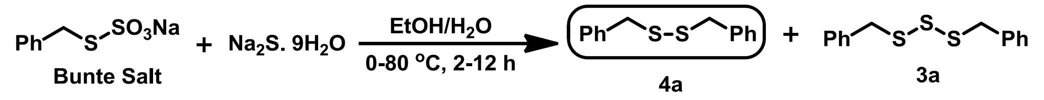

Entry	Na_2S	H_2O: EtOH	Temp (°C)	Time (h)	Yield of **4a** (%)[a]	Yield of **3a** (%)[a]
1	0.5	100 : 0	RT	4	5	61
2	0.5	75 : 25	RT	4	17	54
3	0.5	50 : 50	RT	4	31	35
4	0.5	25 : 75	RT	4	71	5
5	0.5	0 : 100	RT	4	36	21
6	0.5	25 : 75	0	4	43	22
7	0.5	25 : 75	50	4	66	0
8	0.5	25 : 75	80	4	62	0
9	0.5	25 : 75	50	2	64	0
10	0.5	25 : 75	50	8	79	0
11	0.5	25 : 75	50	12	62	0

[a] The relative ratio of disulfide **4a** and trisulfide **3a** has been calculated based on the intensity of -S-CH_2- protons corresponding to disulfide and trisulfide in ^{1}H NMR spectra of the crude product mixture.

Table S3. Synthesis of disulfides **4a-4u**.

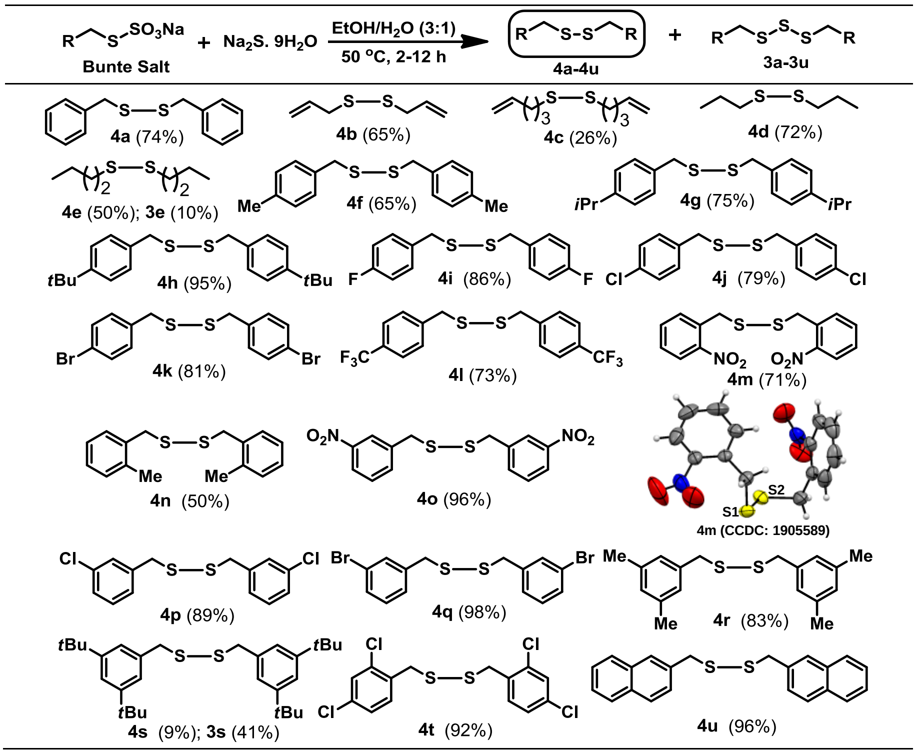

General synthesis of disulfides: To a stirred ethanolic solution (3.5 ml) of Bunte salt (1.36 mmol, 1.0 equiv), was added the aqueous solution (1.5 ml) of sodium sulfide nonahydrate (0.68 mmol, 0.50 equiv) at room temperature and the mixture was heated at 50 °C and the progress of the reaction was monitored by TLC studies. Upon the completion of reaction, the ethanol component was evaporated at reduced pressure and residual mixture was diluted with ethyl acetate and washed with brine solution. The combined organic layer was dried over anhydrous sodium sulfate and the solvent was evaporated under reduced pressure to afford the crude disulfides. For compounds **4b**, **4e**, **4s** and **4u**, sodium sulfite (5.0 equiv) was added in the reaction mixture to enhance the selectivity towards disulfide formation.

Compound 4a: Benzyl bromide (0.23 g, 1.36 mmol) was used to yield the disulfide as white solid product. Reaction time: 4h, Yield: (0.13 g, 74 %); M.P: 69 - 71 °C; R_f = 0.5 (100 % petroleum ether). ^{1}H-NMR ($CDCl_3$, 400 MHz) δ (ppm): 3.60 (s, 2H), 7.23 - 7.34 (m, 5H). ^{13}C-NMR ($CDCl_3$, 150 MHz) δ (ppm): 43.2, 127.4, 128.5, 129.4, 137.3. ESI-MS: *m/z* calcd for $C_{14}H_{14}S_2$ $[M+H]^+$: 247.0615. Observed $[M+H]^+$: 247.0617.

Compound 4b:[3] Allyl bromide (1.00 g, 8.46 mmol) was used in the presence of Na_2SO_3 (5.33 g, 42.33 mmol) to yield the disulfide as a yellow liquid. Reaction time: 8h, Yield (0.40 g, 65 %); R_f = 0.9 (100 % petroleum ether). ^{1}H-NMR ($CDCl_3$, 600 MHz) δ (ppm): 3.33 - 3.35 (d, 2H, *J* = 12.0 Hz), 5.14 - 5.21 (m, 2H), 5.81 - 5.87 (m, 1H). ^{13}C-NMR ($CDCl_3$, 150 MHz) δ (ppm): 42.3, 118.5, 133.5.

Compound 4c: 5-Bromopent-1-ene (0.50 gm, 3.35 mmol) was used to yield the disulfide as a colourless liquid. Reaction time: 12h, Yield (0.20 g, 26 %); R_f = 0.7 (100 % petroleum ether). ^{1}H-NMR ($CDCl_3$, 400 MHz) δ (ppm): 1.75 – 1.82 (m, 2H), 2.13 – 2.19 (m, 2H) 2.66 – 2.70 (t, 2H, *J* = 8.0 Hz), 4.97 - 5.06 (m, 2H), 5.73 - 5.82 (m, 1H). ^{13}C-NMR ($CDCl_3$, 100 MHz) δ (ppm): 27.9, 32.4, 38.1, 115.5, 137.5.

Compound 4d: *n*-Propyl bromide (0.50 g, 4.06 mmol) was used to yield the disulfide as liquid product. Reaction time: 5h, Yield (0.23 g, 72 %); R_f = 0.8 (100 % petroleum ether). ^{1}H-NMR ($CDCl_3$, 400 MHz) δ (ppm): 0.98 - 1.01 (t, 6H, *J* = 8.0 Hz), 1.67 - 1.76 (m, 2H), 2.65 - 2.69 (t, 4H, *J* = 8.0 Hz). ^{13}C-NMR ($CDCl_3$, 100 MHz) δ (ppm): 12.1, 21.5, 40.2. GC-MS: calcd for $C_6H_{14}S_2$ $[M]^+$: 150.0537; observed : 150.

Compound 4e: *n*-Butyl bromide (0.50 g, 4.06 mmol) was used to yield the disulfide as liquid product. Reaction time: 5h, Yield (0.20 g, 50%); R_f = 0.7 (100 % petroleum ether). ^{1}H-NMR ($CDCl_3$, 400 MHz) δ (ppm): 0.91 - 0.95 (t, 3H, *J* = 8.0 Hz), 1.40 - 1.44 (m, 2H), 1.64 - 1.73 (m, 2H), 2.68 - 2.70 (t, 3H, *J* = 8.0 Hz). ^{13}C-NMR ($CDCl_3$, 100 MHz) δ (ppm): 12.7, 20.6, 30.3, 37.9. GC-MS: *m/z* calcd for $C_8H_{18}S_2$ $[M]^+$: 178.0850 ; observed: 178.

Compound 4f: 4-Methylbenzyl bromide (0.25 g, 1.36 mmol) was used to yield the disulfide as white solid. Reaction time: 4h, Yield: (0.12 g, 65 %); M.P: 46 - 48 ºC ; R_f = 0.5 (100 % Petroleum ether). ^{1}H-NMR ($CDCl_3$, 600 MHz) δ (ppm): 2.33 (s, 3H), 3.60 (s, 2H), 7.14 - 7.17 (m, 4H). ^{13}C-NMR ($CDCl_3$, 150 MHz) δ (ppm): 21.2, 43.0, 129.2, 129.3, 134.3, 137.1. ESI-MS: *m/z* calcd for $C_{16}H_{18}S_2$ $[M+H]^+$: 275.0923, Observed $[M+H]^+$: 275.0941.

Compound 4g: 4-Isopropylbenzyl bromide (0.30 g, 1.36 mmol) was used to yield the disulfide as liquid product. Reaction time: 4h, Yield: (0.20 g, 75 %); R_f = 0.5 (100 % petroleum ether). ^{1}H-NMR ($CDCl_3$, 600 MHz) δ (ppm): 1.23 -1.24 (d, 3H, *J* = 6.0 Hz), 2.86 - 2.92 (m, 1H), 3.59 (s, 2H), 7.15 - 7.17 (d, 2H, *J* = 12.0 Hz), 7.17 - 7.19 (d, 2H, *J* = 12.0 Hz). ^{13}C-NMR ($CDCl_3$, 150 MHz) δ (ppm): 24.0, 33.8, 43.0, 126.5, 129.4, 134.6, 148.2. ESI-MS: *m/z* calcd for $C_{20}H_{26}S_2$ $[M+NH_4]^+$: 348.1814, Observed $[M+NH_4]^+$: 348.1951.

Compound 4h: 4- *tert*-Butylbenzyl chloride (0.25 g, 1.36 mmol) was used to yield the disulfide as semi solid product. Reaction time: 16 h, Yield: (0.23 g, 95 %); M.P: 63 - 64 ºC ; R_f = 0.5 (100 % petroleum ether). ^{1}H-NMR (400 MHz, $CDCl_3$,): δ (ppm): 1.31-1.30 (m, 9H), 3.60 (s, 2H) 7.18 - 7.16 (d, 2H, *J* = 8.0 Hz), 7.35 - 7.33 (d, 2H, *J* = 8.0 Hz). ^{13}C-NMR (150 MHz, $CDCl_3$): δ (ppm): 31.4, 43.0, 125.4, 129.1, 134.2, 150.5. ESI-MS: *m/z* calcd for $C_{22}H_{30}S_2$ $[M+NH_4]^+$: 276.2127, Observed $[M+NH_4]^+$: 276.2156.

Compound 4i: 4-Fluorobenzyl bromide (0.26 g, 1.36 mmol) was used to yield the disulfide as white solid product. Reaction time: 4h, Yield: (0.13 g, 86 %); M.P: 59 - 61 ºC; R_f = 0.5 (100 % petroleum ether). ^{1}H-NMR ($CDCl_3$, 600 MHz) δ (ppm): 3.58 (s, 2H), 7.00 - 7.02 (t, 2H, *J* = 6.0 Hz), 7.24 - 7.28 (m, 2H). ^{13}C-NMR ($CDCl_3$, 150 MHz) δ (ppm): 42.4, 115.3, 115.5, 130.8, 130.9, 133.1, 133.1, 161.4, 163.0. ESI-MS: *m/z* calcd for $C_{14}H_{12}F_2S_2$ $[M+H]^+$: 283.0421, Observed $[M+H]^+$: 283.1897.

Compound 4j:[5] 4-Chlorobenzyl chloride (0.22 g, 1.36 mmol) was used to yield the disulfide as white solid product. Reaction time: 5h, Yield (0.20 g, 79 %); M.P: 57-59 ºC; R_f = 0.5 (100 % petroleum ether). ^{1}H-NMR ($CDCl_3$, 600 MHz) δ (ppm): 3.57 (s, 2H), 7.15 - 7.16 (d, 2H, *J* = 6.0 Hz), 7.29 - 7.30 (d, 2H, *J* = 6.0 Hz). ^{13}C-NMR ($CDCl_3$, 150 MHz) δ (ppm): 42.4, 128.7, 130.6, 133.4, 135.8.

Compound 4k: 4-Bromobenzyl bromide (0.34 g, 1.36 mmol) was used to yield the disulfide as reddish amorphous solid. Reaction time: 20 h, Yield: (0.22 g, 81%); M.P: 77 – 79 ºC; R_f = 0.5 (100 % petroleum ether). ^{1}H-NMR ($CDCl_3$, 400 MHz) δ (ppm): 3.72 (s,. 2H), 7.08 – 7.10 (d, *J* = 8.0 Hz), 7.44 – 7.46 (d, *J* = 8.0 Hz). ^{13}C-NMR ($CDCl_3$, 100 MHz) δ (ppm): 42.6, 121.5, 131.0, 131.7, 136.6. ESI-MS: *m/z* calcd for $C_{14}H_{12}Br_2S_2$ $[M+NH_4]^+$: 419.9085, Observed $[M+NH_4]^+$: 419.0412.

Compound 4l:[6] 4-Trifluromethylbenzyl bromide (0.26 g, 1.36 mmol) was used to yield the disulfide as white amorphous solid. Reaction time: 16 h, Yield: (0.20 g, 73%); M.P: 64 – 66 ºC; R_f = 0.5 (100 % petroleum ether).^{1}H-NMR ($CDCl_3$, 400 MHz) δ (ppm): 3.64 (s, 2H), 7.31 - 7.33 (d, 2H, *J* = 8.0 Hz), 7.57 - 7.59 (d, 2H, *J* = 8.0 Hz). ^{13}C-NMR ($CDCl_3$, 150 MHz) δ (ppm): 42.6, 123.2, 125.0, 125.4 - 125.5 (q, J_1 = 12.0 Hz, J_2 = 18.0 Hz), 129.6, 129.7, 129.4.

Compound 4m: 2-Nitrobenzyl bromide (0.30 g, 1.36 mmol) was used to yield the disulfide as yellow solid product. Reaction time: 2h, Yield (0.20 g, 71 %); M.P: 107 - 109 ºC; R_f = 0.5 (10 % ethyl acetate in petroleum ether). ^{1}H-NMR ($CDCl_3$, 600 MHz) δ (ppm): 4.03 (s, 2H), 7.34 - 7.35 (d, 1H, *J* = 6.0 Hz), 7.45 - 7.48 (t, 1H, *J* = 6.0 Hz), 7.57 - 7.60 (t, 1H, *J* = 6.0 Hz), 8.04 - 8.06 (d, 1H, *J* = 6.0 Hz). ^{13}C-NMR ($CDCl_3$, 150 MHz) δ (ppm):

41.0, 125.5, 128.7, 132.8, 133.4, 133.4, 147.9. ESI-MS: *m/z* calcd for $C_{14}H_{12}N_2O_4S_2$ $[M + Na]^+$: 359.0136, Observed $[M+Na]^+$: 359.0223.

Compound 4n: 2-Methylbenzyl bromide (0.25 g, 1.36 mmol) was used to yield the disulphide as white solid. Reaction time: 16 h, Yield (0.10 g, 50%); M.P: 77 – 78 ºC; R_f = 0.5 (in 100% Petroleum ether). ^{1}H-NMR ($CDCl_3$, 600 MHz) δ (ppm): ^{1}H-NMR (400 MHz, $CDCl_3$,): δ (ppm): 2.37 (s, 3H), 3.66 (s, 2H), 7.13-7.19 (m, 4H). ^{13}C-NMR (100 MHz, $CDCl_3$): δ (ppm):19.3, 41.6, 125.9, 127.8, 130.5, 130.5, 135.1, 136.8. ESI-MS: *m/z* calcd for $C_{16}H_{18}S_2$ $[M + H]^+$ = 275.0923, Observed $[M+H]^+$: 275.0973.

Compound 4o: 3-Nitrobenzyl bromide (0.23 g, 1.36 mmol) was used to yield the disulfide as white amorphous solid. Reaction time: 30 h, Yield: (0.22 g, 96 %); M.P: 101-102 ºC; R_f = 0.5 (10% ethyl acetate in petroleum ether).^{1}H-NMR ($CDCl_3$, 400 MHz) δ (ppm): 3.72 (s, 2H), 7.58 -7.53 (m, 2H), 8.06 (s, 1H), 8.14 - 8.17 (dt, 2H, J_1 = 8.0 Hz, J_2 = 2.0 Hz). ^{13}CNMR ($CDCl_3$, 100 MHz) δ (ppm): 42.1, 122.7, 124.1, 129.6, 135.3, 139.3. ESI-MS: *m/z* calcd for $C_{14}H_{12}N_2O_4S_2$ $[M + Na]^+$: 359.0136, Observed $[M+Na]^+$: 359.0155.

Compound 4p: 3- Chlorobenzyl chloride (0.22 g, 1.36 mmol) was used to yield the disulfide as white amorphous solid. Reaction time: 18 h, Yield: (0.10 g, 89 %); M.P: 122 – 123 ºC; R_f = 0.8 (100 % petroleum ether).^{1}H-NMR ($CDCl_3$, 400 MHz) δ (ppm): 3.56 (s, 2H), 7.13 - 7.10 (m, 1H), 7.23 (s, 1H), 7.23 - 7.27 (m, 2H). ^{13}C-NMR ($CDCl_3$, 100 MHz) δ (ppm): 42.7, 127.5, 127.7, 129.5, 129.8, 134.3, 139.3. ESI-MS: *m/z* calcd for $C_{14}H_{12}Cl_2S_2$ $[M + NH_4]^+$ = 332.0096, Observed $[M+ NH_4]^+$: 332.2070.

Compound 4q: 3-Bromobenzyl bromide (0.34 g, 1.36 mmol) was used to yield the disulfide as reddish amorphous solid. Reaction time: 21 h, Yield: (0.27 g, 98 %); M.P: 56 - 58 ºC; R_f = 0.5 (100% petroleum ether).^{1}H-NMR ($CDCl_3$, 400 MHz) δ (ppm): 3.96 (s, 2H), 7.17 - 7.24 (m, 2H), 7.40 - 7.42 (d, 1H, *J* = 8.0 Hz), 7.46 (s, 1H). ^{13}C-NMR ($CDCl_3$, 100 MHz) δ (ppm): 42.4, 122.6,128.1, 130.2, 130.7, 132.4, 138.8. ESI-MS: *m/z* calcd for $C_{14}H_{12}Br_2S_2$ $[M + K]^+$ = 440.8384, Observed $[M + K]^+$ = 440.1956.

Compound 4r: 3,5-Dimethylbenzyl bromide (0.27 g, 1.36 mmol) was used to yield the disulfide as reddish semi solid compound. Reaction time: 21 h, Yield: (0.17 g, 83 %); R_f = 0.6 (100 % petroleum ether). ^{1}H-NMR ($CDCl_3$, 400 MHz): δ (ppm): 2.31 (s, 6H), 3.57 (s, 2H), 6.86 (s, 1H). 6.90 (s, 2H). ^{13}C-NMR ($CDCl_3$, 100 MHz): δ (ppm): 21.2, 43.4, 127.2, 129.1, 137.1, 138.0.

Compound 4s: In this reaction, the corresponding trisulfide **3s** was obtained as the major product even in the presence of 5 equiv of sodium sulfite.

Compound 4t:[7] 2,4- Dichlorobenzyl chloride (0.27 g, 1.36 mmol) was used to yield the disulfide as white amorphous solid. Reaction time: 24 h, Yield: (0.24 g, 92 %); M.P: 119 – 120 ºC; R_f = 0.8 (100 % petroleum ether). ^{1}H-NMR ($CDCl_3$, 400 MHz) δ (ppm): 3.76 (s, 2H), 7.20 - 7.17 (m, 2H), 7.40 – 7.39 (d, *J* = 4Hz, 1H). ^{13}C-NMR ($CDCl_3$, 150 MHz) δ (ppm): 40.4, 127.0, 129.6, 132.2, 133.5, 134.1, 134.8.

Compound 4u: 2-(Chloromethyl)naphthalene (0.30 g, 1.36 mmol) was used in the presence of Na_2SO_3 (0.34 g, 2.72 mmol) to yield the disulfide as white solid. Reaction time: 4h, Yield: (0.25 g, 96 %); M.P: 121 – 122 ºC; R_f = 0.5 (100 % petroleum ether). ^{1}H-NMR ($CDCl_3$, 400 MHz) δ (ppm): 3.72 (s,. 2H), 7.32 - 7.34 (m, 1H), 7.46 - 7.51 (m, 3H), 7.75 – 7.82 (s, 3H). ^{13}C-NMR ($CDCl_3$, 100 MHz) δ (ppm): 43.7, 126.0, 126.7, 127.3, 127.7, 127.8, 128.2, 128.3, 132.7, 133.3, 134.6. ESI-MS: *m/z* calcd for $C_{22}H_{18}S_2$ $[M+H]^+$: 347.0923; observed $[M+H]^+$: 347.2515.

Synthesis of unsymmetrical disulfide 4v: To an ethanolic solution (3.5 ml) of the column purified Bunte salts **6** and **7** (0.92 mmol) of 4-Methylbenzyl bromide (**6**) and 4-Isopropylbenzyl bromide (**7**), was added an aqueous solution (1.5 ml) of sodium sulfide nonahydrate (0.92 mmol) in a drop-wise manner at 50 °C and the mixture was stirred for 3h at that temperature. The progress of the reaction was monitored by TLC study. Upon the completion, the reaction mixture was diluted with ethyl acetate and washed with brine solution. The combined organic layer was dried over anhydrous sodium sulfate and the solvent was evaporated under reduced pressure to afford crude disulfide mixture (**4f**, **4g** and **4v**) at reasonably good yields. The crude mixture was then analyzed by a reverse-phase C-18 column in an analytical HPLC system to identify the disulfides present in the mixture (Figures S97).

Synthesis of monosulfide 5m

To a stirred solution of sodium sulfide nonahydrate (0.05g, 0.23 mmol) in ethanol (5.0 ml), 2-nitrobenzyl bromide (0.10 g, 0.46 mmol) was added at room temperature and the mixture was stirred at room temperature for 3h. The progress of the reaction was monitored by TLC study. After completion of the reaction, ethanol was evaporated under reduced pressure and the reaction mixture was diluted with ethyl acetate and washed with brine solution. The combined organic layer was dried over anhydrous sodium sulfate and the solvent was evaporated under reduced pressure to afford the crude monosulfide as crystalline yellow solid. Yield: (0.04 g, 58%); M.P: 118 - 122 ºC; R_f = 0.5 (10% ethyl acetate in petroleum ether). ^{1}H-NMR ($CDCl_3$, 400 MHz) δ (ppm):

4.02 (s, 4H), 7.37 - 7.41 (m, 4H), 7.49 - 7.53 (m, 2.04), 7.92 - 7.94 (d, 2H, *J* = 8.0 Hz). ^{13}C-NMR ($CDCl_3$, 100 MHz) δ (ppm): 32.6, 124.3, 127.3, 130.8, 132.0, 132.4, 147.7. ESI-MS: *m/z* calcd for $C_{14}H_{12}N_2O_4S$ $[M+H]^+$: 305.0591, observed $[M+H]^+$: 305.0281.

HPLC analysis

Purity of the synthesized compounds was analysed by high-performance liquid chromatography (HPLC) using Waters 2489 instrument having waters 600 controller and 600 pump or Agilent 1220 infinity II LC system using reverse-phase C-18 column (Luna ®, 5μM, 100 Å, 205×4.6 mm). The HPLC analysis of the test compounds was performed using HPLC grade solvents. 2-Nitro-substituted benzylic compounds **3m**, **4m**, and **5m** were analysed using (70 to 95%) of acetonitrile and (30 to 5%) water system for 10 min in a linear gradient mode and (95:5) ratio of acetonitrile and water system in isocratic mode for another 10 min, respectively (Figure S91). Compounds **3f**, **3g** and **3v** were analysed using (85 to 97%) acetonitrile and (15 to 3%) water system for 10 min in a linear gradient mode followed by (97:3) acetonitrile and water system in an isocratic mode for another 10 min (Figure S94). Compounds **4f**, **4g** and **4v** were analysed by using acetonitrile (92 to 98%) and water (8 to 2%) in a linear gradient mode for 10 min followed by (98:2) ratio of acetonitrile and water in an isocratic mode for another 10 min (Figure S97). Final test compounds for biological study were purified by reverse-phase semi-prep column (Luna ®, polar C-18, 250×21.2 mm) on a semi-prep HPLC system (Thermo scientific Dionex, Ultimate 3000 pump with DAD).

Preparation of MS samples and analysis

High resolution mass spectra (HR-MS) and GC-MS were obtained using an Agilent 6520 Accurate-Mass Quadrupole Time-of-Flight (Q-TOF) LC/MS spectrometer and PerkinElmer Clarus 680 GC/600C MS, respectively. Samples were prepared for MS analysis by taking minimum amount (~1 mg/ml) and dissolved in HPLC grade methanol or acetonitrile. The solution was then filtered using 0.22 micron syringe filters. The samples were injected to the MS systems via auto-sampler using usual protocol. HPLC grade acetonitrile and water system was used as mobile phase in HR-MS and helium gas was used as mobile phase in GC-MS. The samples were analysed in ESI +ve ion mode.

X-Ray Crystallography

Single crystal X-ray diffraction data was collected on a Bruker AXS SMART APEX CCD diffractometer or Super Nova, Single source at offset, Eos diffractometer. The data refinement and cell reductions were carried out by CrysAlisPro at room temperature (293 K). The X-ray generator was operated at 50 KV and 35 mA using Mo-Kα radiation (λ = 0.71073 Å). The data was collected using SMART software package. The data were reduced by SAINTPLUS, an empirical absorption correction was applied using the package SADABS and XPREP were used to determine the space group. The crystal structure was solved by direct methods using SIR92[8] and refined by full-matrix least-squares method using SHELXL-97.[9] All non-hydrogen atoms were refined anisotropically and hydrogen atoms were assigned at idealized locations. **CCDC 1905587** (compound **5m**), **CCDC 1905588** (compound **3m**) and **CCDC 1905589** (compound **4m**) contain the supplementary crystallographic data for this paper. These data can be obtained free of charge from The Cambridge Crystallographic Data Centre *via* www.ccdc.cam.ac.uk/data_request/cif.

Crystal data for **3m**: $C_{14}H_{12}N_2O_4S_3$; M_r = 368.5; monoclinic; space group P*21*; a = 4.6759 (12), b = 14.3551 (42), c = 12.2530(35); β = 90.125(20); V = 822.46(2) $Å^3$; Z = 2; ρ_{calcd} = 1.49 g/cm^3; Mo-Ka radiation (λ = 0.71073 Å); T = 293(2) K; R_1 = 0.047, wR_2 = 0.108 (I>2σ(I)); R_1= 0.100, wR_2=0.127 (all data).

Crystal data for **4m**: $C_{14}H_{12}N_2O_4S_2$; M_r = 336.4; monoclinic; space group P*21/n*; a = 13.6592 (5), b = 7.8745 (3), c = 14.1331(5); β = 99.026(2); V = 1501.32(5) $Å^3$; Z = 4; ρ_{calcd} = 1.49 g/cm^3; Mo-Ka radiation (λ = 0.71073 Å); T = 293(2) K; R_1 = 0.042, wR_2 = 0.109 (I>2σ(I)); R_1= 0.058, wR_2=0.117 (all data).

Crystal data for **5m**: $C_{14}H_{12}N_2O_4S$; M_r = 304.3; monoclinic; space group C*2/c*; a = 7.5711 (4), b = 14.0965 (8), c = 13.1401(7); β = 90.629(5); V = 1402.31(2) $Å^3$; Z = 4; ρ_{calcd} = 1.44 g/cm^3; Mo-Ka radiation (λ = 0.71073 Å); T = 293(2) K; R_1 = 0.041, wR_2 = 0.102 (I>2σ(I)); R_1= 0.051, wR_2=0.109 (all data).

Cell Culture

Human breast carcinoma cell line MCF-7 was obtained from the National Centre for Cell Science (NCCS), India. MCF-7 was cultured in DMEM medium (Gibco) supplemented with 10% (v/v) FBS (Gibco) and 1% Pen-Strep (Gibco). Cells were cultured as a monolayer in a humidified incubator at 37 °C in the presence of 5% CO_2 level.

Cellular morphology and viability studies

The synthesized compounds were primarily screened in breast cancer cell line (MCF-7, passage no 41-50). Stock solution of the synthesized compounds was prepared in DMSO (HiMedia) and serially diluted in the culture media for the preparation of working solutions of different concentrations. The cells were seeded at a density of 1×10^4 cells per 100 µl in 96-well plates and incubated overnight. The cells were treated with test compounds (10.0 µM and 25.0 µM) and incubated for 72h in the CO_2 incubator. Cellular morphology was carefully observed and imaged in a Bio-rad ZOE^{TM} fluorescent cell imager before and after (24h, 48h and 72h interval) the treatment of test compounds. Preliminary screening with cell viability assay was performed for the cells in the presence of test compounds after 72h and compared with the control experiments without any test compound.

Trisulfides that exhibited significant potencies in preliminary studies were selected and purified further by a reverse-phase HPLC method. The purified trisulfides were screened for their anti-proliferative activities. Stock solution of the synthesized compounds was prepared in DMSO (HiMedia) and serially diluted in the culture media for the preparation of working solutions of different concentrations. The cells (MCF-7) were plated in 96-well culture plates at a density of 1×10^4 cells/100 µl/well and treated with test compounds (upto 25.0 µM) for 0h (Set 1) and 72h (Set 2). At the end of treatment period, the cells were washed with DPBS and 100.0 µL of 0.5 mg/mL of MTT in fresh DPBS was added to each well (Set 1) and incubated for 2h. Following the 2h incubation, the culture media from the plate was removed and the purple formazan crystals were dissolved using 100 µl of DMSO (HiMedia) and the absorbance at 570 nm was measured using a microplate reader (Multiskan Go microplate reader). In Set 2, similar MTT treatment protocol was followed only after 72h. The mean ΔOD values were calculated by the subtraction of mean OD values of 0h plate (Set 1) from the mean OD values of identical wells at 72h plate (Set 2) and the percentage proliferation was calculated keeping the mean ΔOD of untreated control as 100%.

Detection of Hydrogen sulfide release by MB assay

Generation of hydrogen sulfide by the synthesized trisulfides and disulfides in the presence of thiols such as glutathione (GSH) was monitored using methylene blue assay in an UV-Vis spectrophotometer.[10] Hydrogen sulfide generation was initiated by adding trisulfide or disulfide donors (50 µM) into PBS buffer (pH 7.4, 50 mM) solution containing thiol (500 µM). This mixture was pre-incubated in the working buffer (pH 7.4) to ensure the generation of H_2S, which might exist as HS^- in buffer. Formation of methylene blue was monitored at 670 nm in UV-Vis spectrophotometer in different time intervals after adding 500 µl of the above solution to 500 µl of methylene blue cocktail (100.0 µL of zinc acetate (1% w/v), 200 µL of *N,N*-dimethyl-1,4-phenylenediamine sulfate (20 mM in 7.2 M HCl), and 200 µL of ferric chloride (30 mM in 1.2 M HCl)) in a cuvette. The H_2S concentration of each sample was calculated against a calibration curve, which was obtained using known concentrations of $Na_2S.9H_2O$ solution under identical condition without any thiols. To understand the possible interference by the added GSH with the produced MB during the assay, several control experiments were performed with the know concentration of GSH and pure MB in buffer as well as in MB cocktail. These results show that presence of GSH probably produces an unknown complex having an absorbance at around 450 nm and also it reduces the absorbance of pure MB at 670 nm (Figure S119A-C). This indicates that the measurement of H_2S release by MB assay in the presence of an excess thiol may not be completely quantitative, rather a qualitative/relatve aspect.

H_2S release from 3f in cellular medium and its detection using fluorescent probe 8

MCF-7 cells were cultured in high glucose Dulbecco's modified Eagle's medium (DMEM) supplemented with 10% fetal bovine serum (FBS) and 1% penicillin/streptomycin at 37 °C under 5% CO_2. Cells were then plated (0.7×10^4 cells/well) in poly-D-lysine coated plates (Merck) containing 2.0 mL of DMEM and incubated at 37 ºC under 5% CO_2 for 24 h. The confluent cells were washed with PBS and incubated with compound **8** for 10 min. After washing with PBS, cells were fixed and imaged to check the level of endogenous H_2S in the treated MCF-7 cells. In another experiment, compound **3f** (1.0 µM) was added to the adhered cells and kept for 10 min at 37 °C under 5% CO_2. After the incubation, cells were washed (5 times) with PBS and compound **8** was added. The cells were incubated for 10 min in the incubator and washed with PBS. The cells were fixed with 4% formaldehyde and imaged under fluorescence microscope (Biorad ZOE Fluoroscent Cell Imager).

DFT Calculations

The geometries of the all the considered reactants, transition states (TS) and products were fully optimized at M06/6-31+G(d) level of theory using Gaussian-09 program.[11] Effect of water solvent we included in all the calculations using IEF-PCM method.[12] The optimizations were followed by frequency calculations at the same level to characterize the obtained stationary points as minima or transition state on the potential energy surface.

Intrinsic reaction coordinate (IRC) calculations,[13] with mass weighted coordinates at the same level of theory, were also performed wherever necessary to validate the reaction path and to follow the reaction profile. Single point energy calculations at various levels were carried out to analyse the effect of methods and basis set on the energy profile of the reaction, Table S4. Effect of zero point correction and Gibbs free energy on the profile is summarized in Table S4.

NMR Spectra of Trisulfides

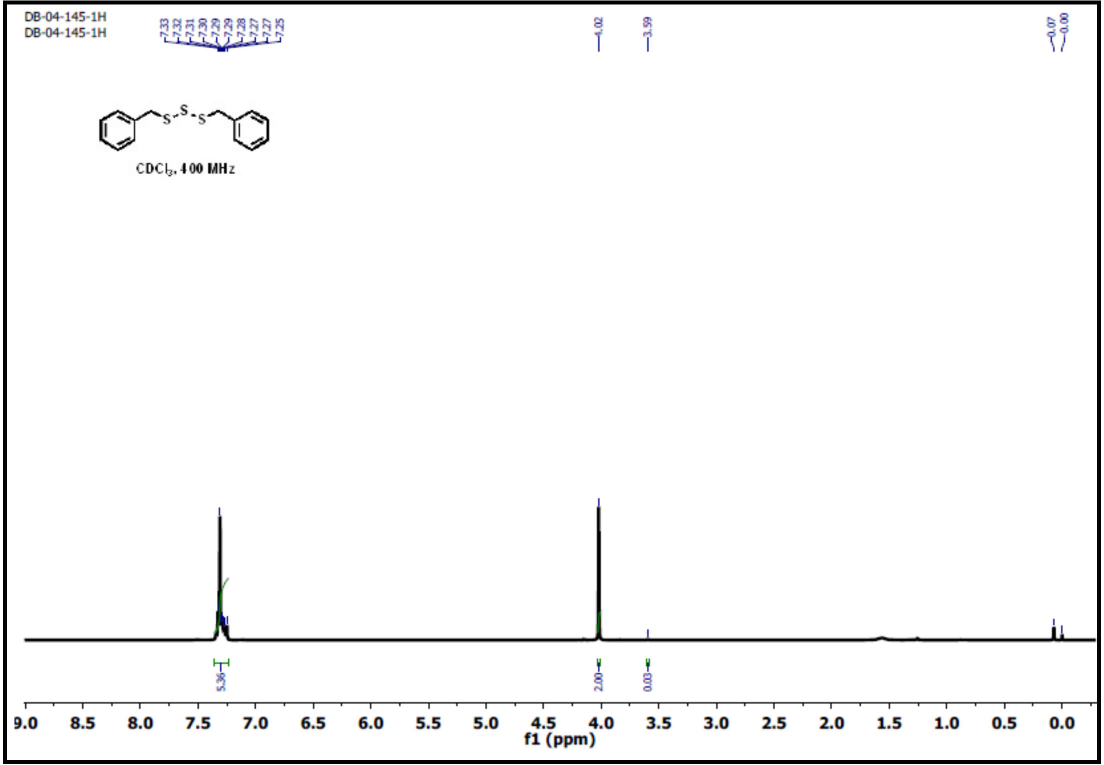

Figure S1: ^{1}H- NMR ($CDCl_3$, 400 MHz, ppm) spectrum of compound **3a**.

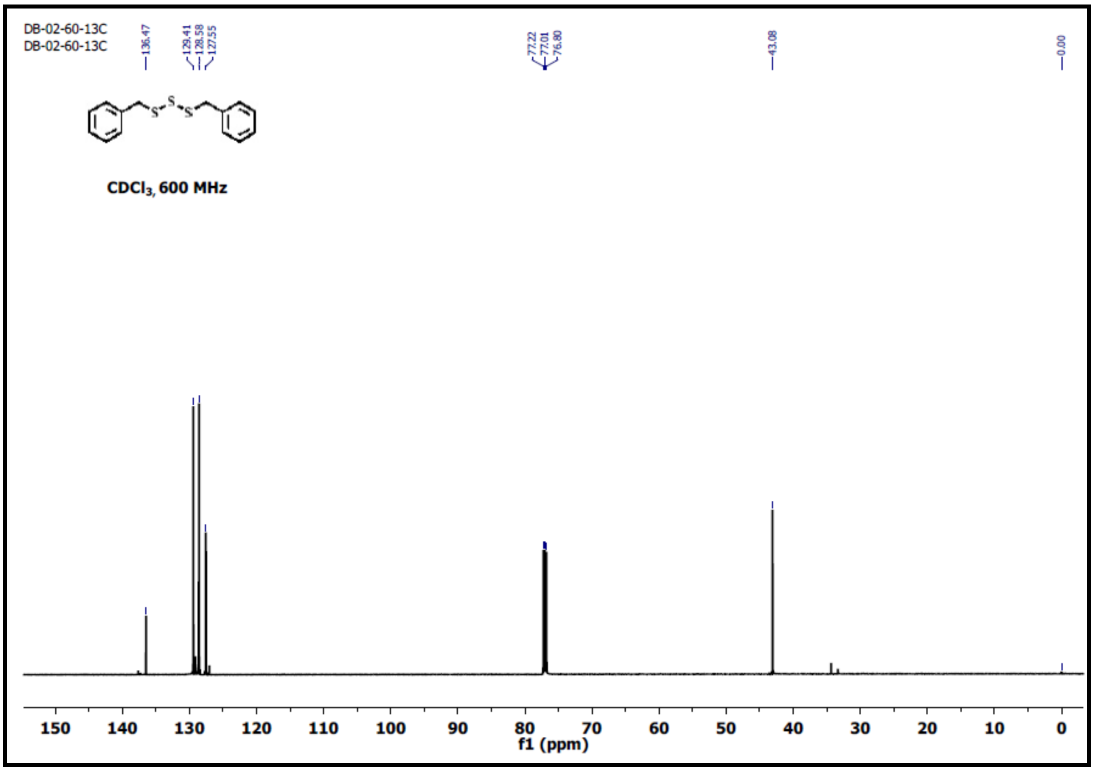

Figure S2: ^{13}C- NMR ($CDCl_3$, 150 MHz, ppm) spectrum of compound **3a**.

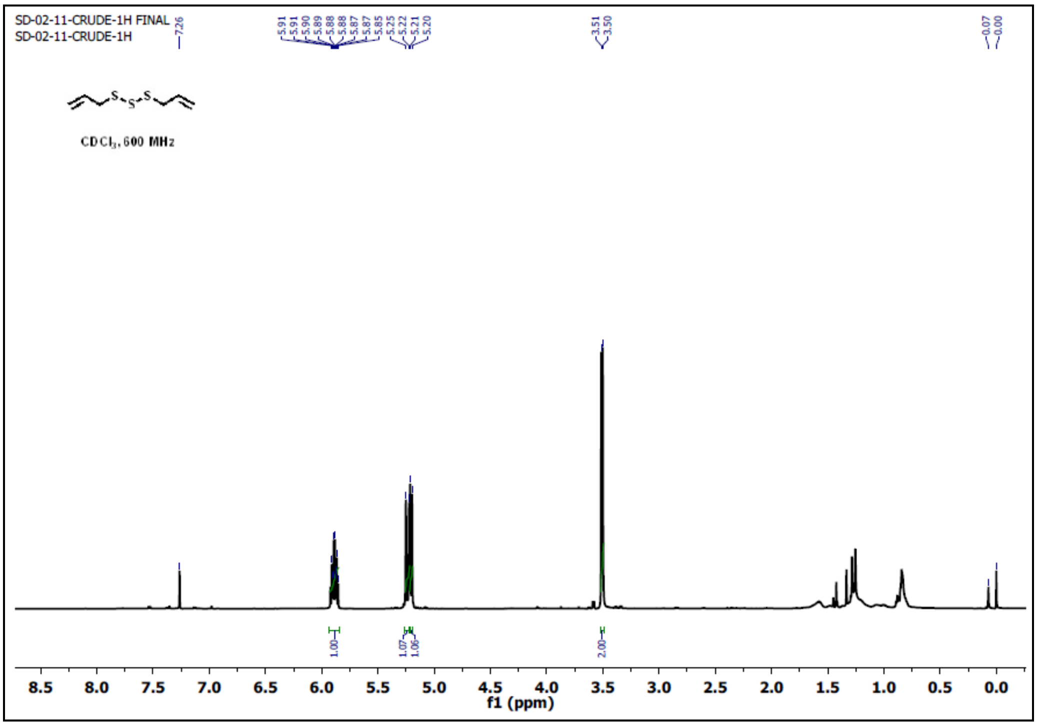

Figure S3: ^{1}H- NMR (CDCl$_3$, 600 MHz, ppm) spectrum of compound **3b**.

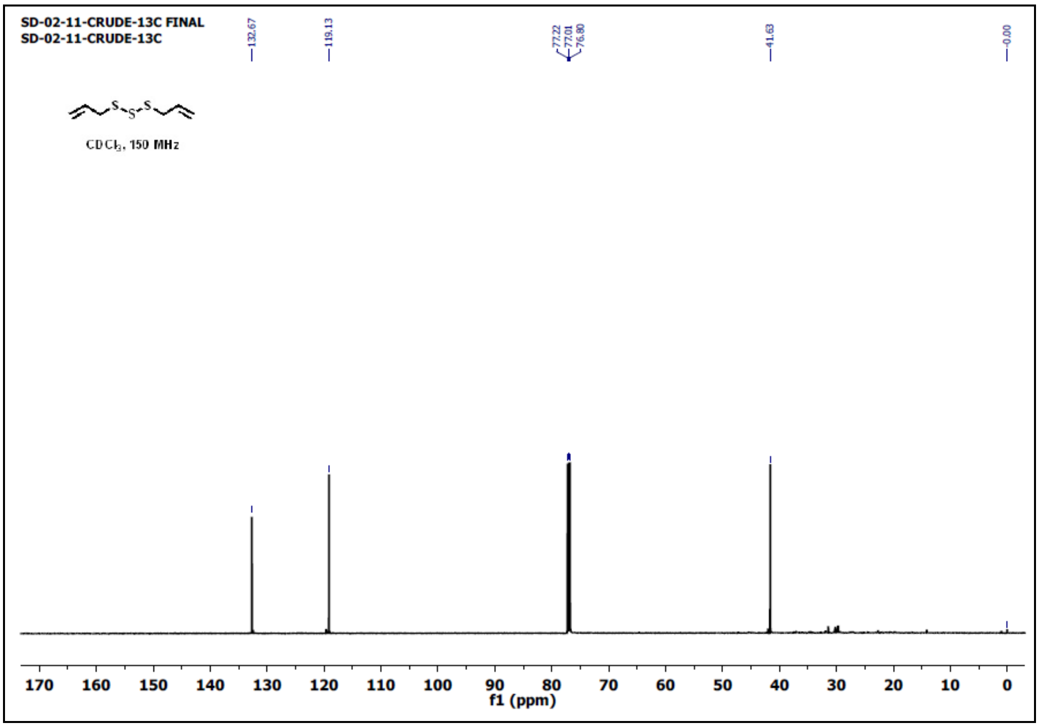

Figure S4: ^{13}C- NMR (CDCl$_3$, 150 MHz, ppm) spectrum of compound **3b**.

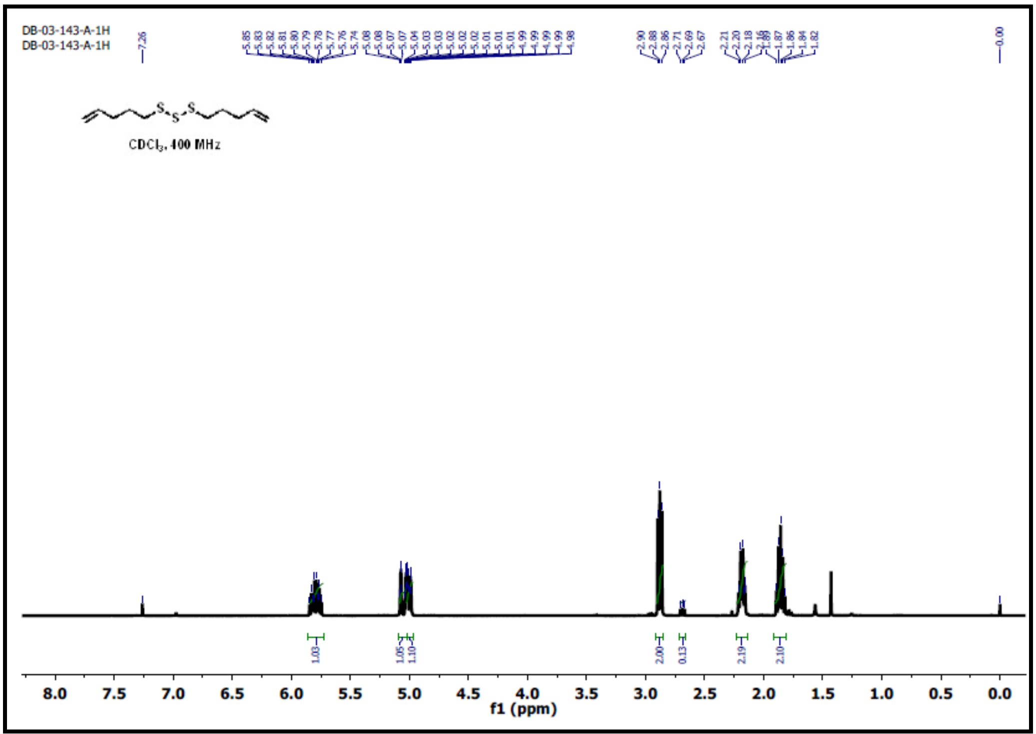

Figure S5: ^{1}H- NMR (CDCl$_3$, 400 MHz, ppm) spectrum of compound **3c**.

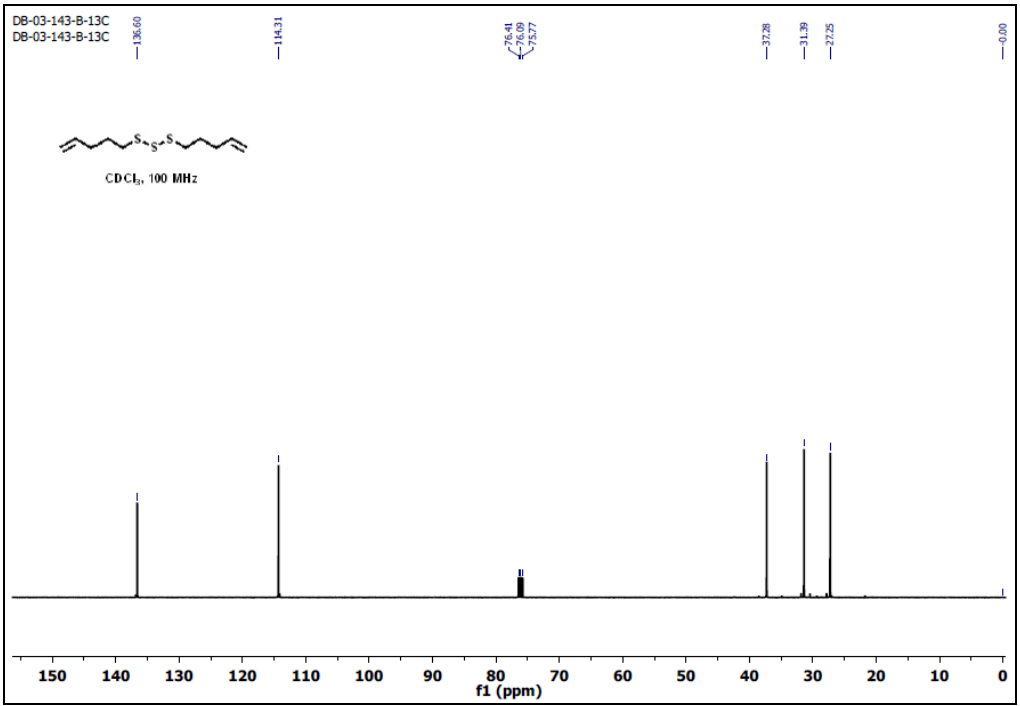

Figure S6: ^{13}C- NMR (CDCl$_3$, 100 MHz, ppm) spectrum of compound **3c.**

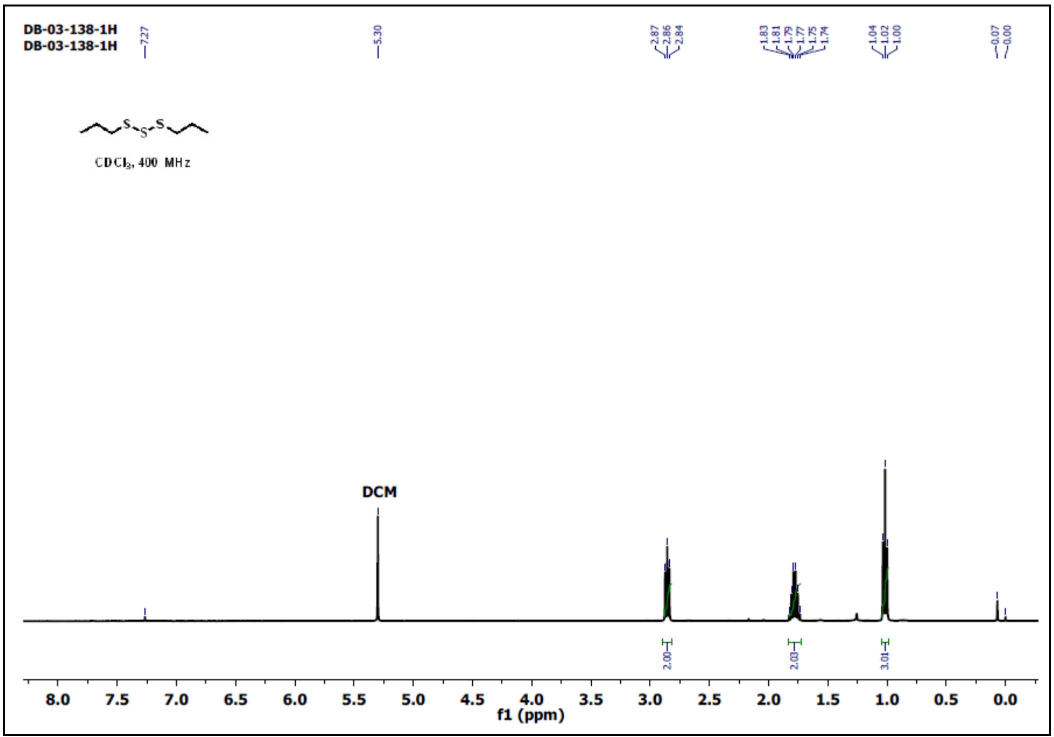

Figure S7: ^{1}H- NMR ($CDCl_3$, 400 MHz, ppm) spectrum of compound **3d**.

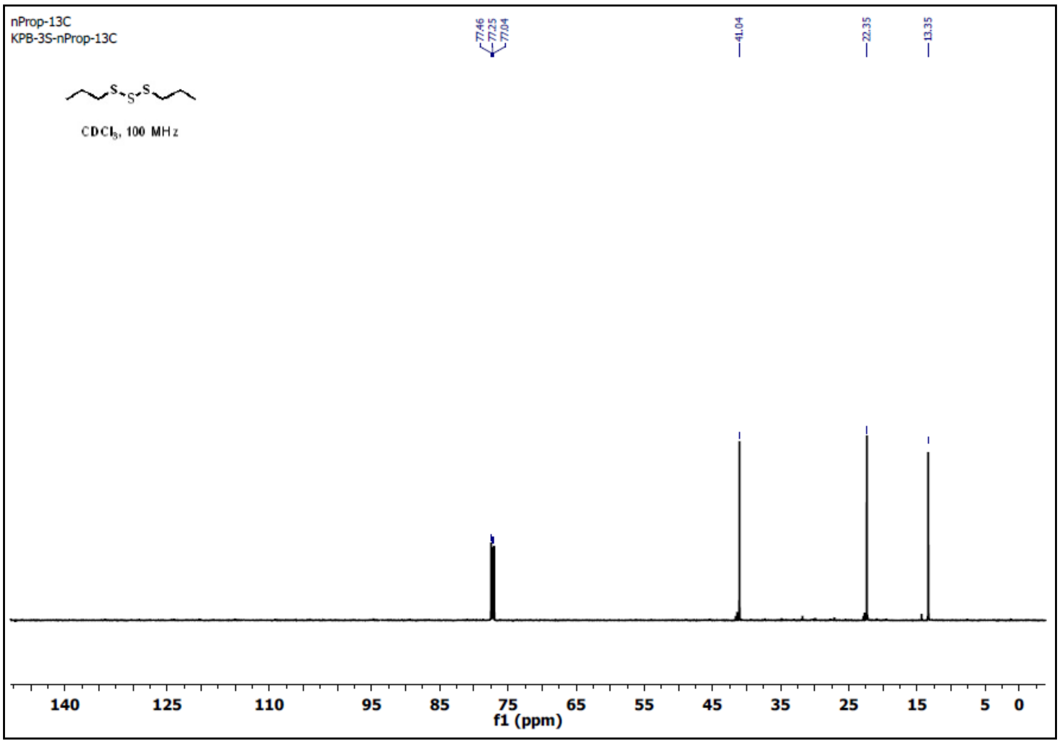

Figure S8: ^{13}C- NMR ($CDCl_3$, 100 MHz, ppm) spectrum of compound **3d**.

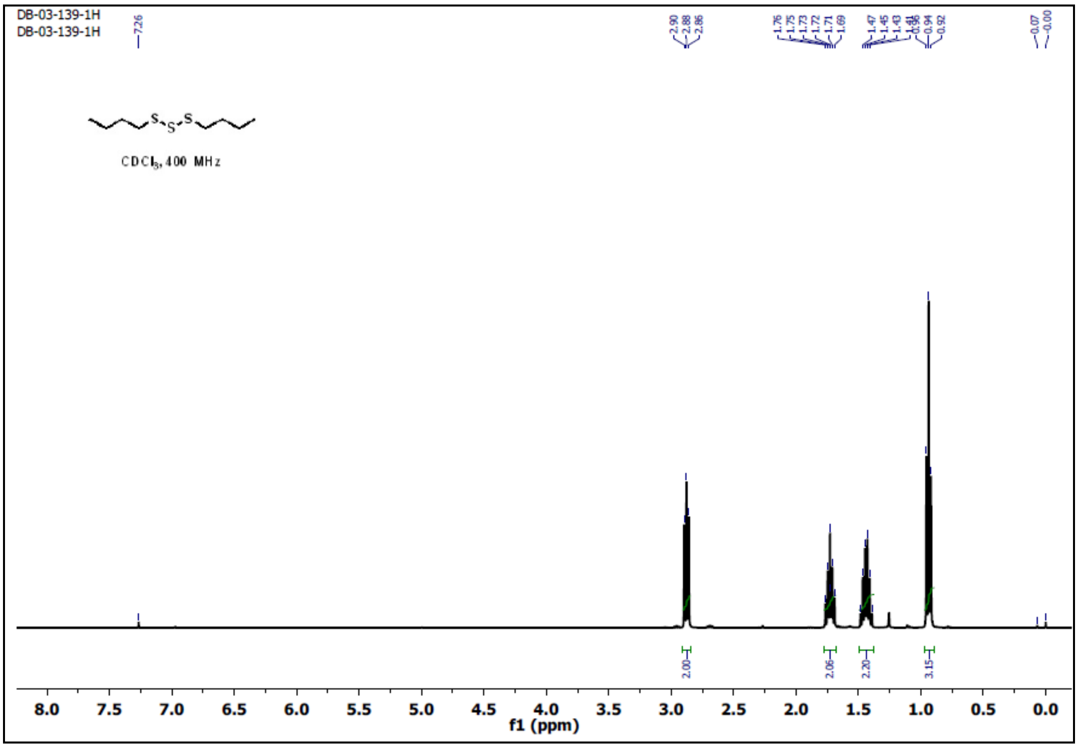

Figure S9: ^{1}H- NMR (CDCl$_3$, 400 MHz, ppm) spectrum of compound **3e**.

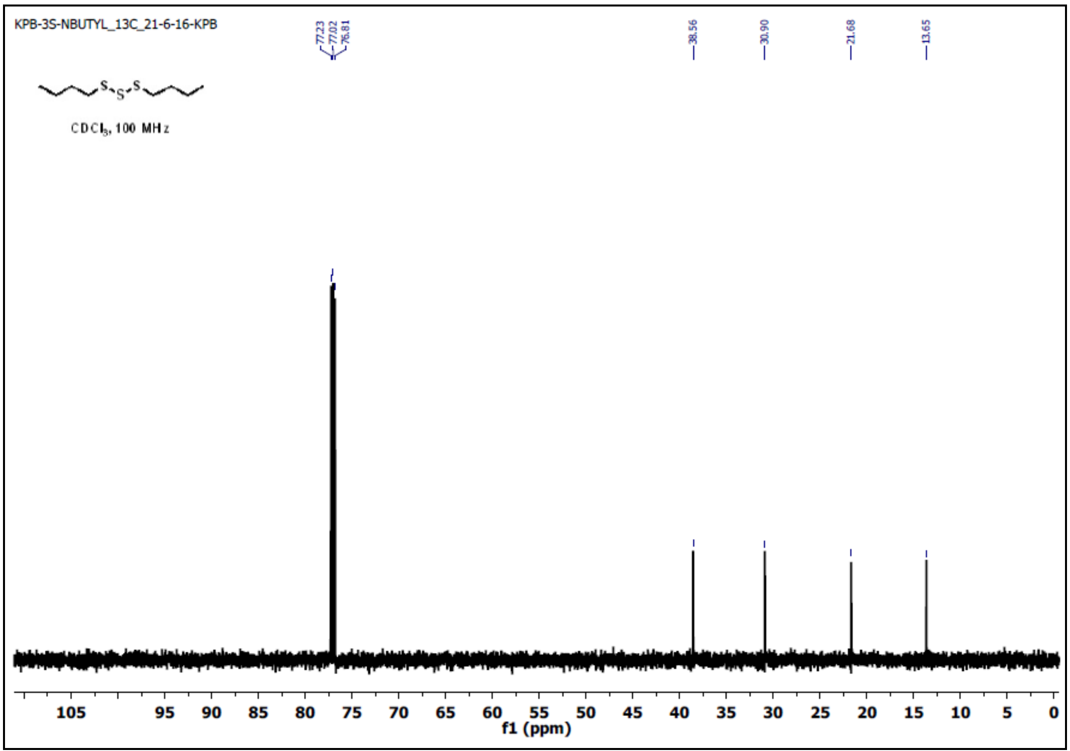

Figure S10: ^{13}C- NMR (CDCl$_3$, 100 MHz, ppm) spectrum of compound **3e**.

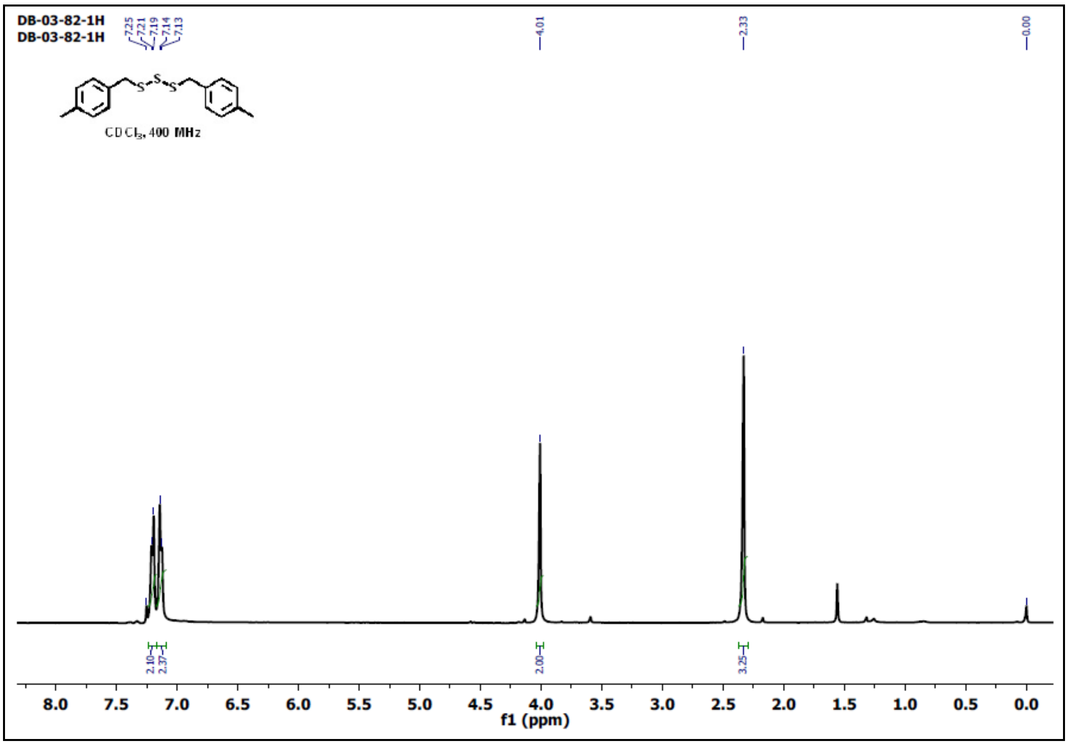

Figure S11: ^{1}H- NMR ($CDCl_3$, 400 MHz, ppm) spectrum of compound **3f**.

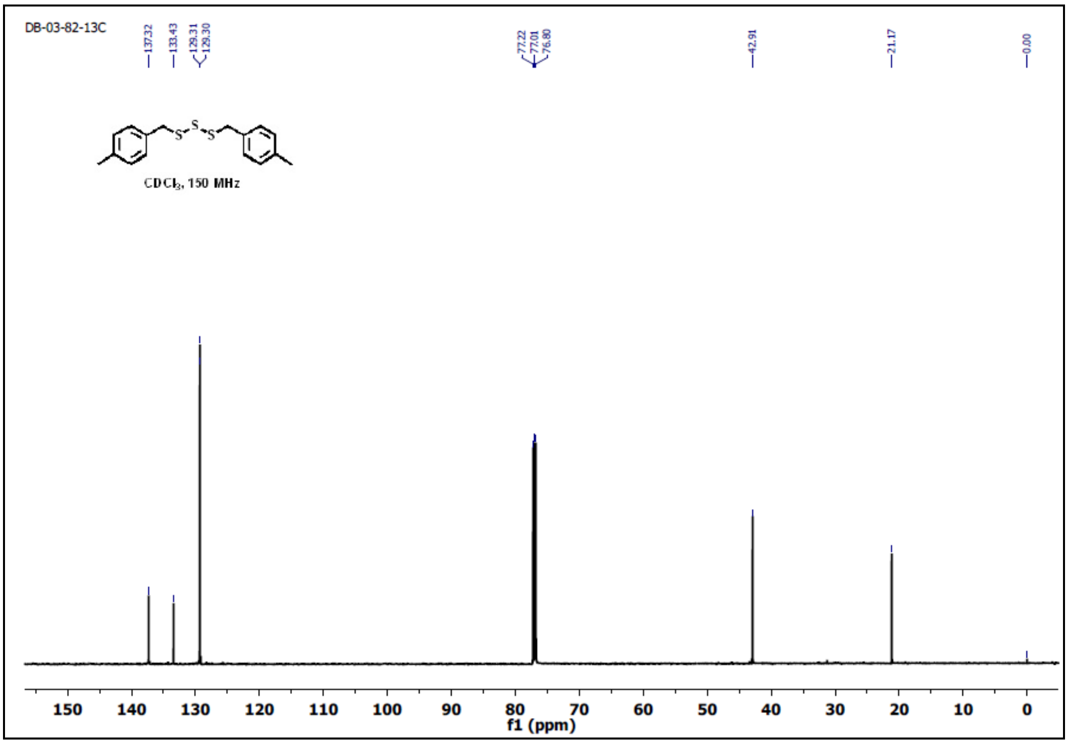

Figure S12: ^{13}C- NMR ($CDCl_3$, 150 MHz, ppm) spectrum of compound **3f**.

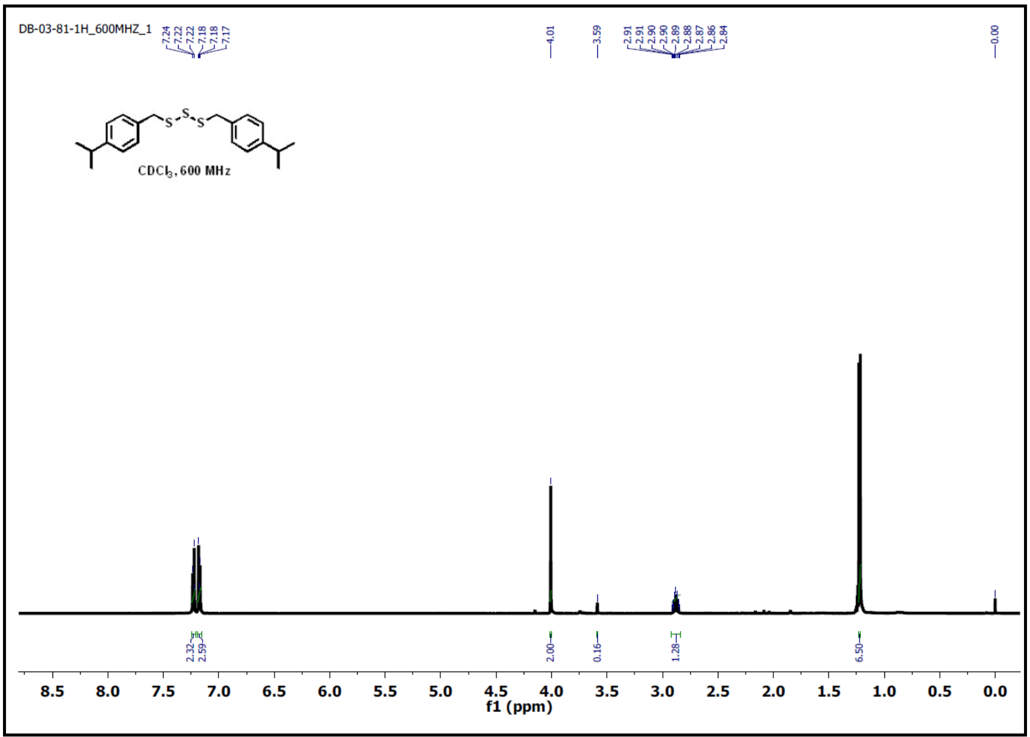

Figure S13: ^{1}H- NMR (CDCl$_3$, 600 MHz, ppm) spectrum of compound **3g**.

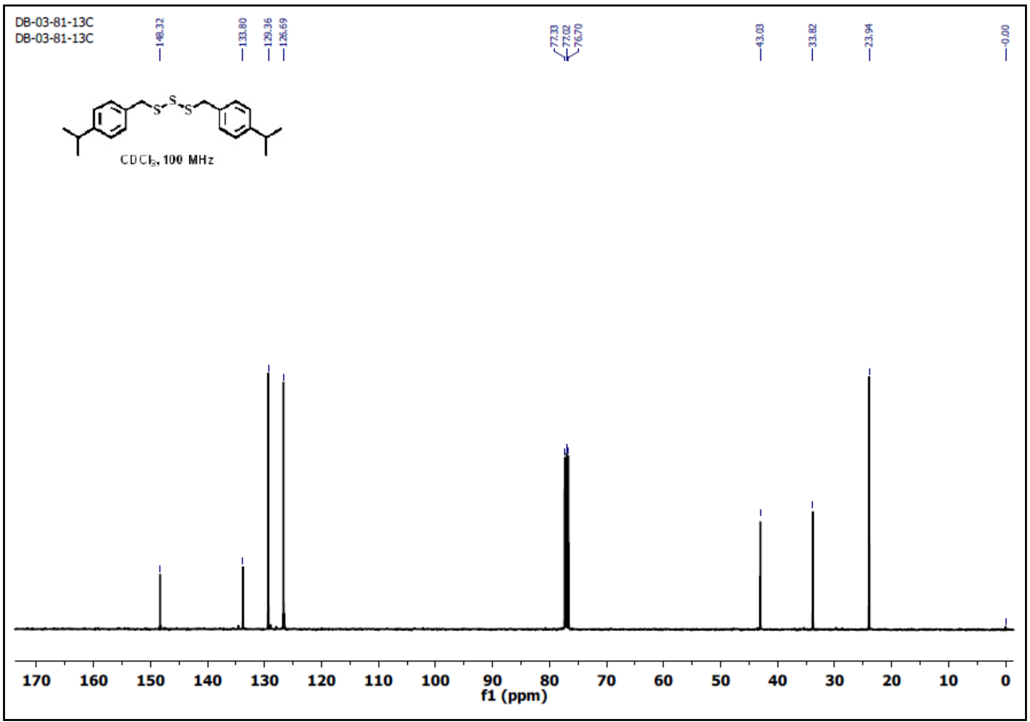

Figure S14: ^{13}C- NMR (CDCl$_3$, 100 MHz, ppm) spectrum of compound **3g**.

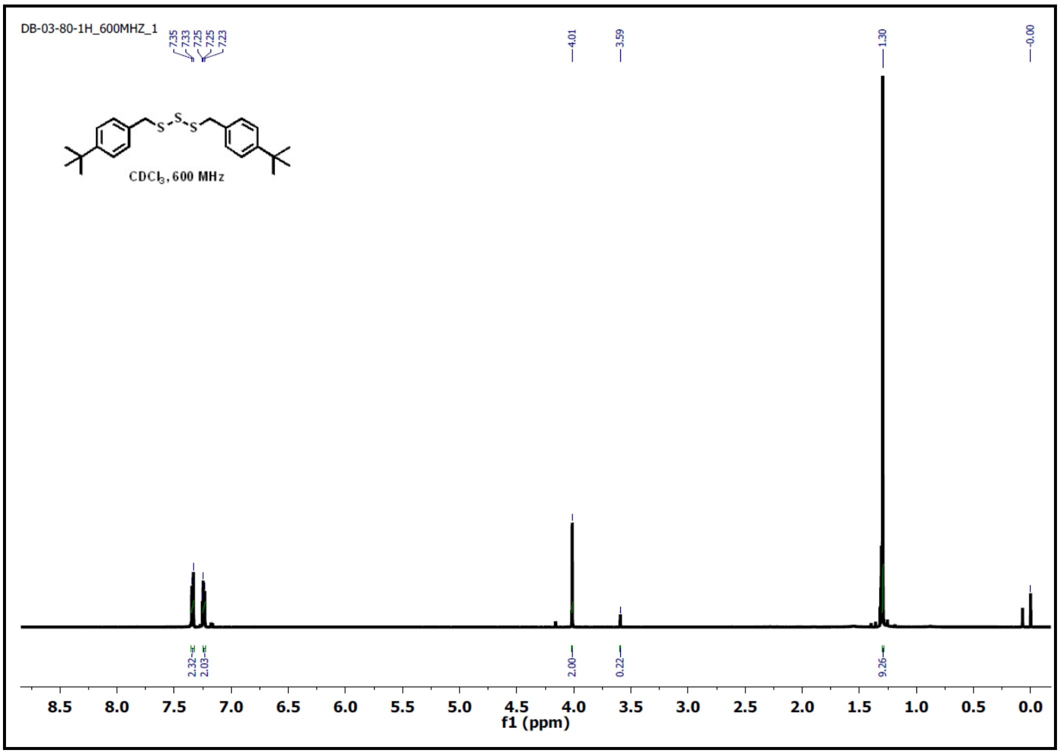

Figure S15: ^{1}H- NMR (CDCl$_3$, 600 MHz, ppm) spectrum of compound **3h**.

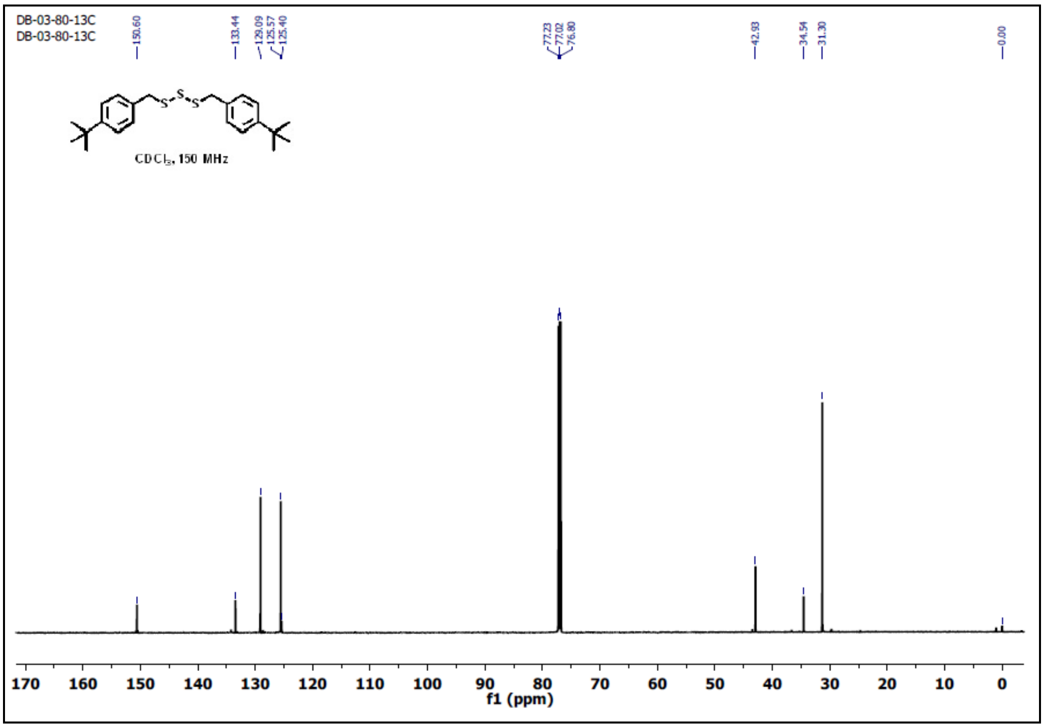

Figure S16: ^{13}C- NMR (CDCl$_3$, 150 MHz, ppm) spectrum of compound **3h**.

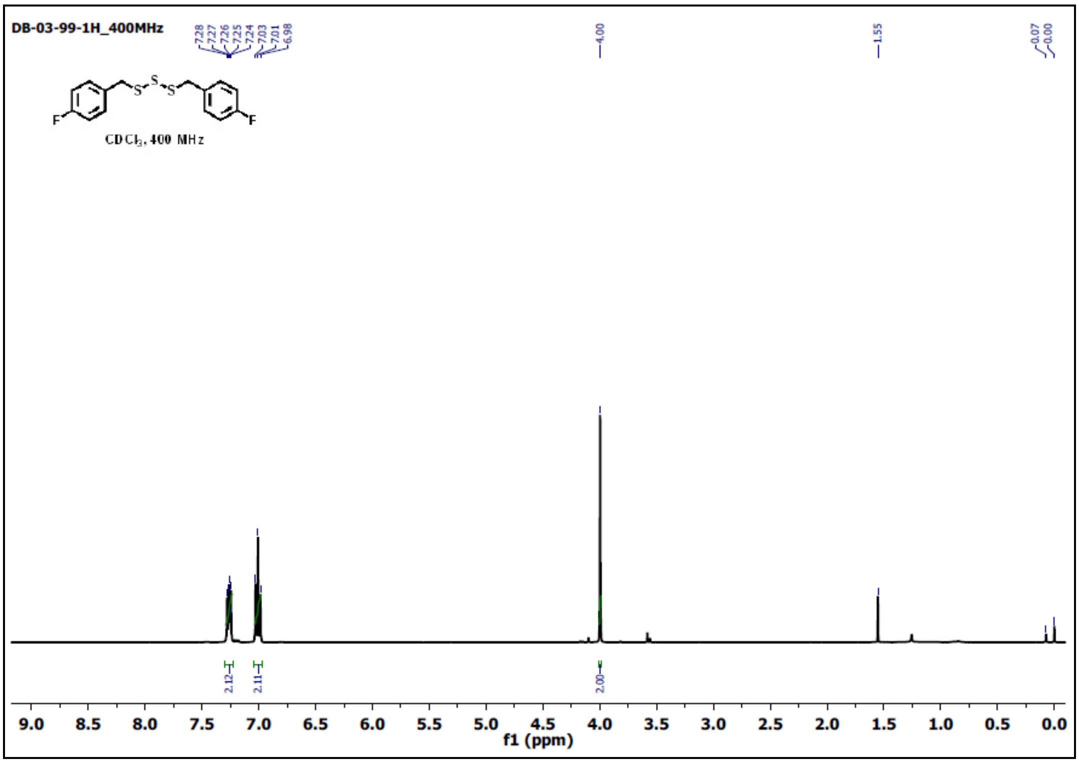

Figure S17: ^{1}H- NMR ($CDCl_3$, 400 MHz, ppm) spectrum of compound **3i**.

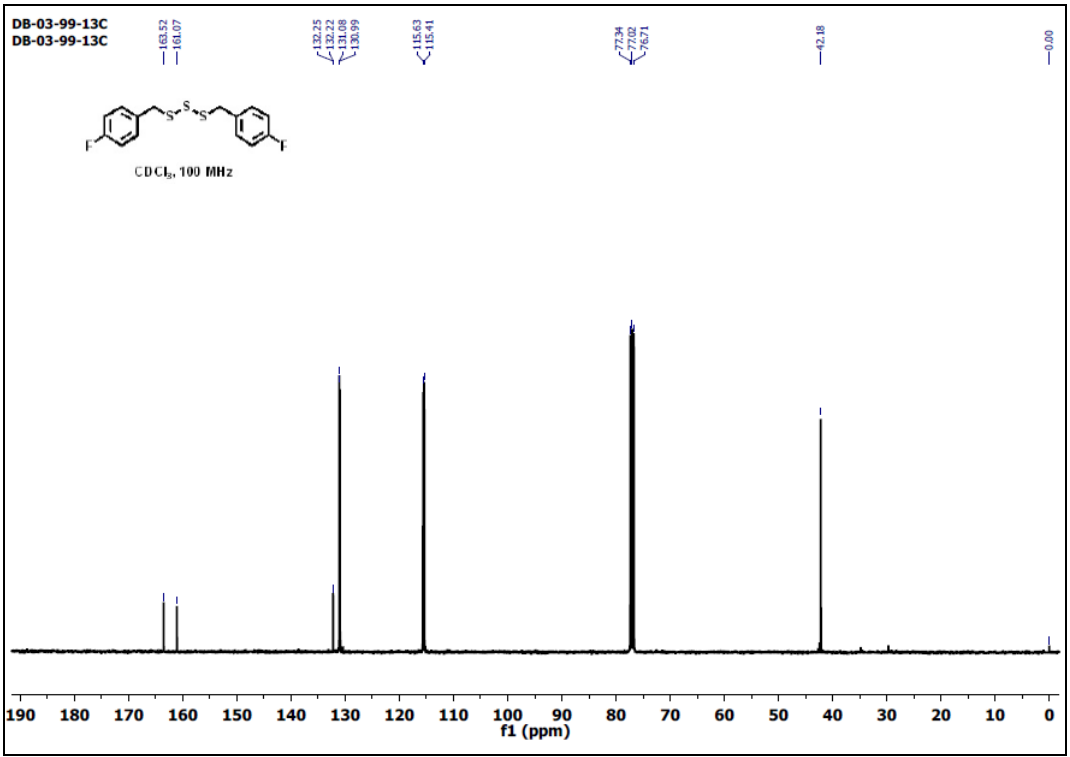

Figure S18: ^{13}C- NMR ($CDCl_3$, 100 MHz, ppm) spectrum of compound **3i**.

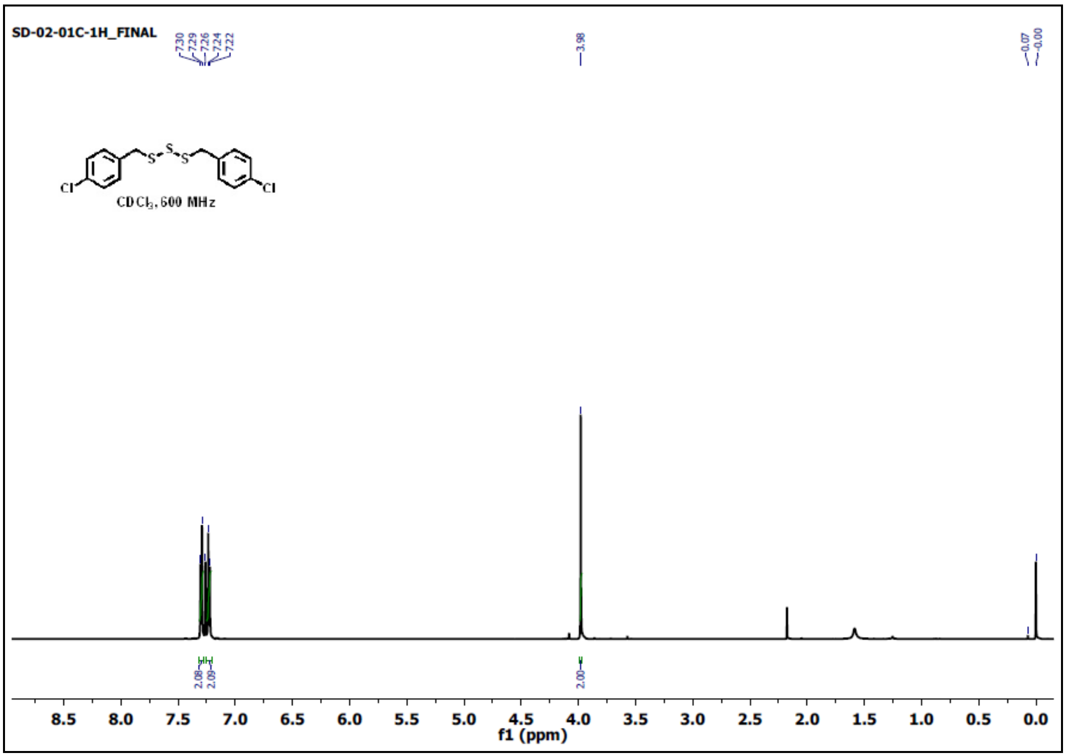

Figure S19: ^{1}H- NMR (CDCl$_3$, 600 MHz, ppm) spectrum of compound **3j**.

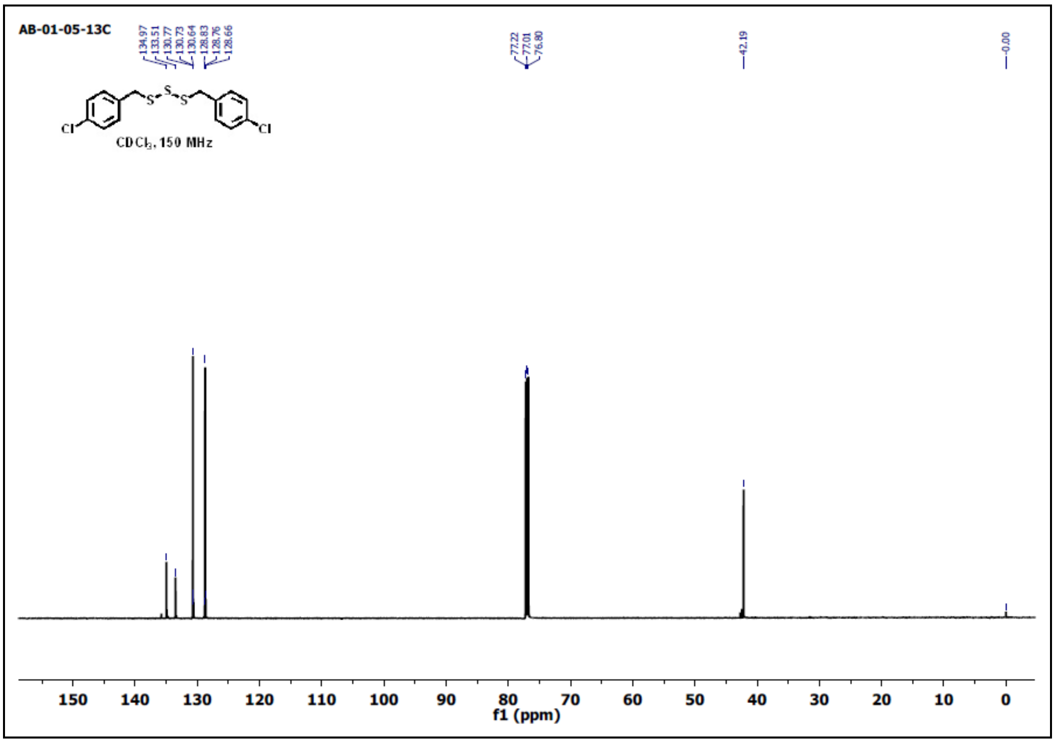

Figure S20: ^{13}C- NMR (CDCl$_3$, 150 MHz, ppm) spectrum of compound **3j**.

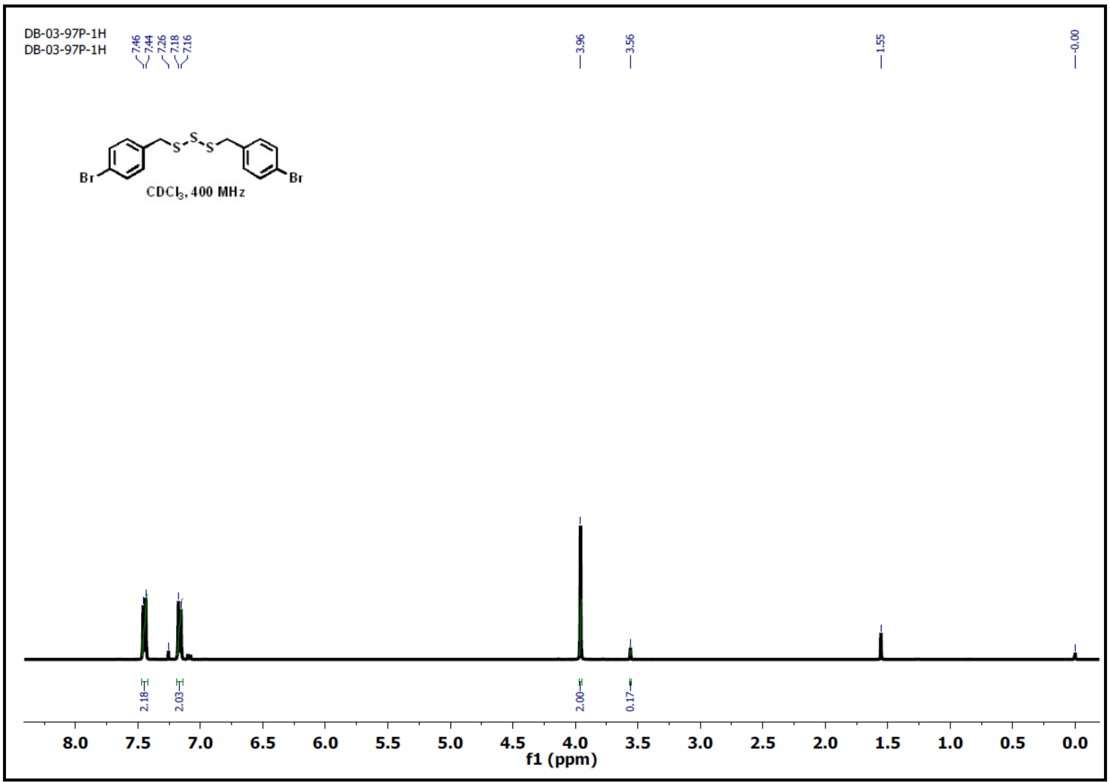

Figure S21: ^{1}H- NMR (CDCl$_3$, 400 MHz, ppm) spectrum of compound **3k**.

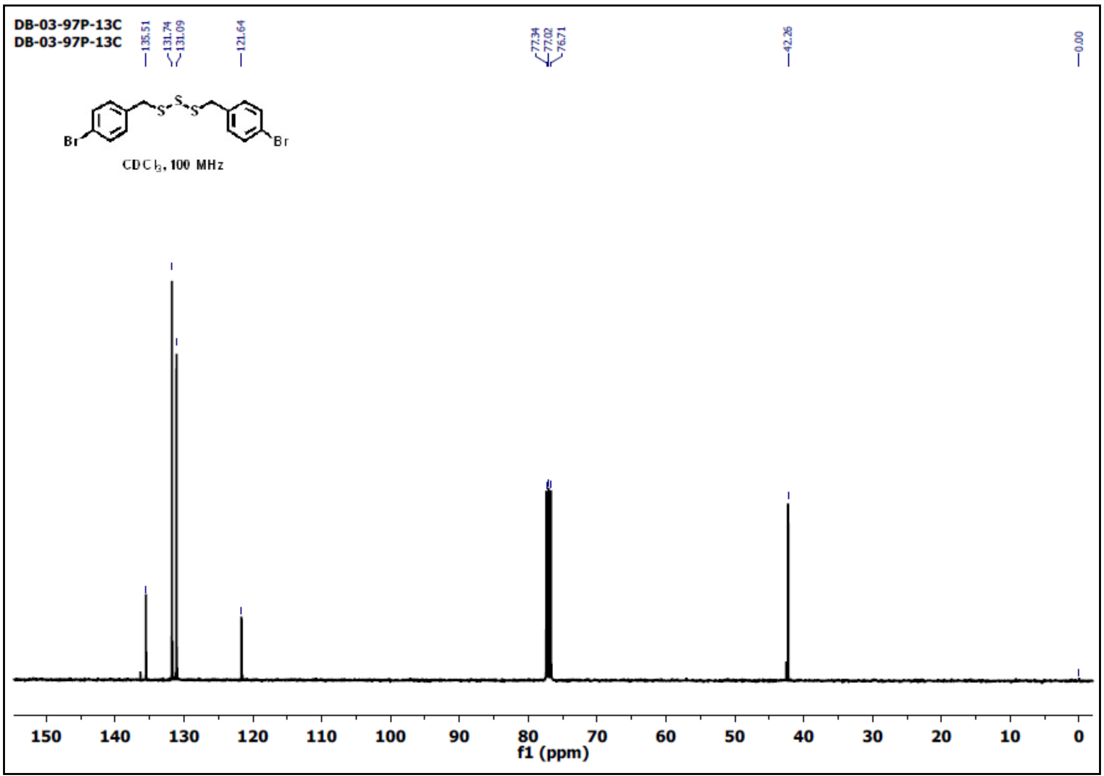

Figure S22: ^{13}C- NMR (CDCl$_3$, 100 MHz, ppm) spectrum of compound **3k.**

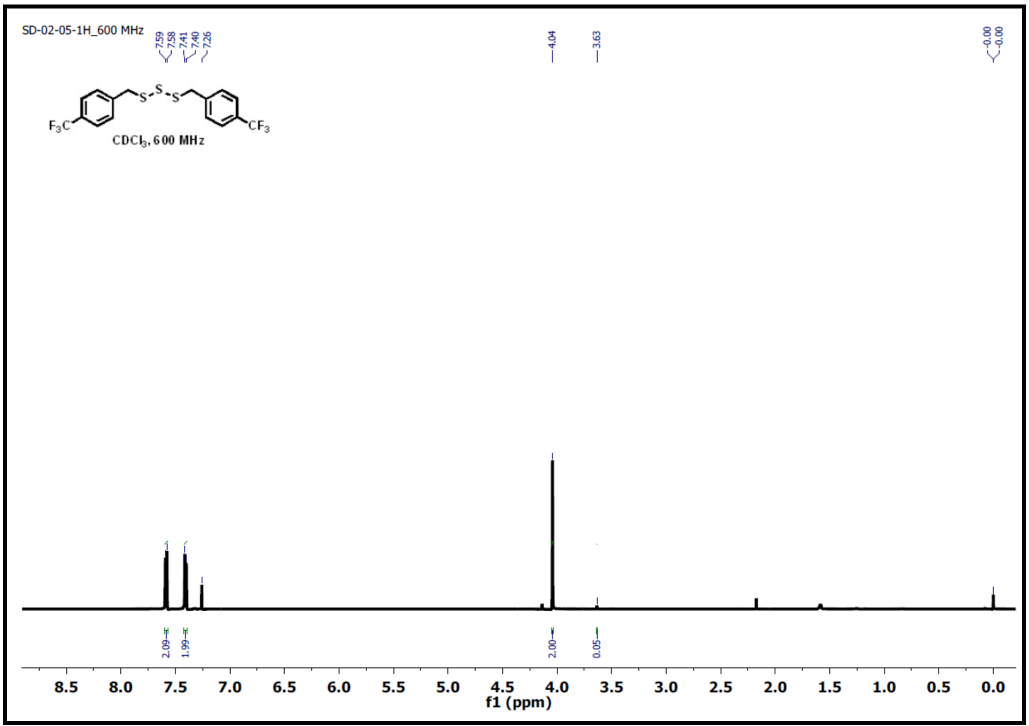

Figure 23: ^{1}H- NMR (CDCl$_3$, 600 MHz, ppm) spectrum of compound **3l.**

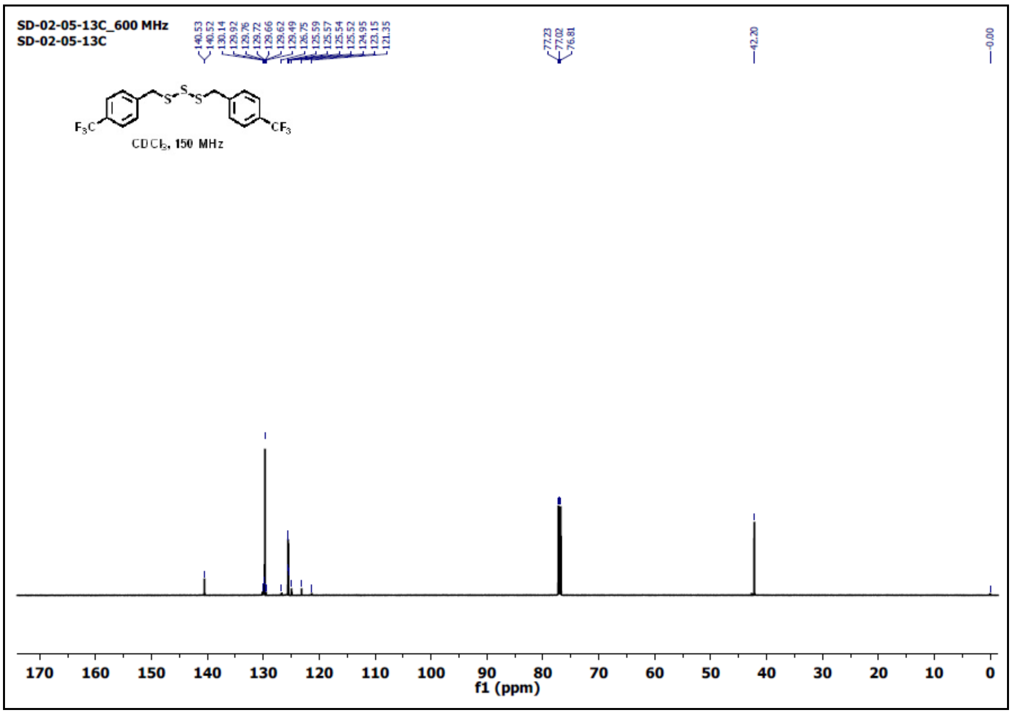

Figure S24: ^{13}C- NMR (CDCl$_3$, 150 MHz, ppm) spectrum of compound **3l**.

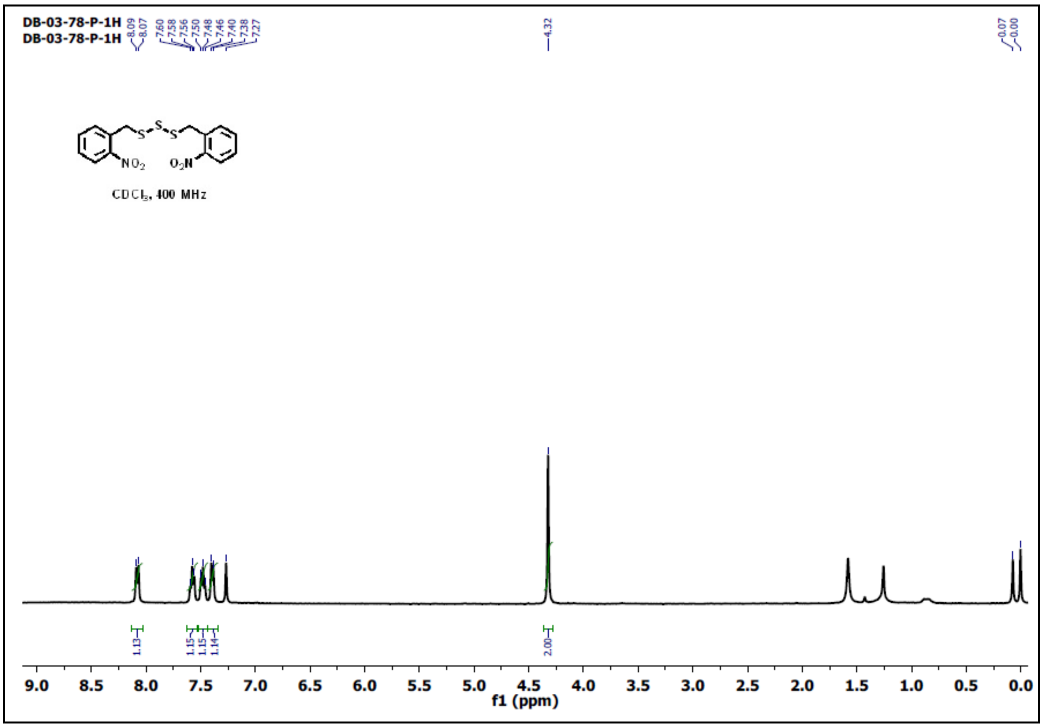

Figure S25: ^{1}H- NMR (CDCl$_3$, 400 MHz, ppm) spectrum of compound **3m**.

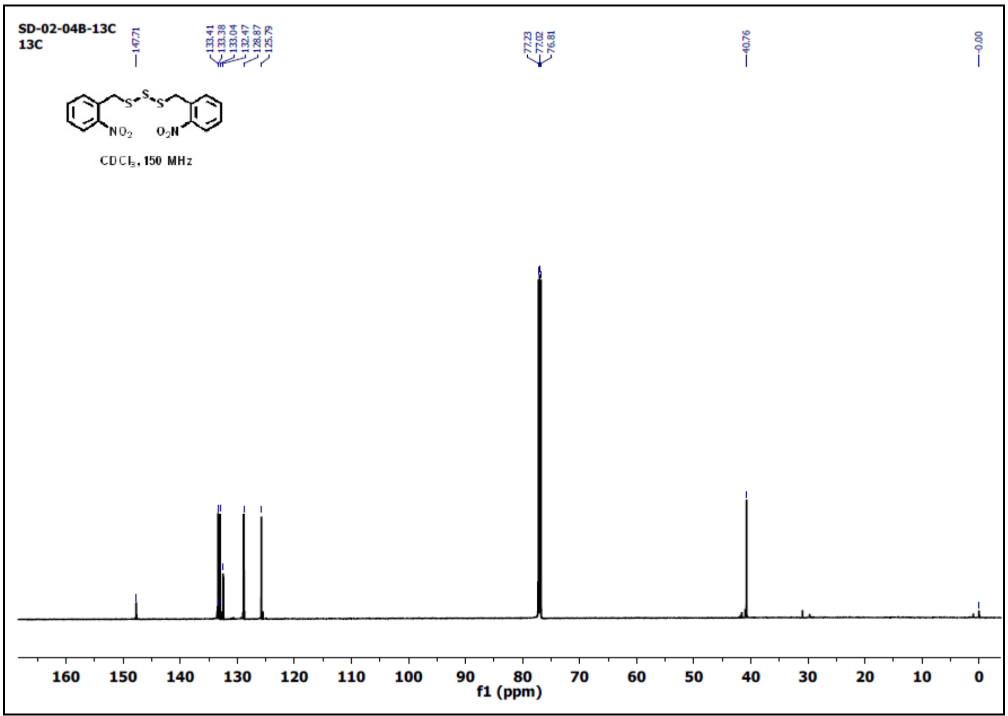

Figure S26: ^{13}C- NMR (CDCl$_3$, 150 MHz, ppm) spectrum of compound **3m**.

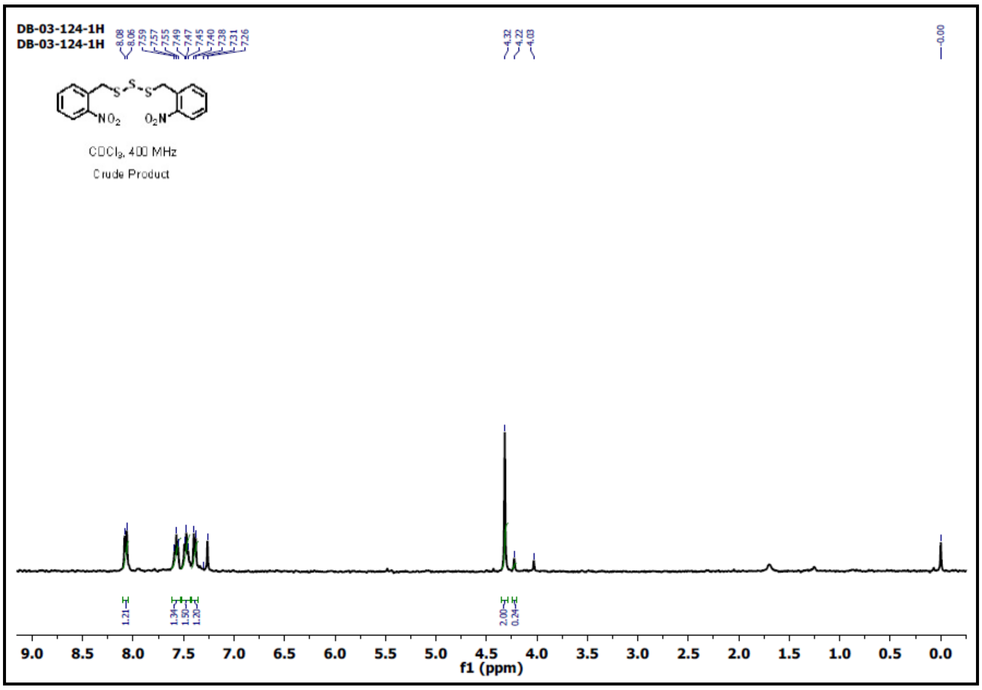

Figure S27: ^{1}H- NMR ($CDCl_3$, 400 MHz, ppm) spectrum of crude (before purification) compound **3m**.

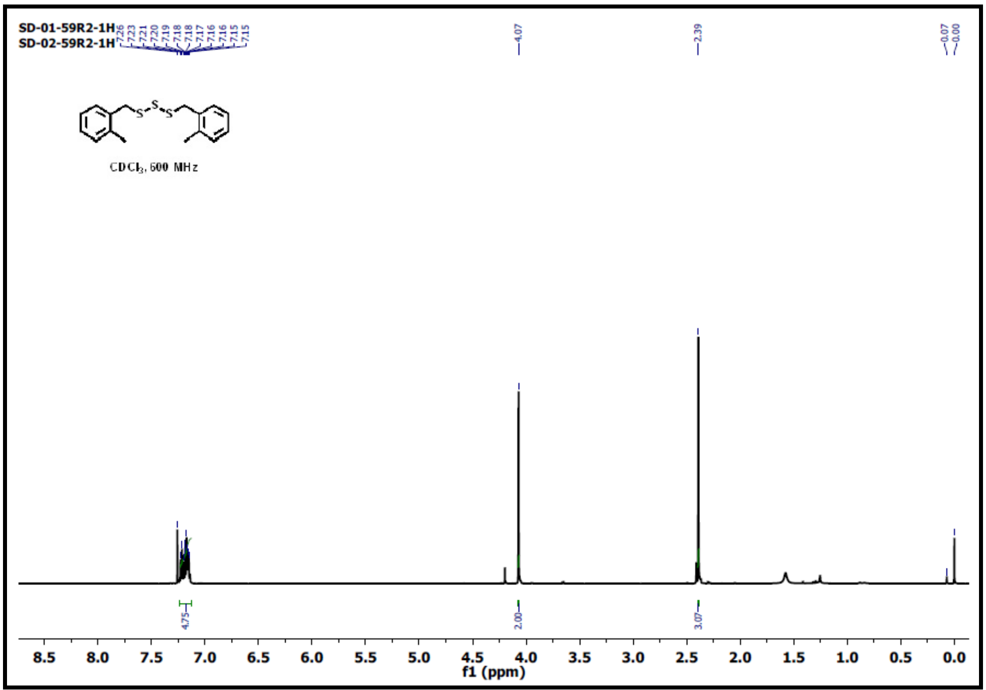

Figure S28: ^{1}H- NMR ($CDCl_3$, 600 MHz, ppm) spectrum of compound **3n**.

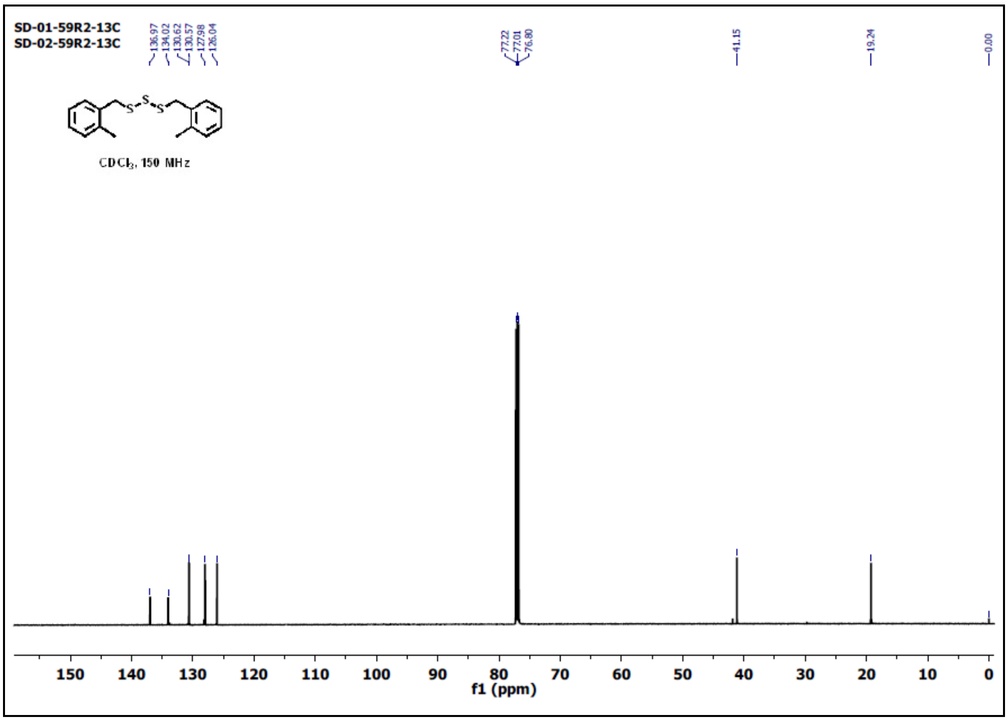

Figure S29: ^{13}C- NMR (CDCl$_3$, 150 MHz, ppm) spectrum of compound **3n**.

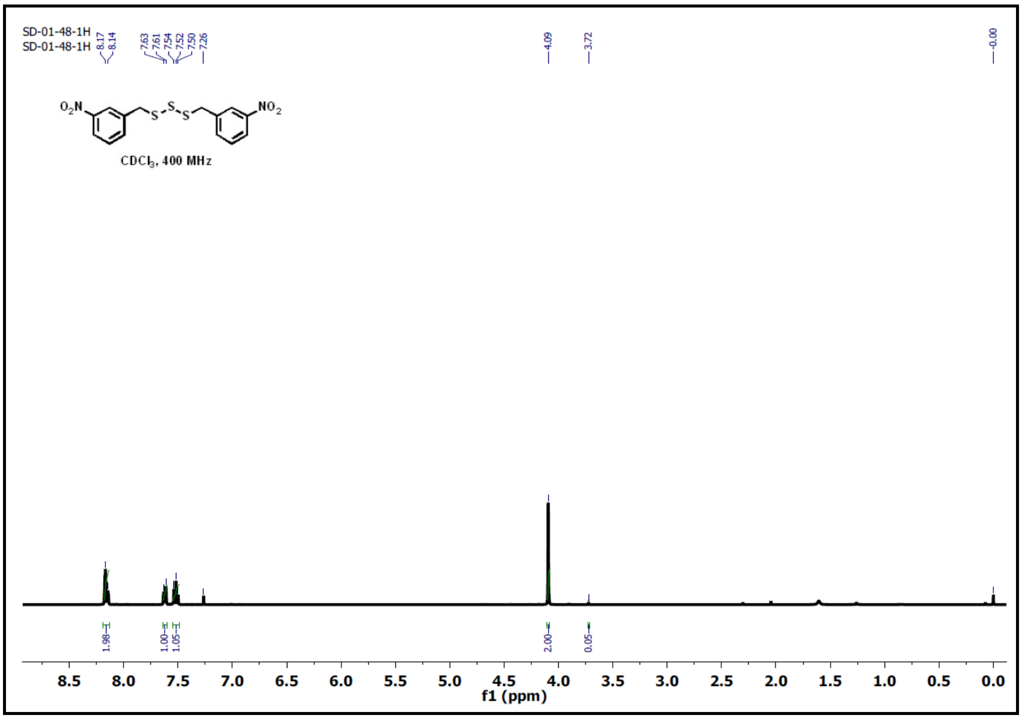

Figure S30: ^{1}H- NMR (CDCl$_3$, 400 MHz, ppm) spectrum of compound **3o**.

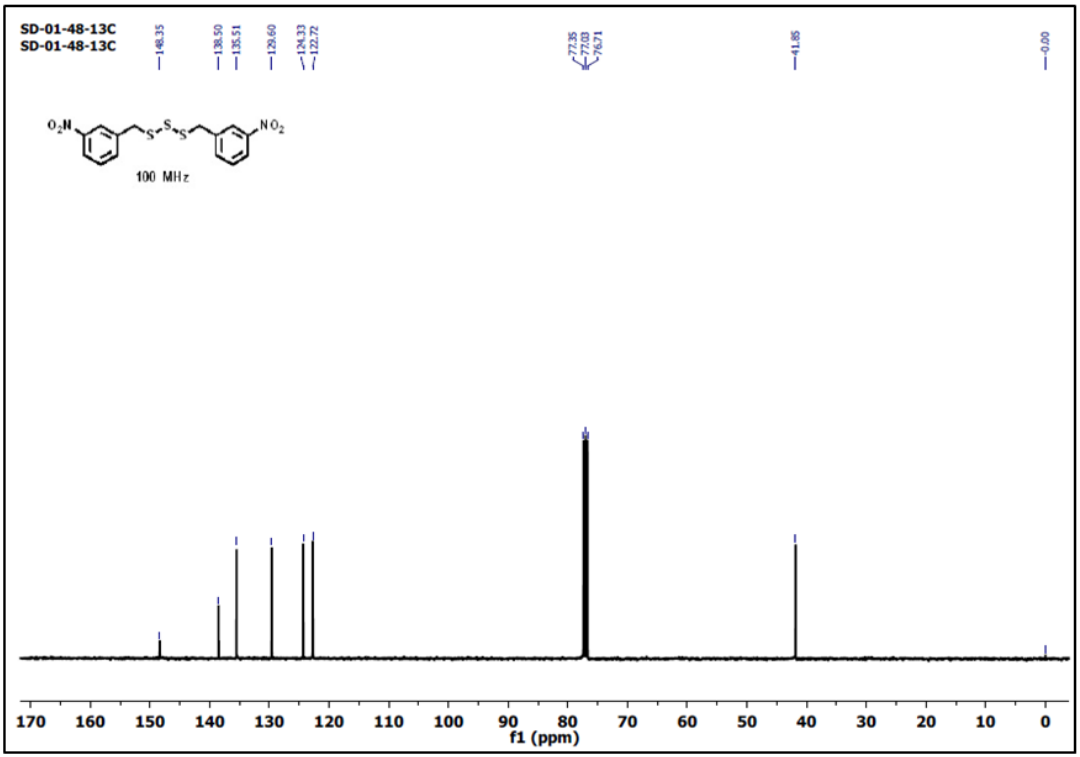

Figure S31: ^{13}C- NMR ($CDCl_3$, 100 MHz, ppm) spectrum of compound **3o**.

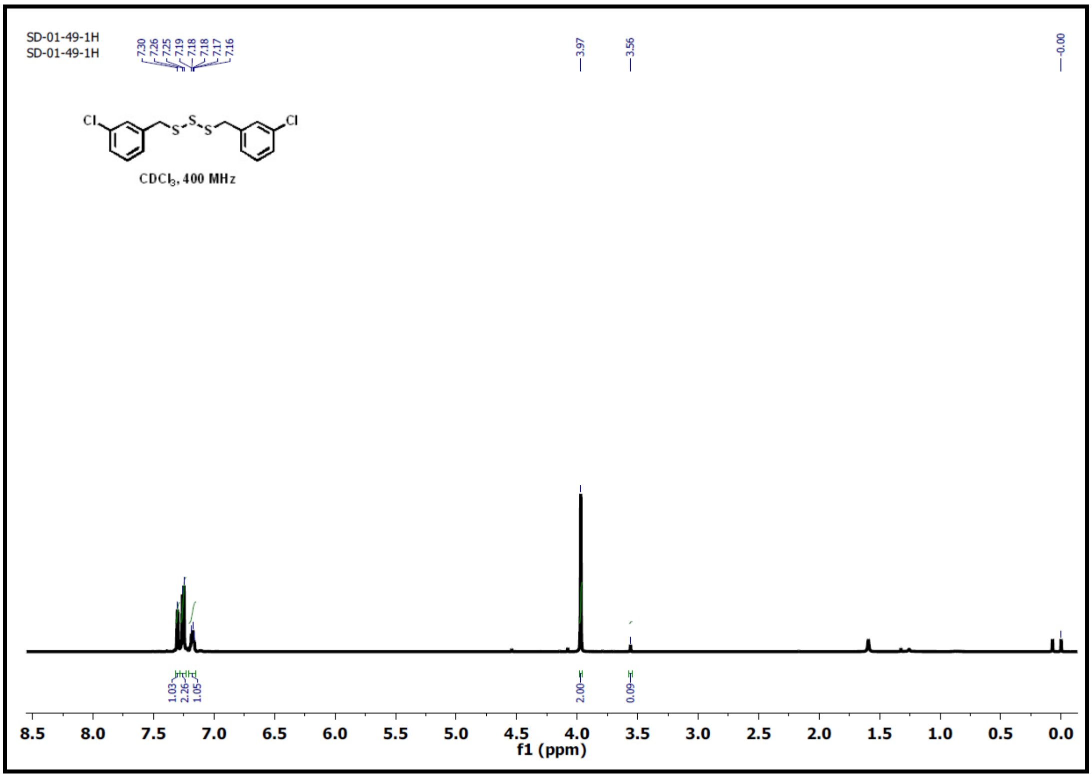

Figure S32: ^{1}H- NMR ($CDCl_3$, 400 MHz, ppm) spectrum of compound **3p**.

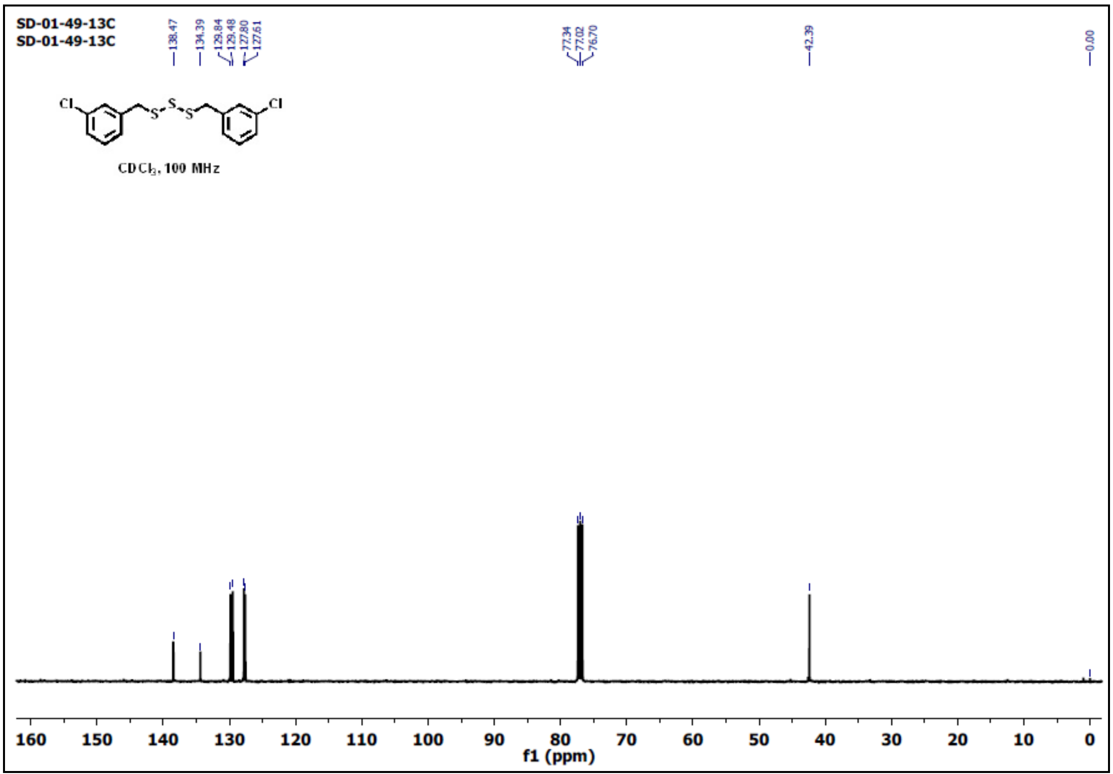

Figure S33: ^{13}C- NMR (CDCl$_3$, 100 MHz, ppm) spectrum of compound **3p**.

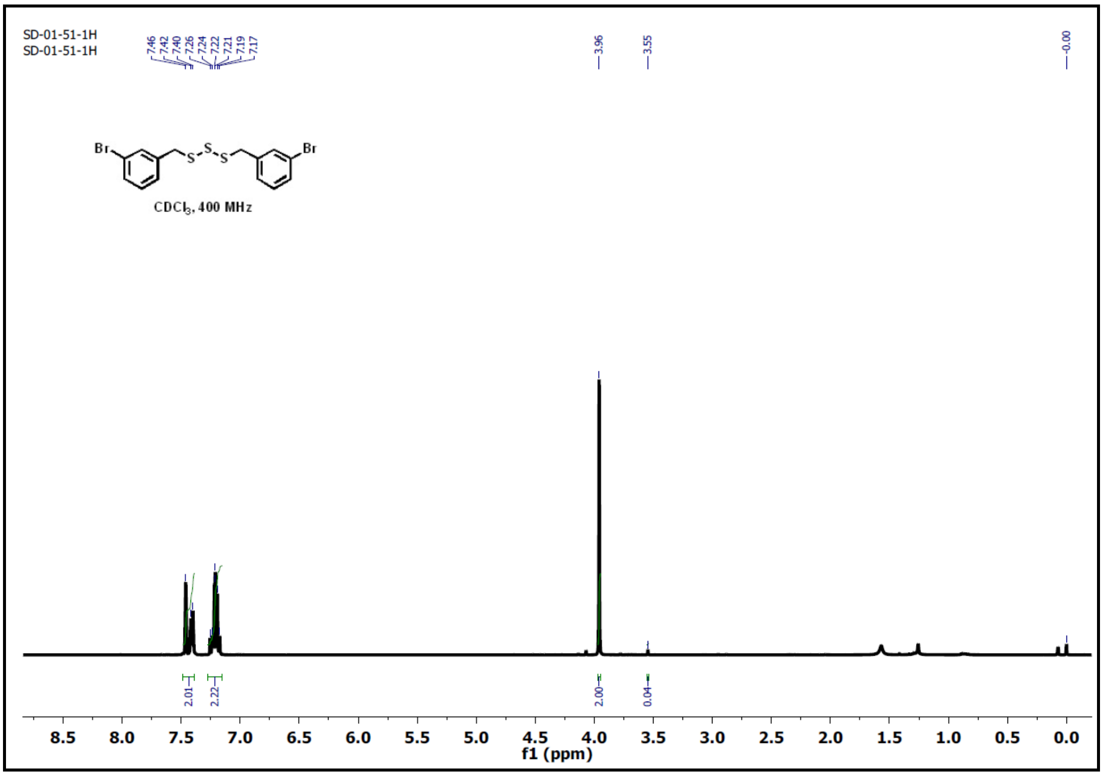

Figure S34: ^{1}H- NMR (CDCl$_3$, 400 MHz, ppm) spectrum of compound **3q**.

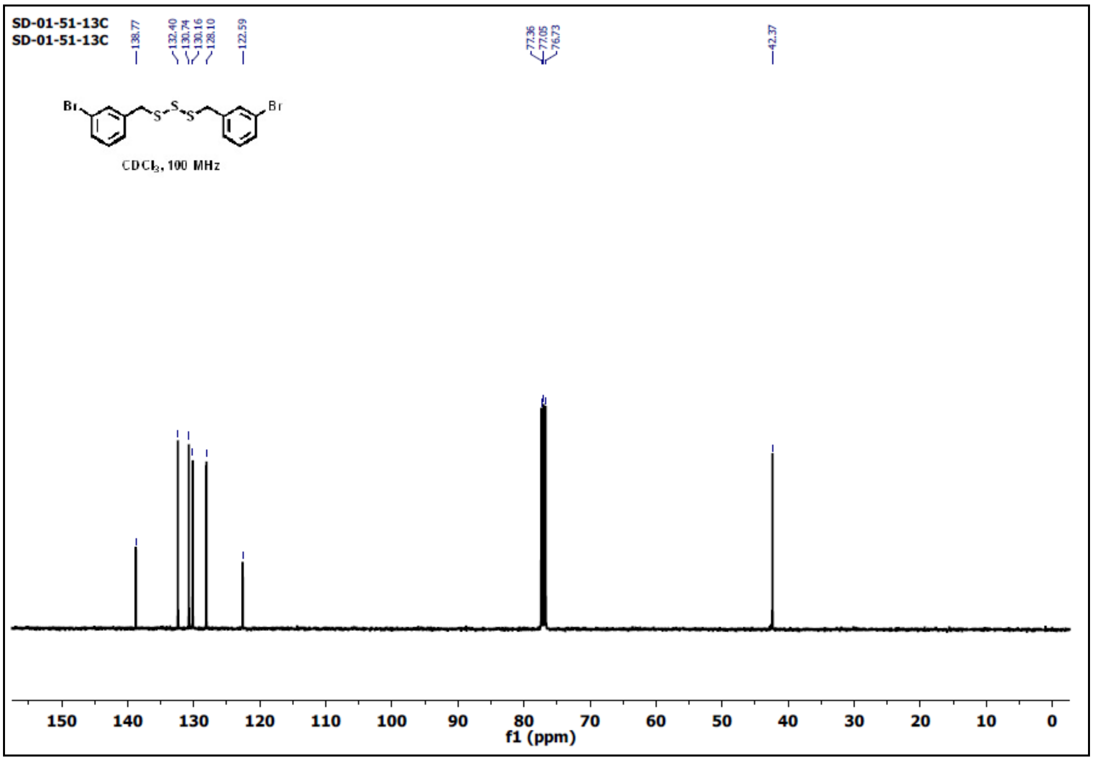

Figure S35: ^{13}C- NMR (CDCl$_3$, 100 MHz, ppm) spectrum of compound **3q**.

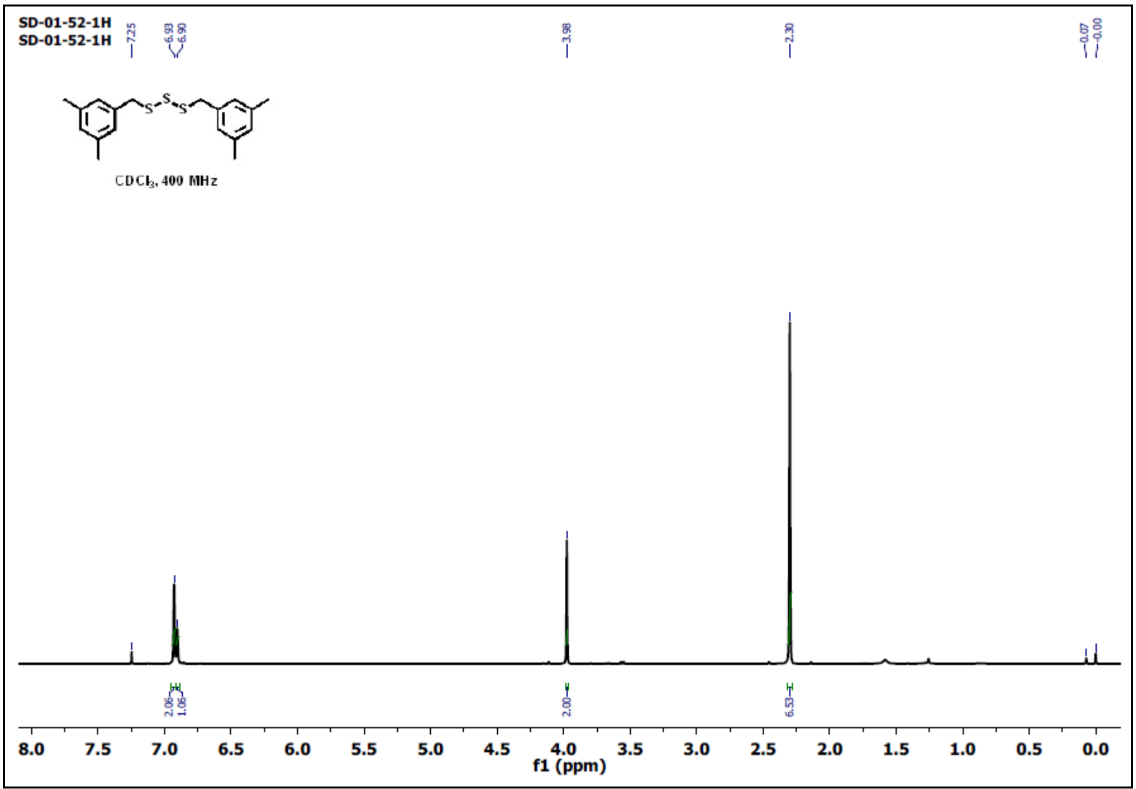

Figure S36: ^{1}H- NMR (CDCl$_3$, 400 MHz, ppm) spectrum of compound **3r**.

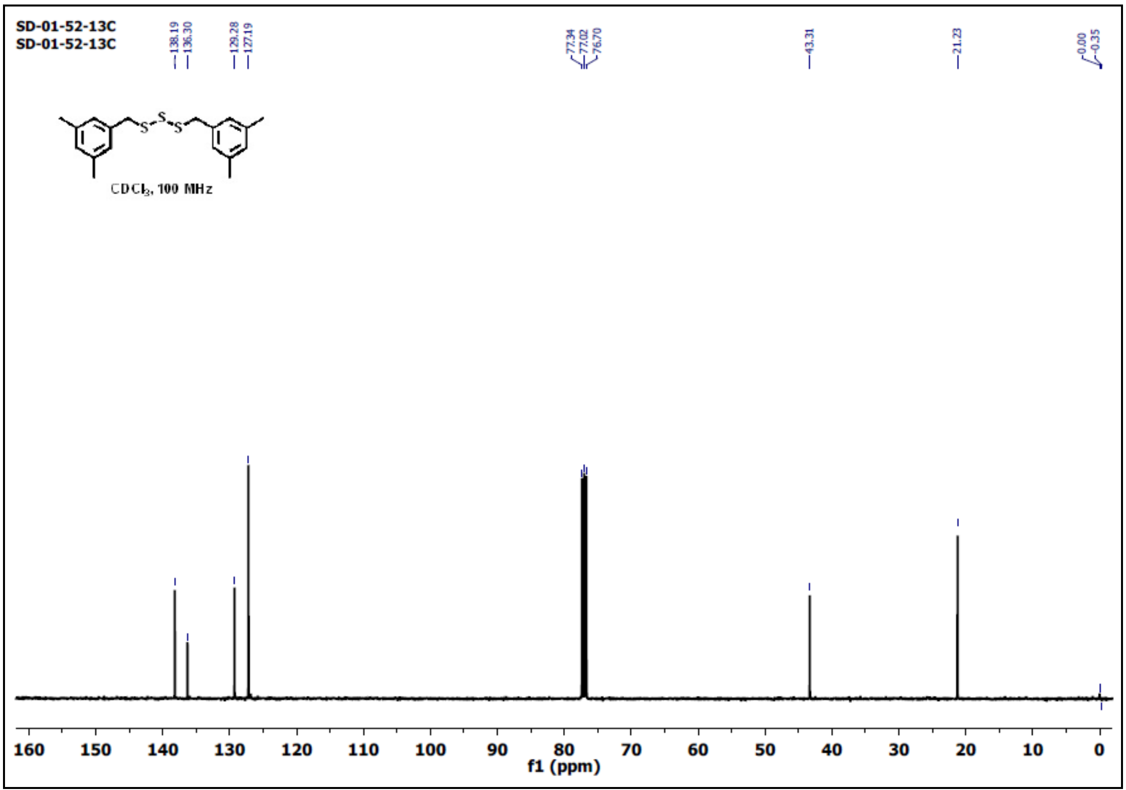

Figure S37: ^{13}C- NMR ($CDCl_3$, 100 MHz, ppm) spectrum of compound **3r**.

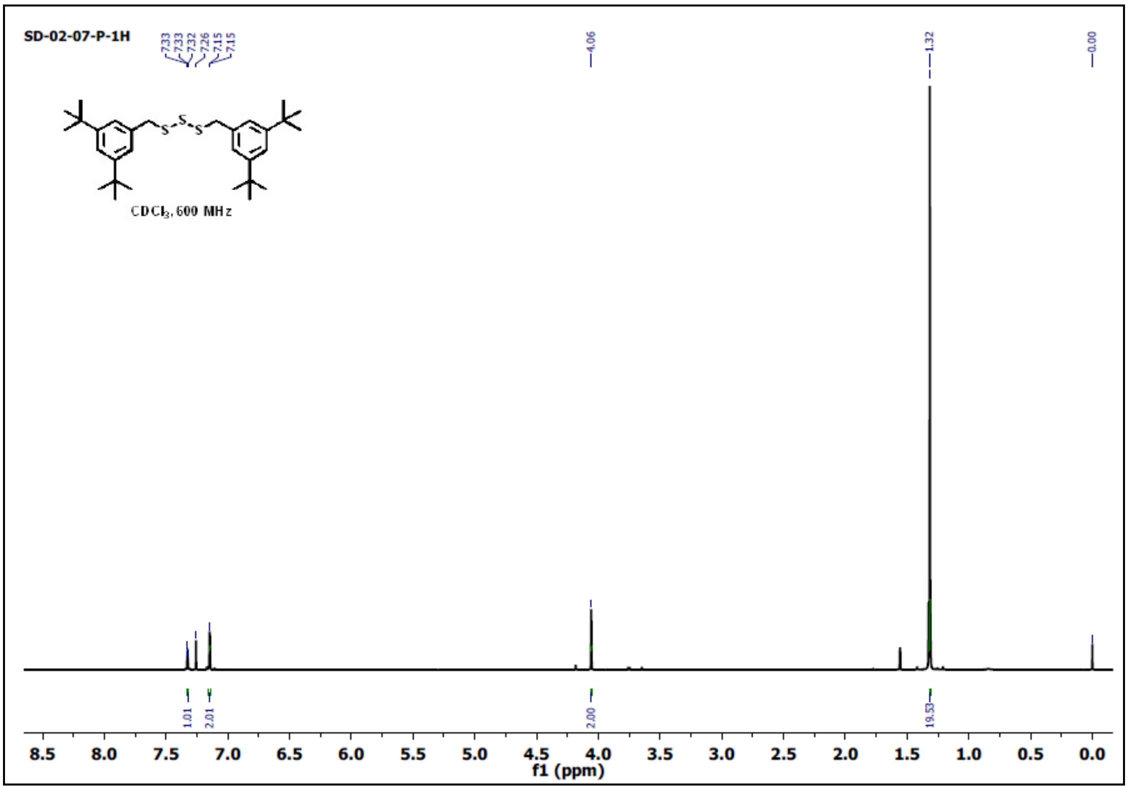

Figure S38: ^{1}H- NMR ($CDCl_3$, 600 MHz, ppm) spectrum of compound **3s**.

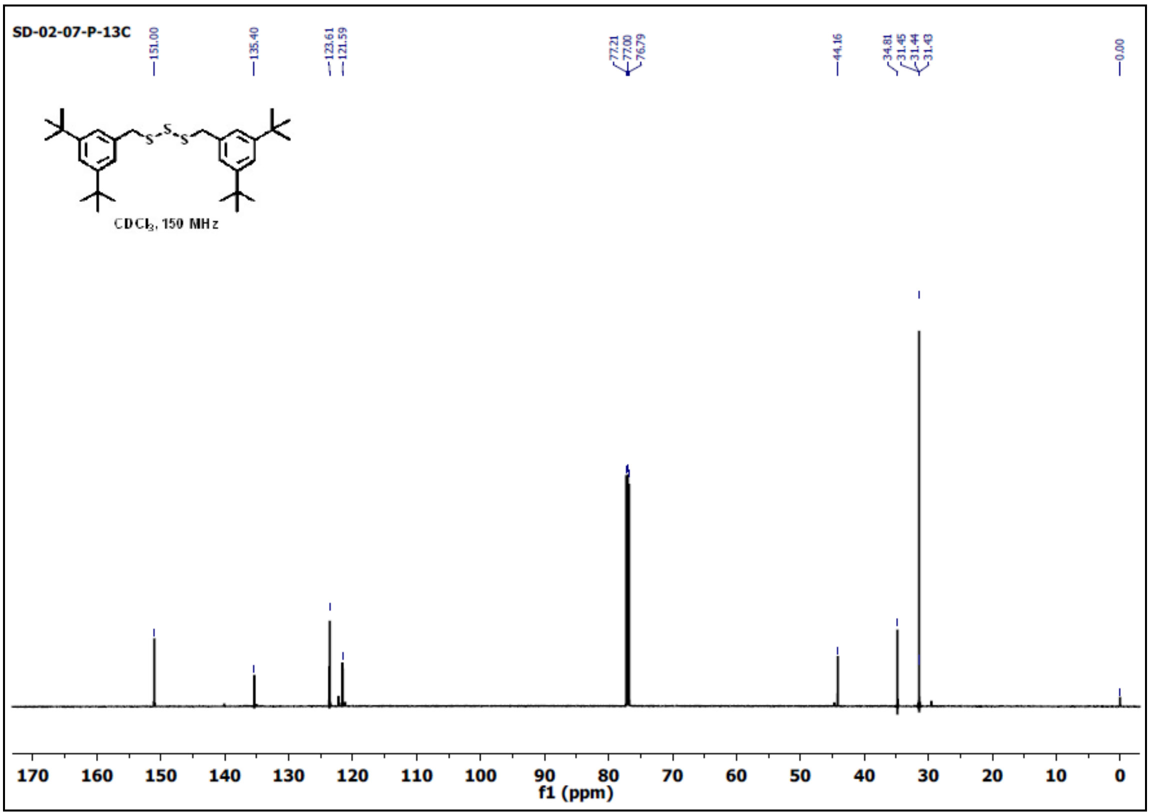

Figure S39: ^{13}C- NMR ($CDCl_3$, 150 MHz, ppm) spectrum of compound **3s**.

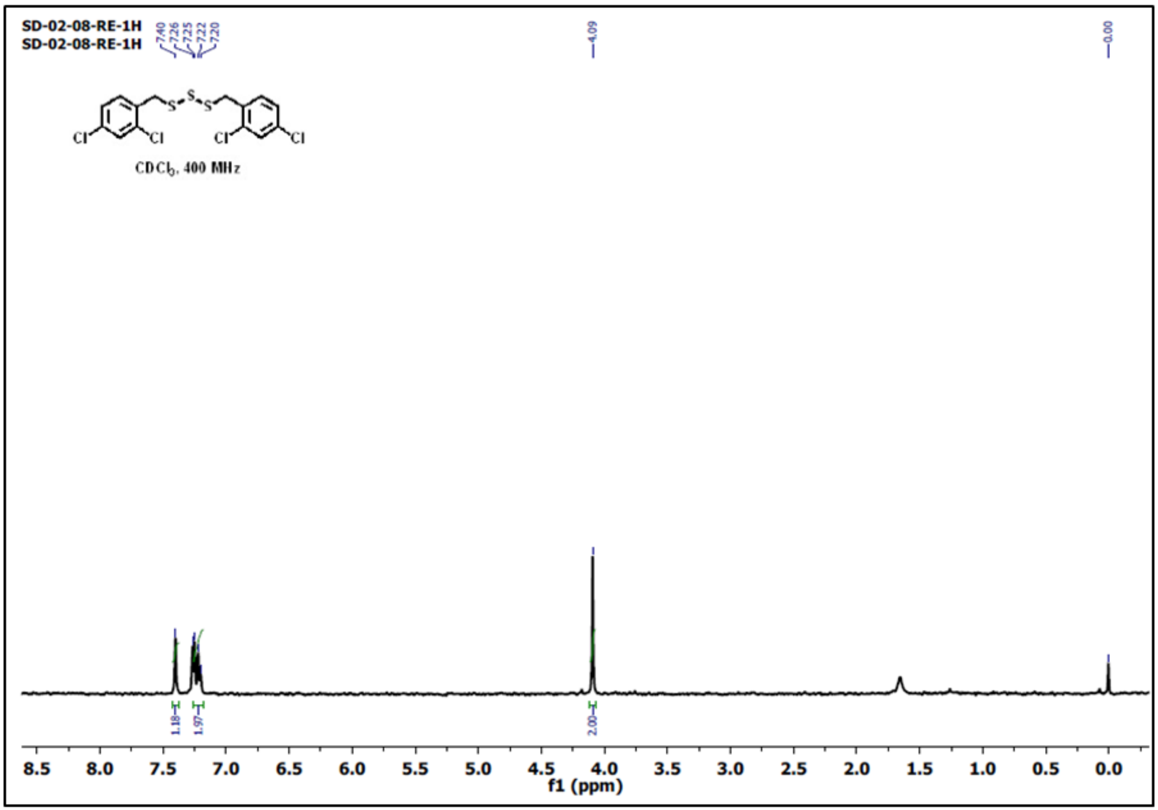

Figure S40: ^{1}H- NMR ($CDCl_3$, 400 MHz, ppm) spectrum of compound **3t**.

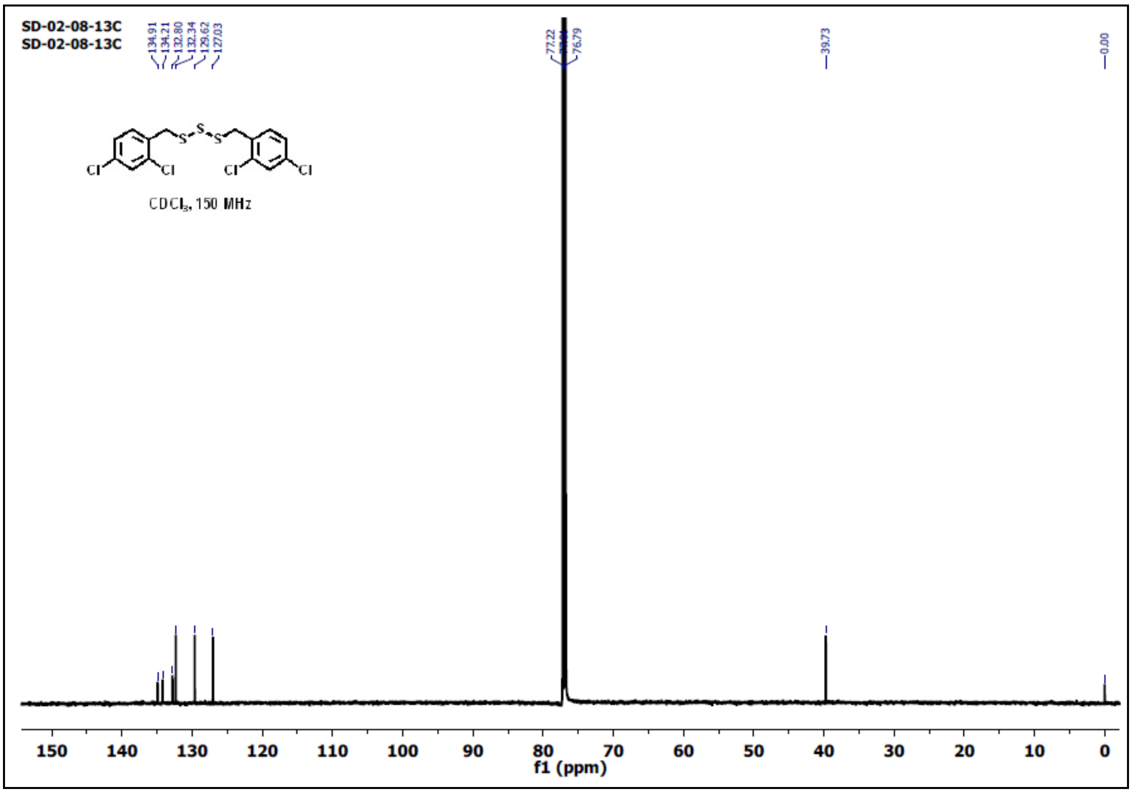

Figure S41: ^{13}C- NMR ($CDCl_3$, 150 MHz, ppm) spectrum of compound **3t**.

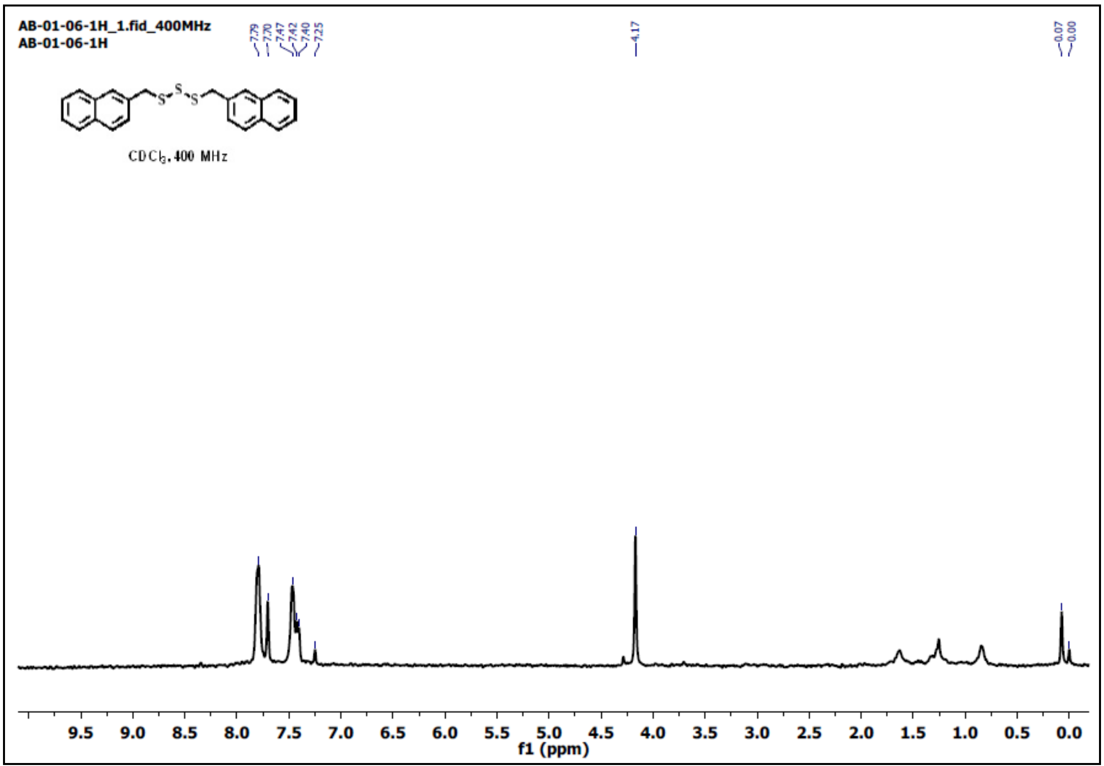

Figure S42: ^{1}H- NMR ($CDCl_3$, 400 MHz, ppm) spectrum of compound **3u**.

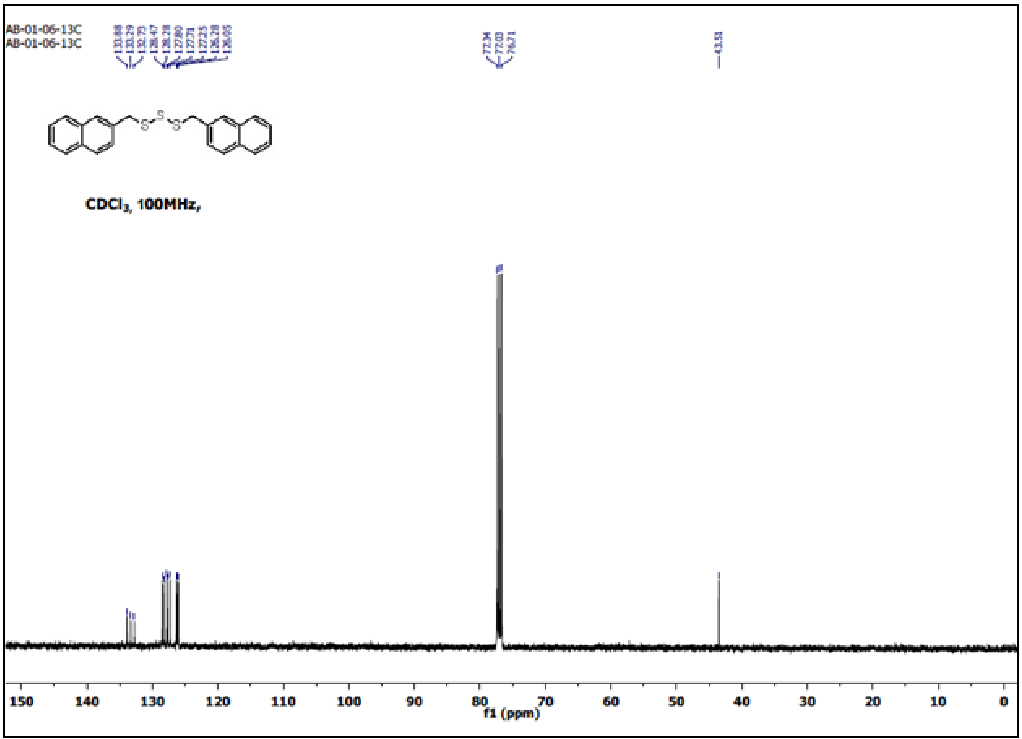

Figure S43: ^{13}C-NMR ($CDCl_3$, 100 MHz, ppm) spectrum of compound **3u**.

NMR spectra of disulfides

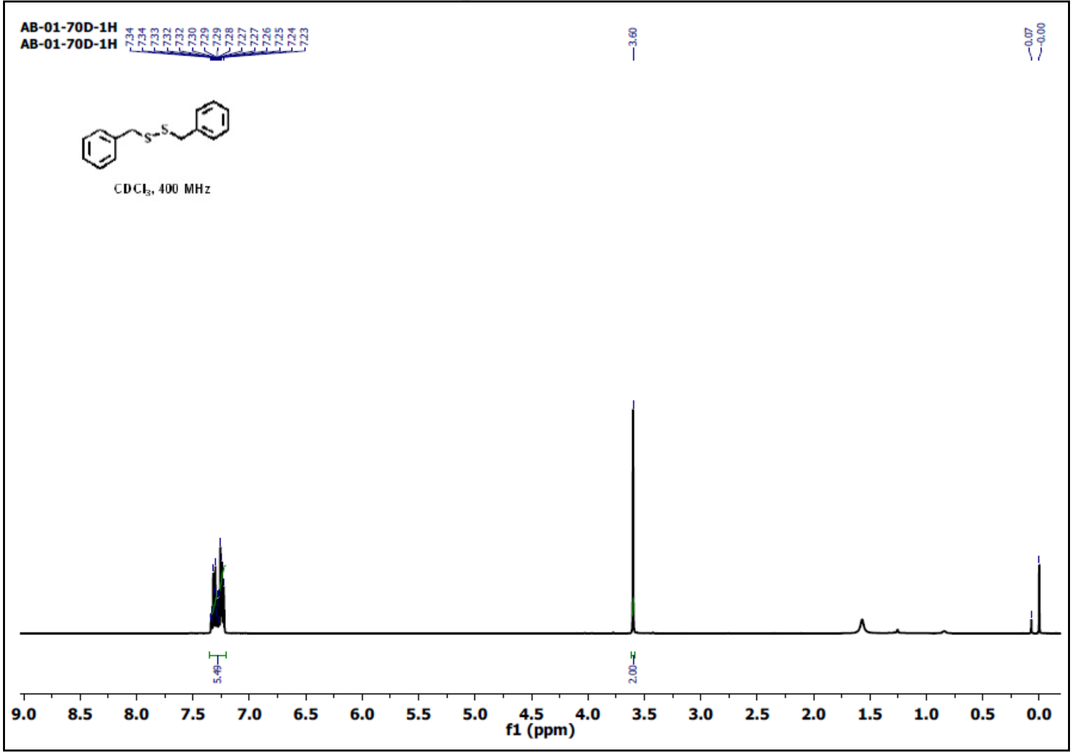

Figure S44: ^{1}H- NMR ($CDCl_3$, 400 MHz, ppm) spectrum of compound **4a**.

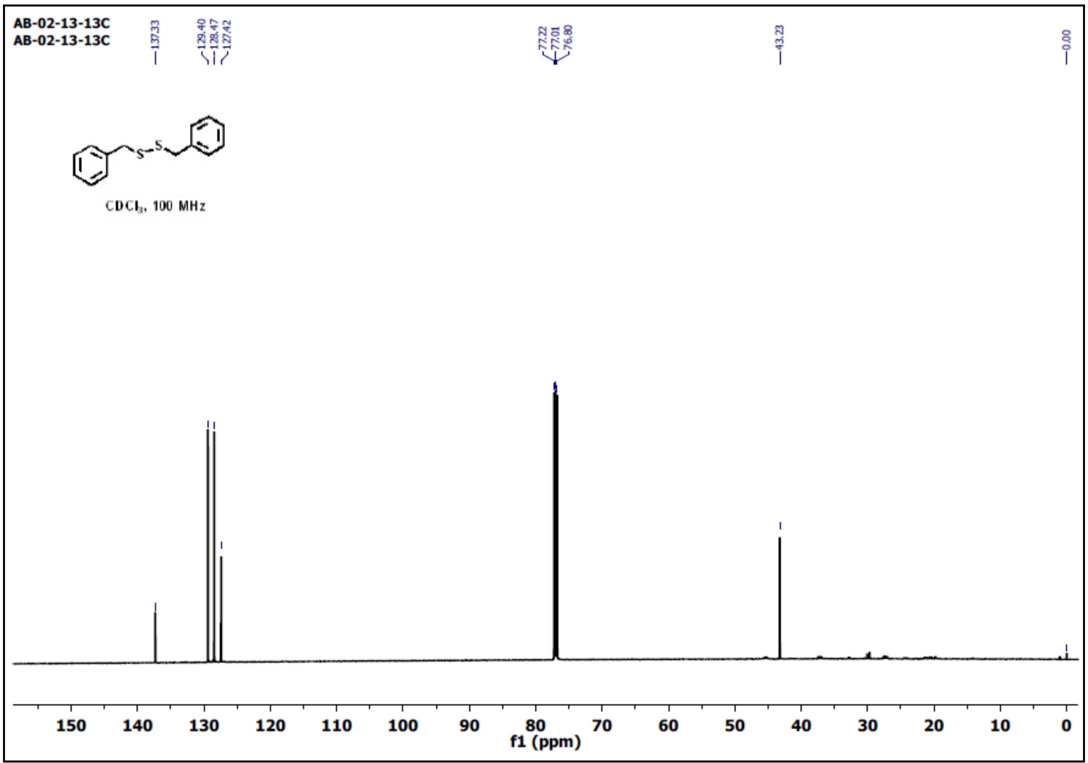

Figure S45: ^{13}C- NMR (CDCl$_3$, 100 MHz, ppm) spectrum of compound **4a**.

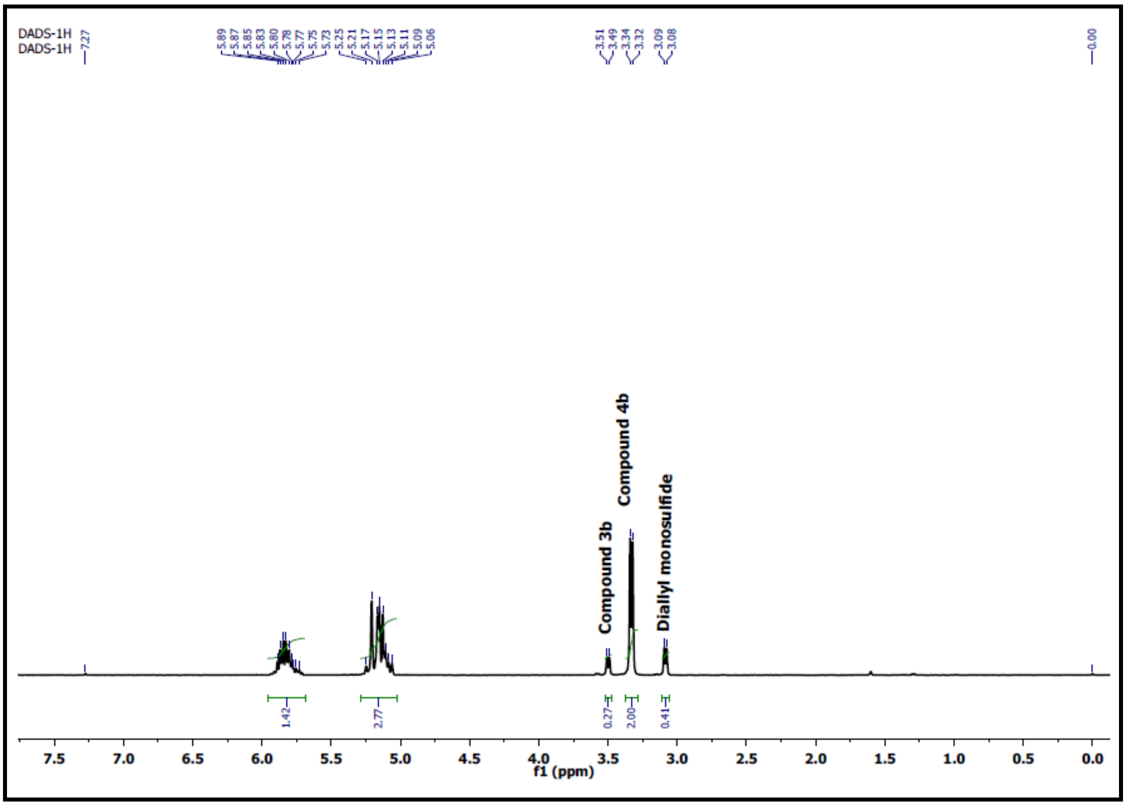

Figure S46: ^{1}H- NMR (CDCl$_3$, 400 MHz, ppm) spectrum of compound **4b**. Here the corresponding monosulfide (Diallyl monosulfide) and compound **3b** was found to be the predominant product.

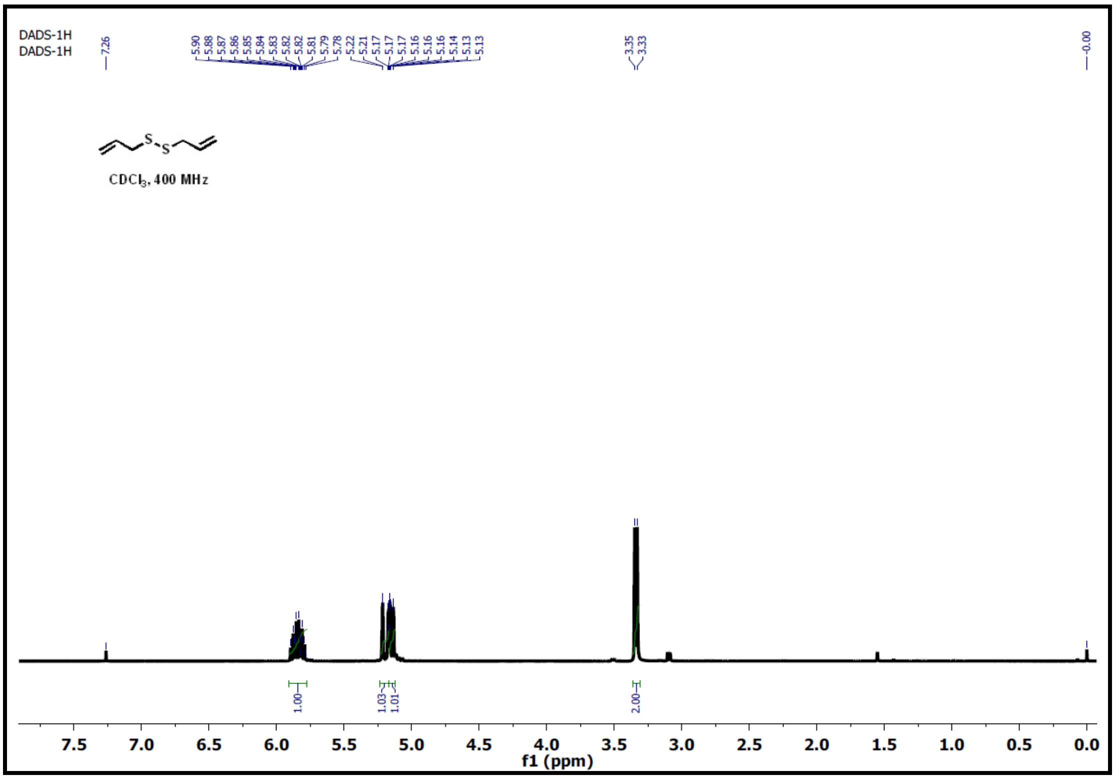

Figure S47: ^{1}H- NMR ($CDCl_3$, 400 MHz, ppm) spectrum of compound **4b** upon the addition of 5 equiv of Na_2SO_3 into the reaction.

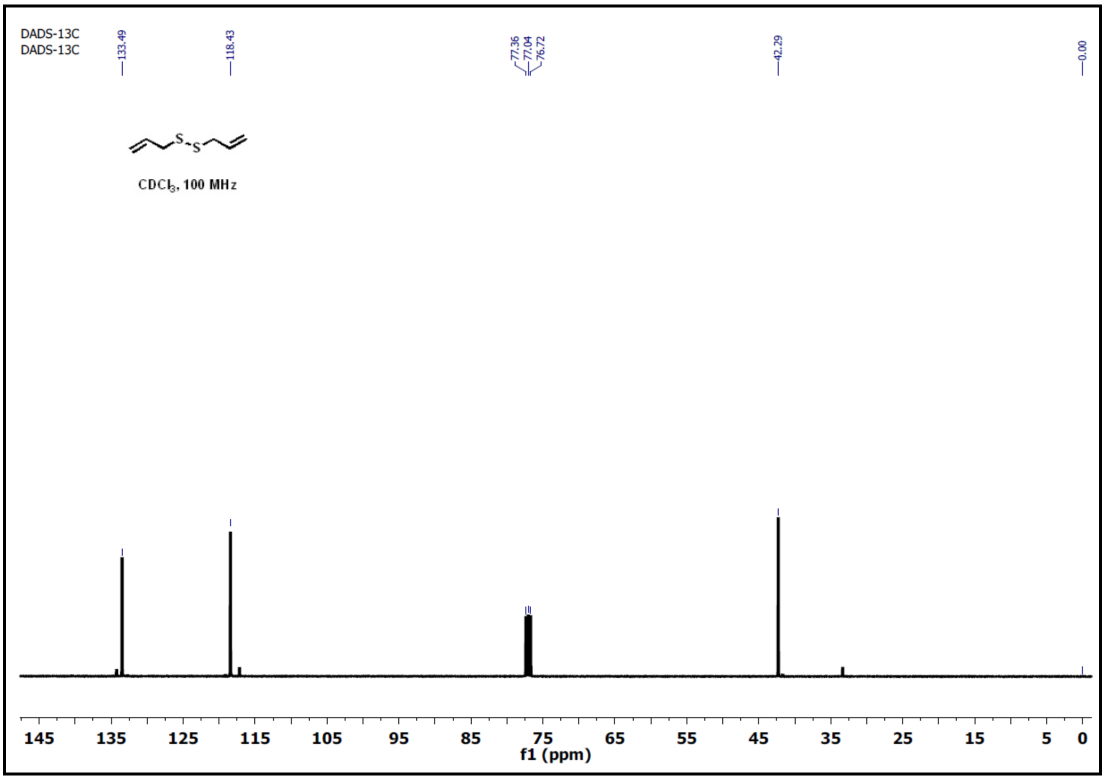

Figure S48: ^{13}C- NMR ($CDCl_3$, 100 MHz, ppm) spectrum of compound **4b** upon the addition of 5 equiv of Na_2SO_3 into the reaction.

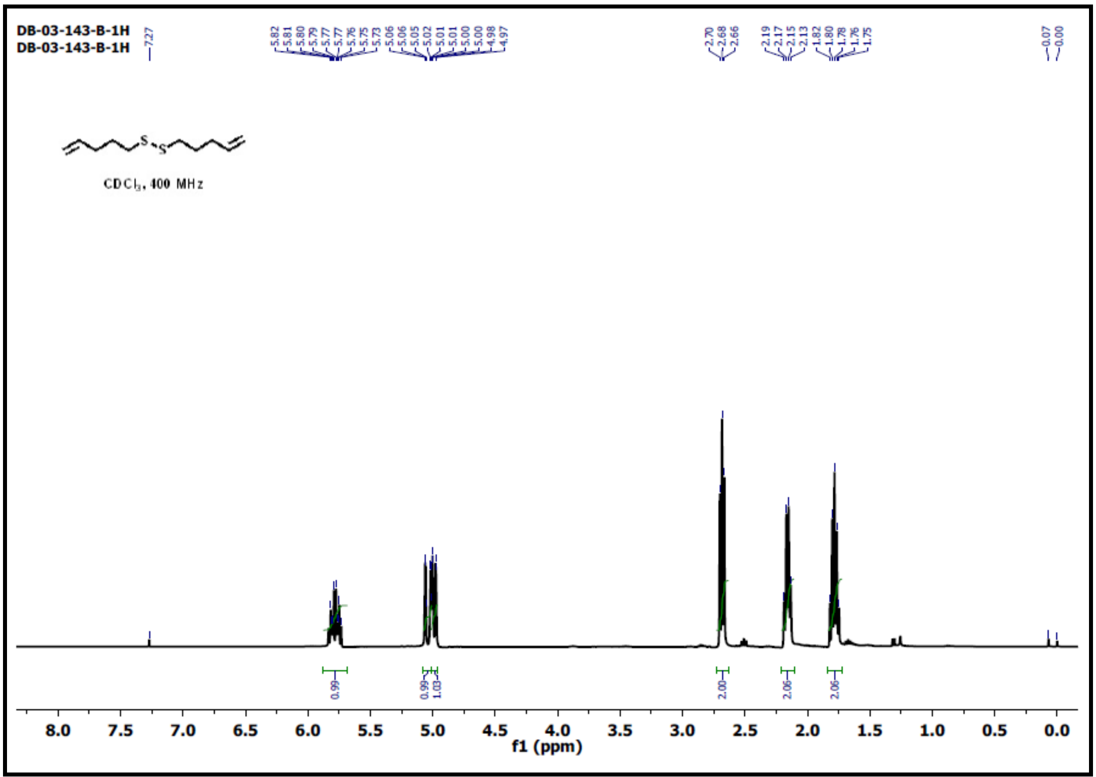

Figure S49: ^{1}H- NMR ($CDCl_3$, 400 MHz, ppm) spectrum of compound **4c**.

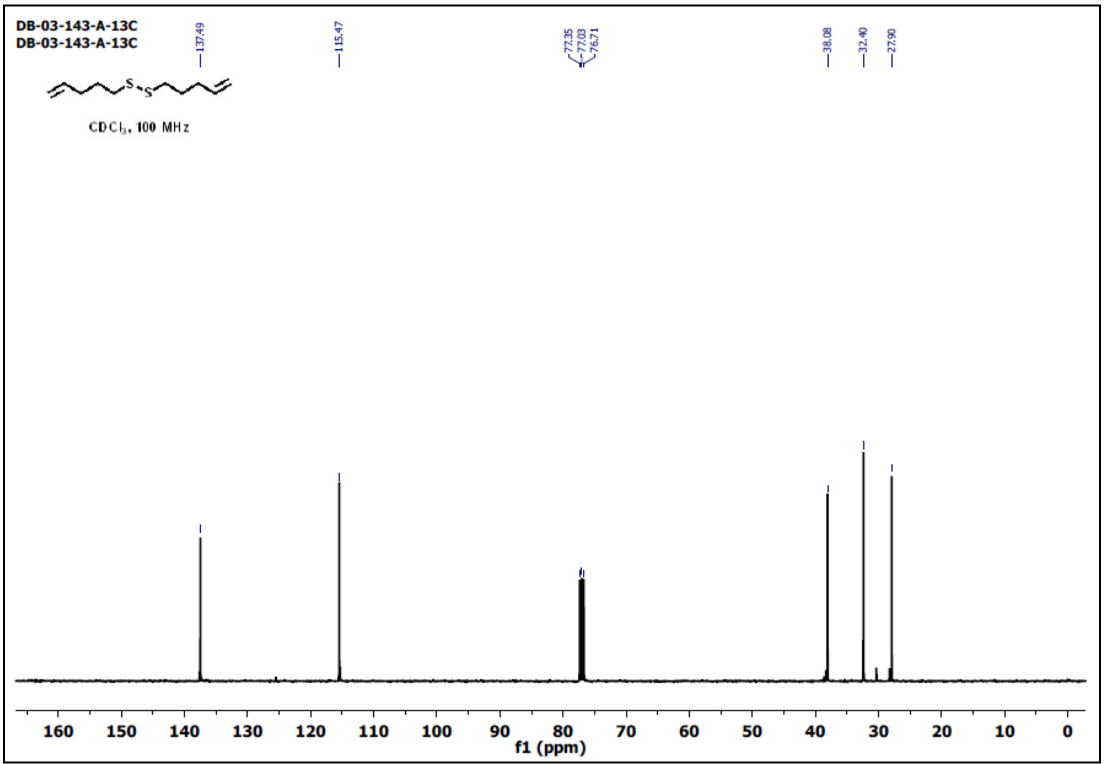

Figure S50: ^{13}C- NMR ($CDCl_3$, 100 MHz, ppm) spectrum of compound **4c**.

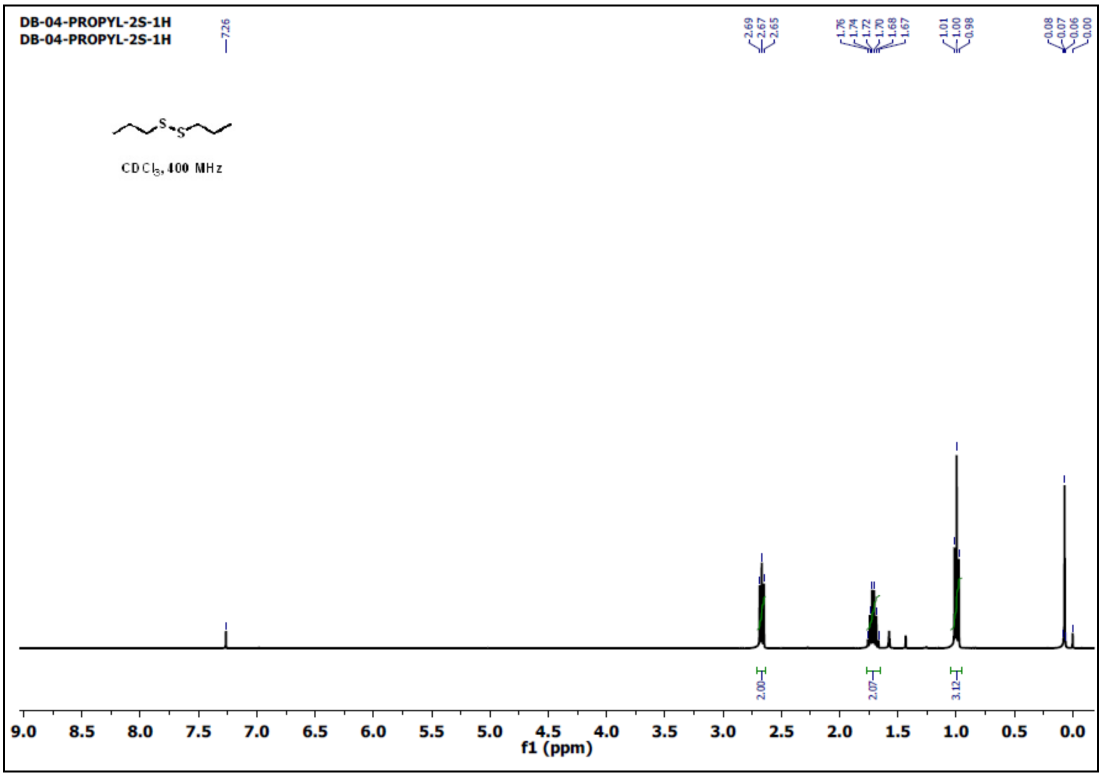

Figure S51: ^{1}H- NMR ($CDCl_3$, 400 MHz, ppm) spectrum of compound **4d.**

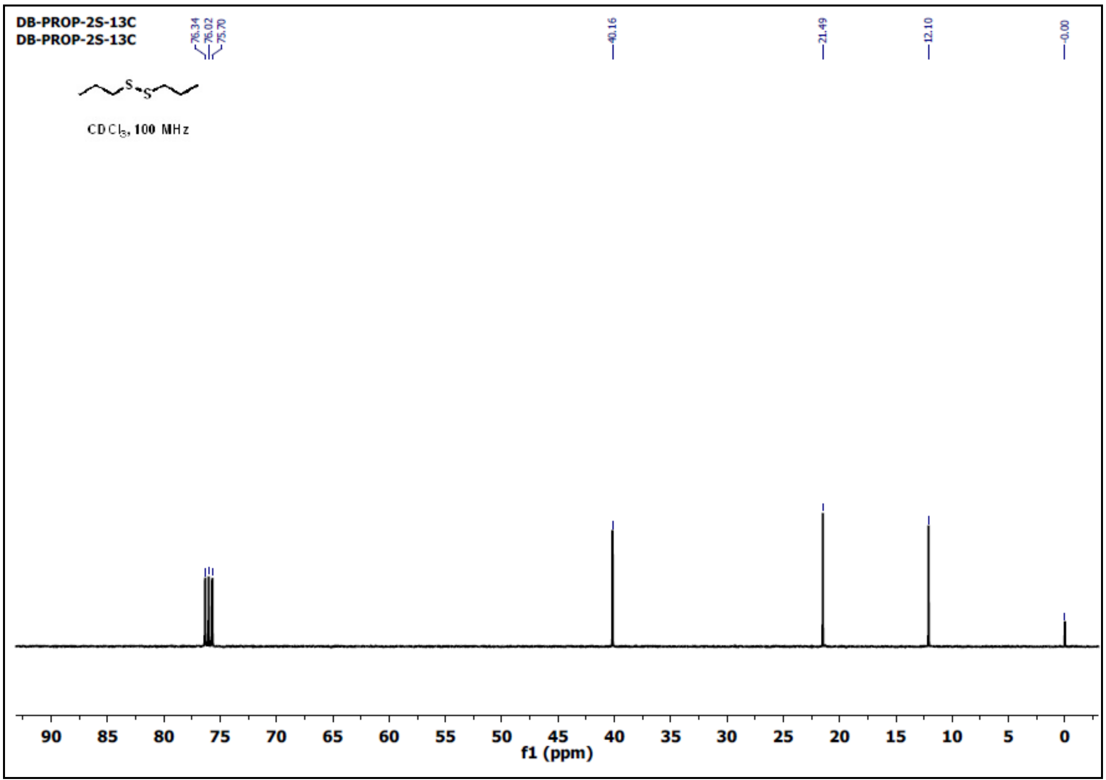

Figure S52: ^{13}C-NMR ($CDCl_3$, 100 MHz, ppm) spectrum of compound **4d**.

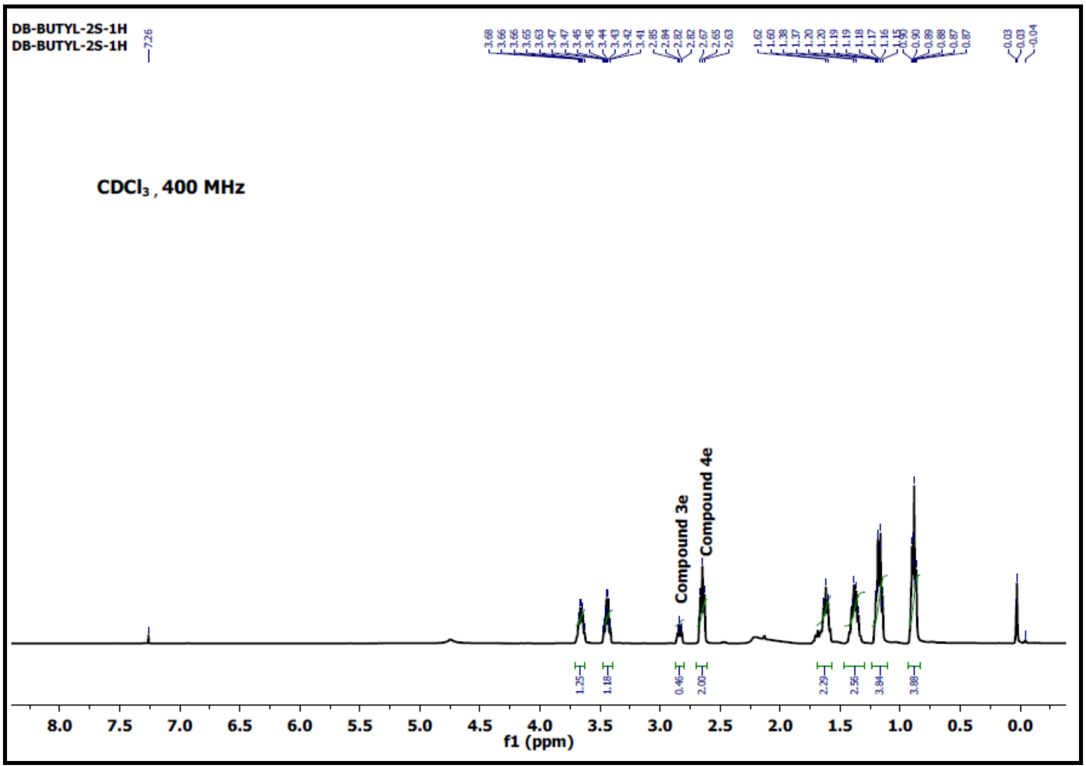

Figure S53: ^{1}H- NMR (CDCl$_3$, 400 MHz, ppm) spectrum of compound **4e**. Here the corresponding trisulfide **3e** and other polysulfides were found to be present.

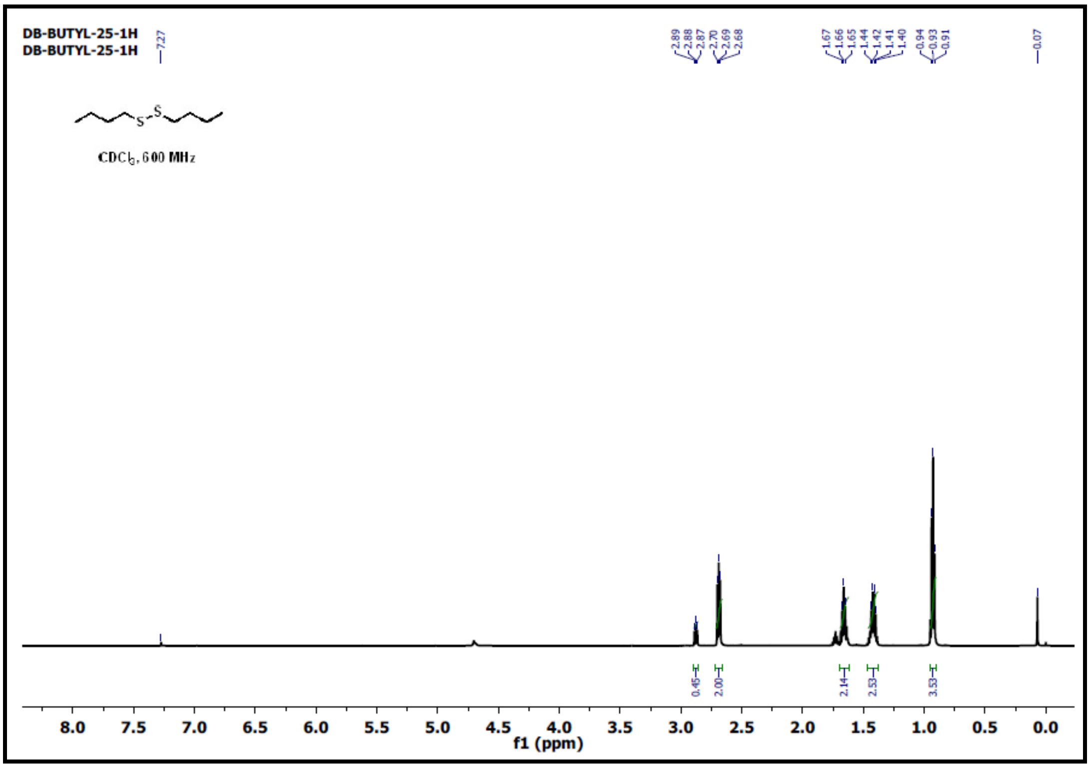

Figure S54: ^{1}H- NMR (CDCl$_3$, 600 MHz, ppm) spectrum of compound **4e** upon the addition of 5 equiv of Na$_2$SO$_3$ into the reaction.

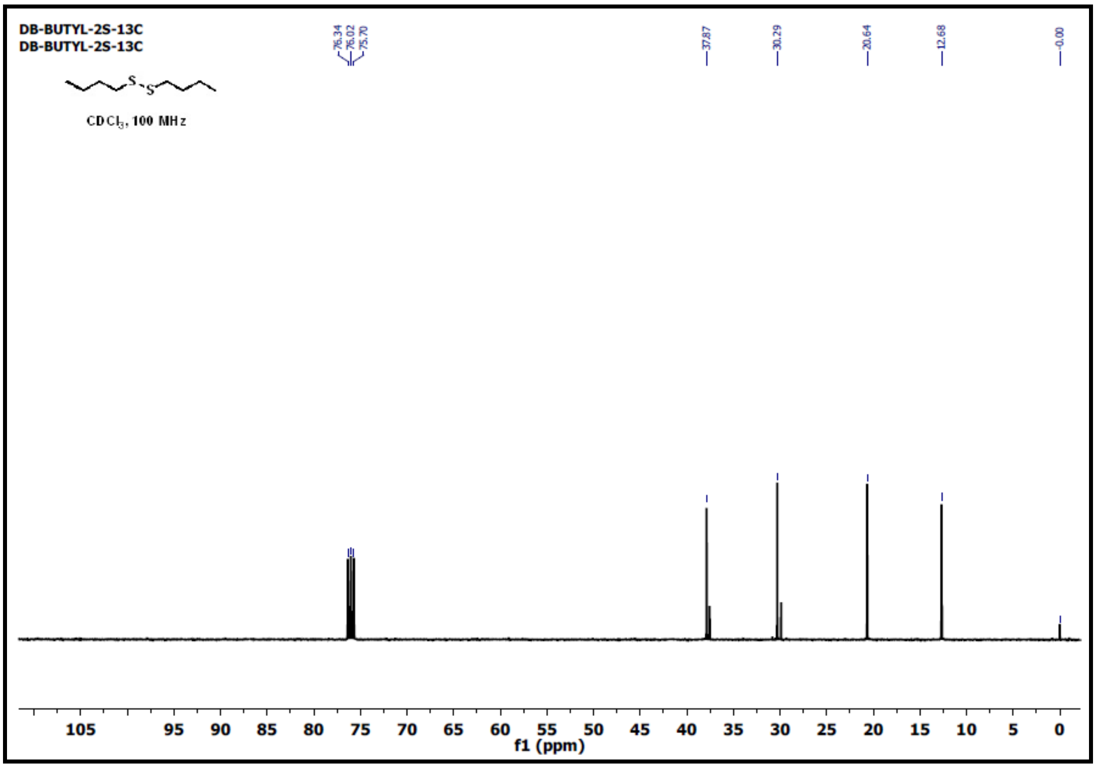

Figure S55: ^{13}C- NMR ($CDCl_3$, 100 MHz, ppm) spectrum of compound **4e** upon the addition of 5 equiv of Na_2SO_3 into the reaction.

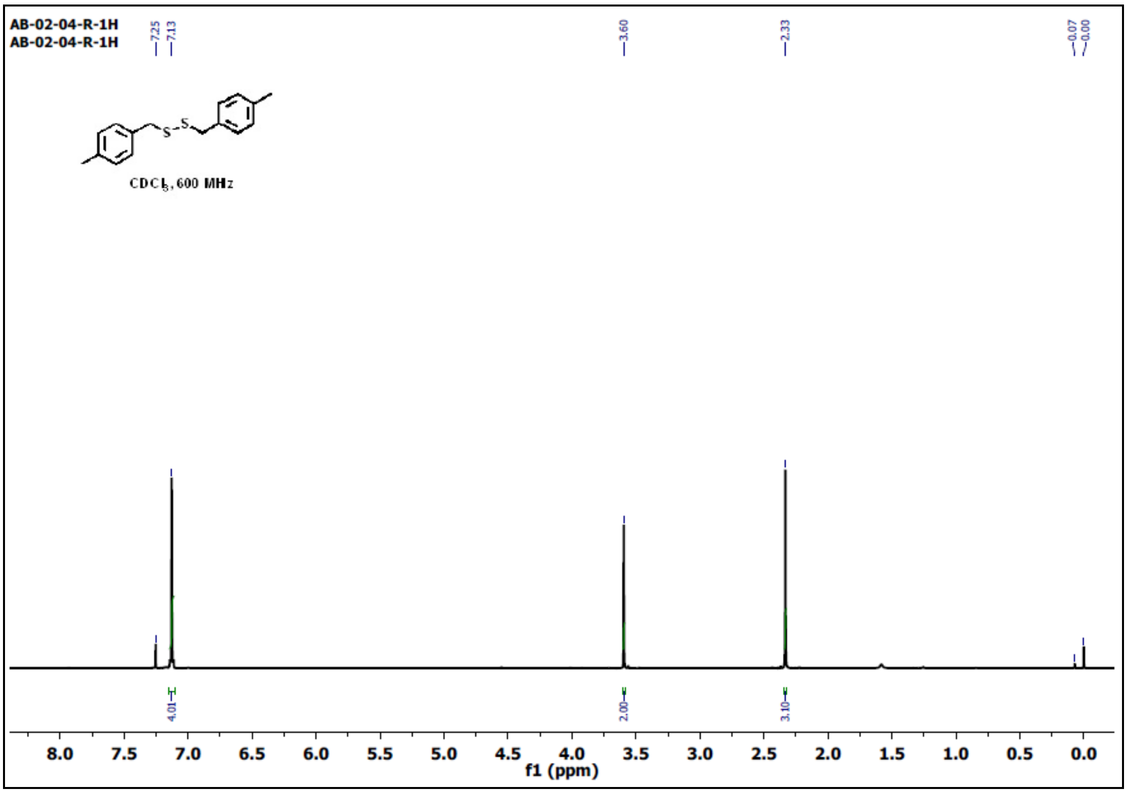

Figure S56: ^{1}H- NMR ($CDCl_3$, 600 MHz, ppm) spectrum of compound **4f**.

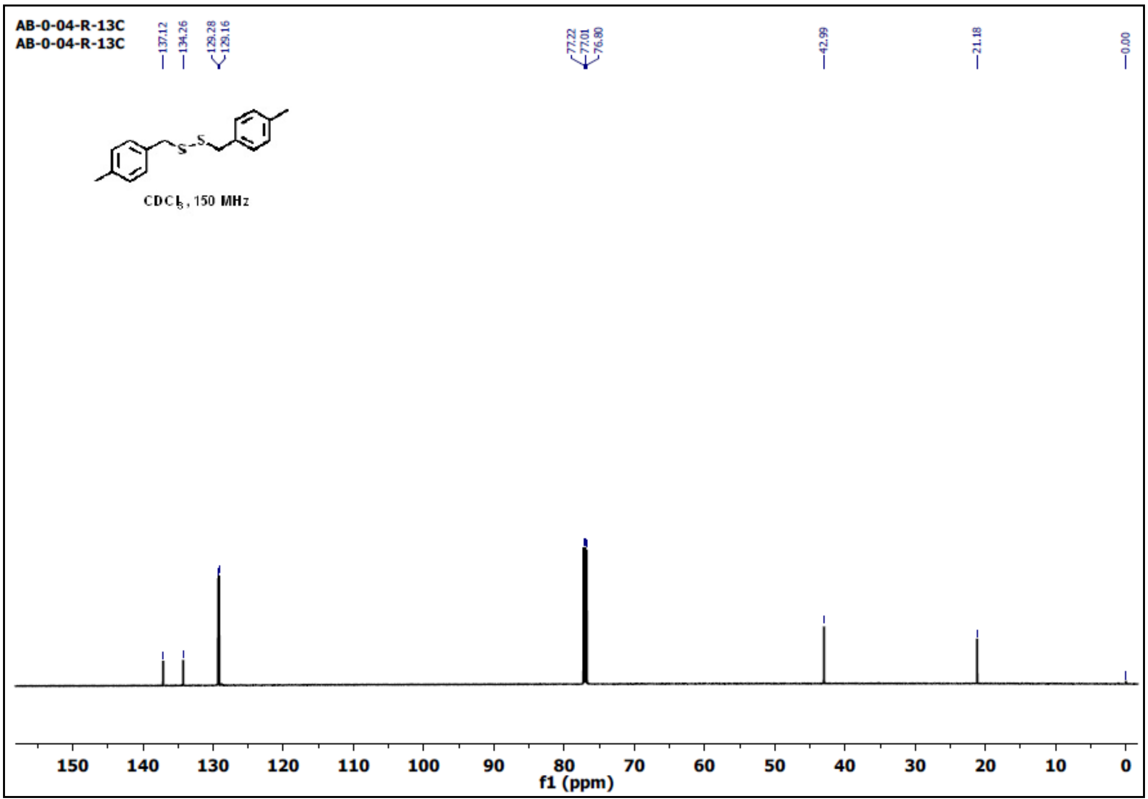

Figure S57: ^{13}C-NMR (CDCl$_3$, 150 MHz, ppm) spectrum of compound **4f**.

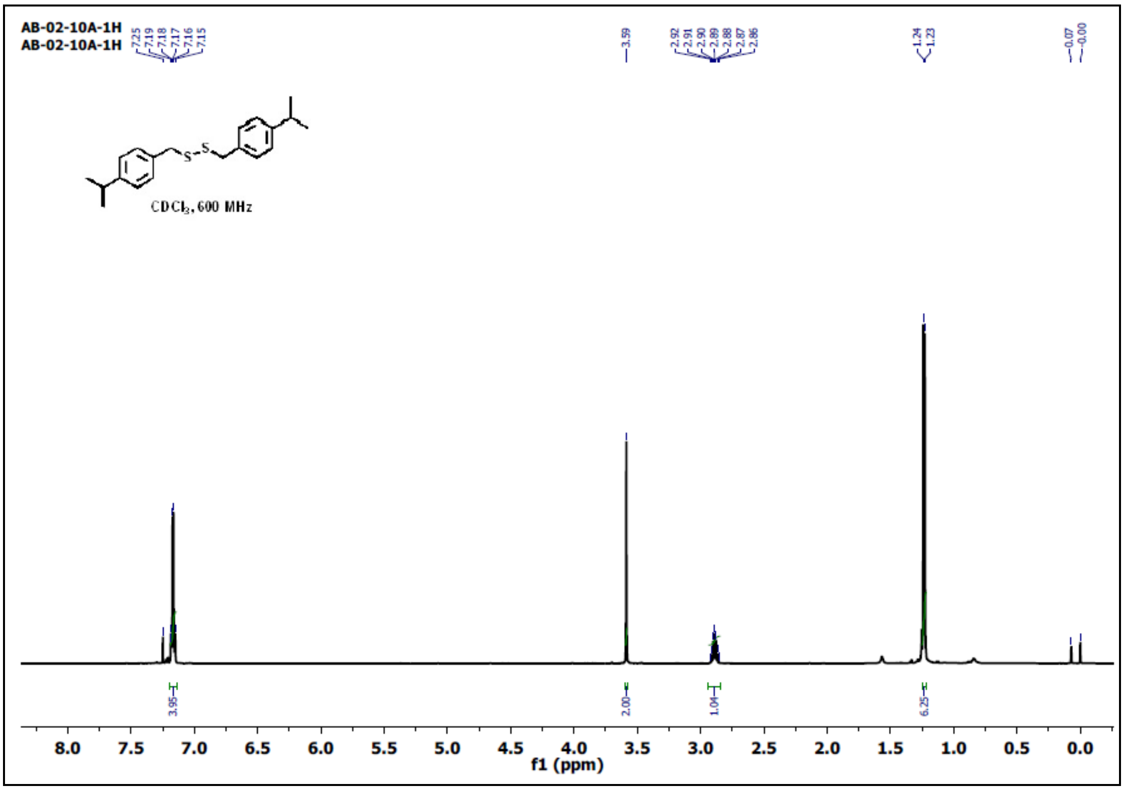

Figure S58: ^{1}H- NMR (CDCl$_3$, 600 MHz, ppm) spectrum of compound **4g**.

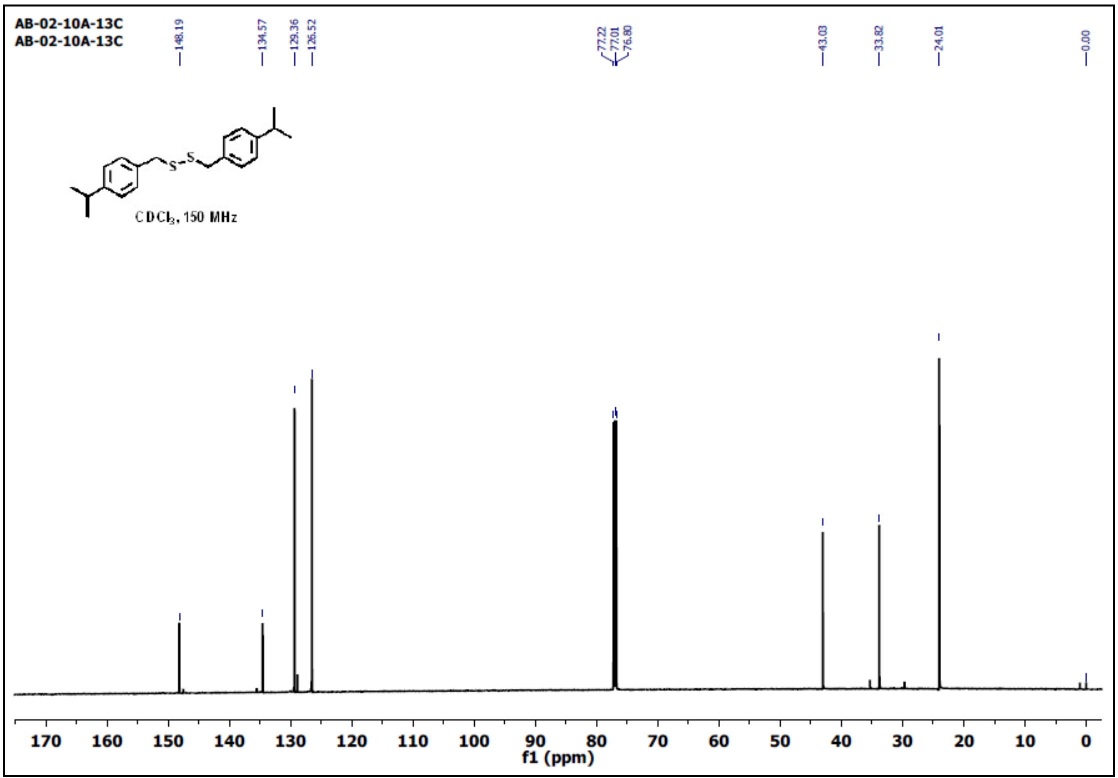

Figure S59: ^{13}C- NMR ($CDCl_3$, 150 MHz, ppm) spectrum of compound **4g**.

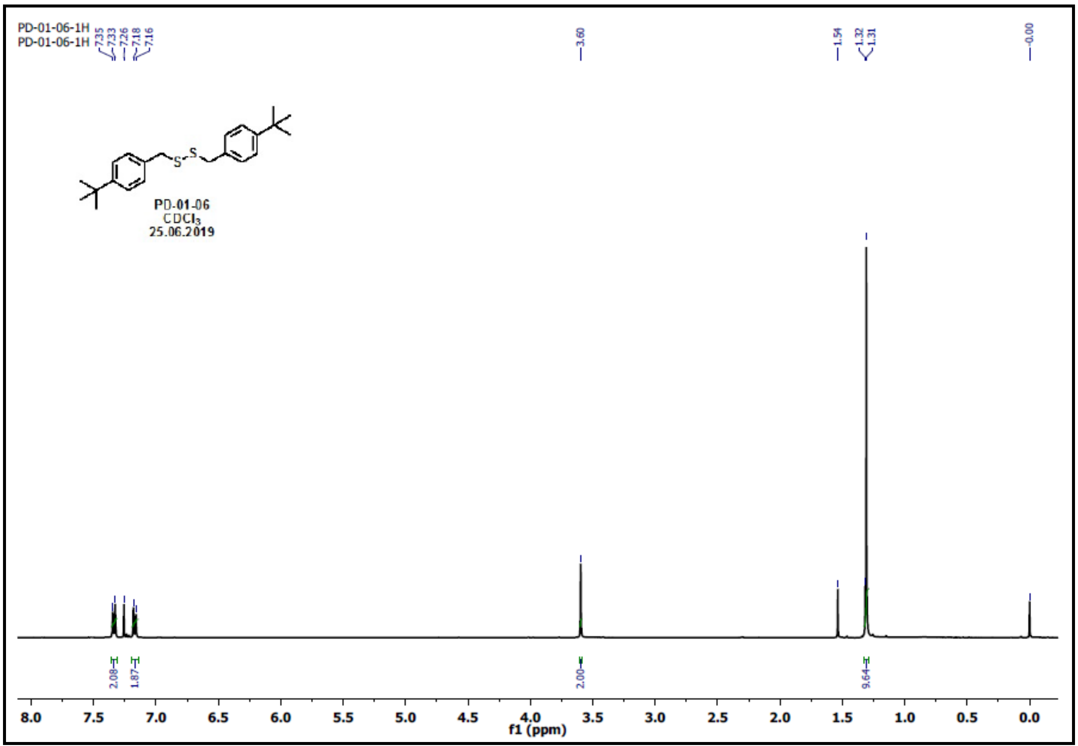

Figure S60: ^{1}H- NMR ($CDCl_3$, 400 MHz, ppm) spectrum of compound **4h**.

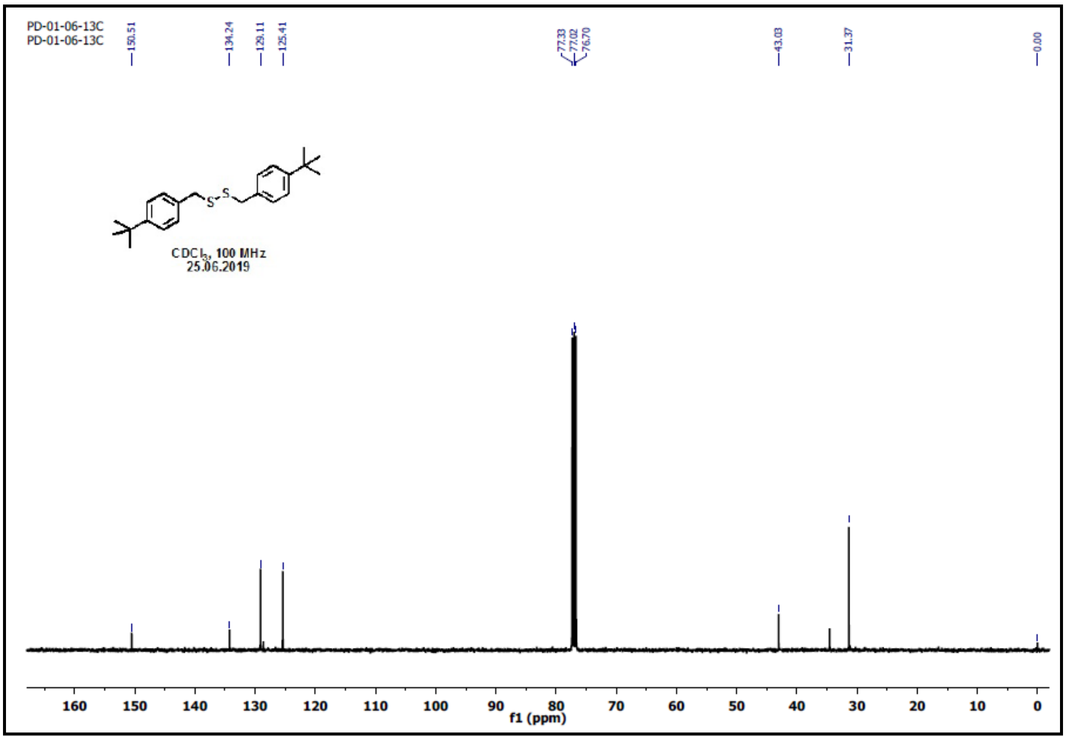

Figure S61: ^{13}C- NMR ($CDCl_3$, 100 MHz, ppm) spectrum of compound **4h**.

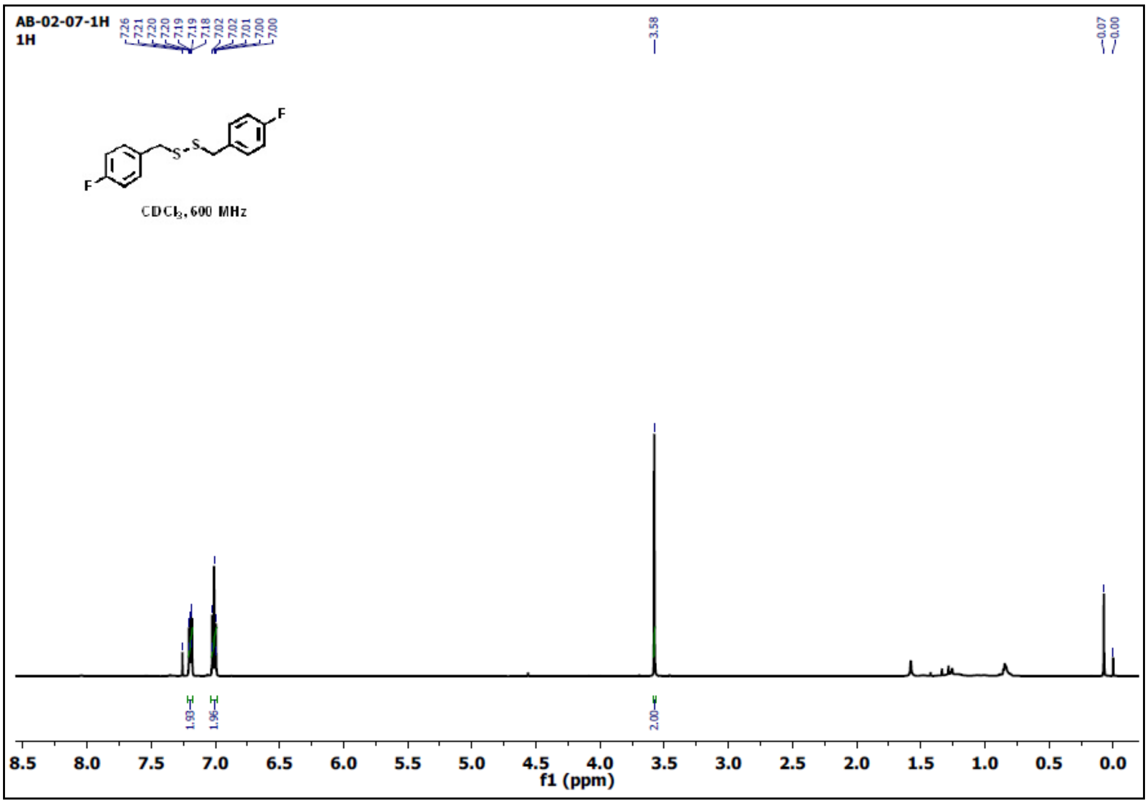

Figure S62: ^{1}H- NMR ($CDCl_3$, 600 MHz, ppm) spectrum of compound **4i**.

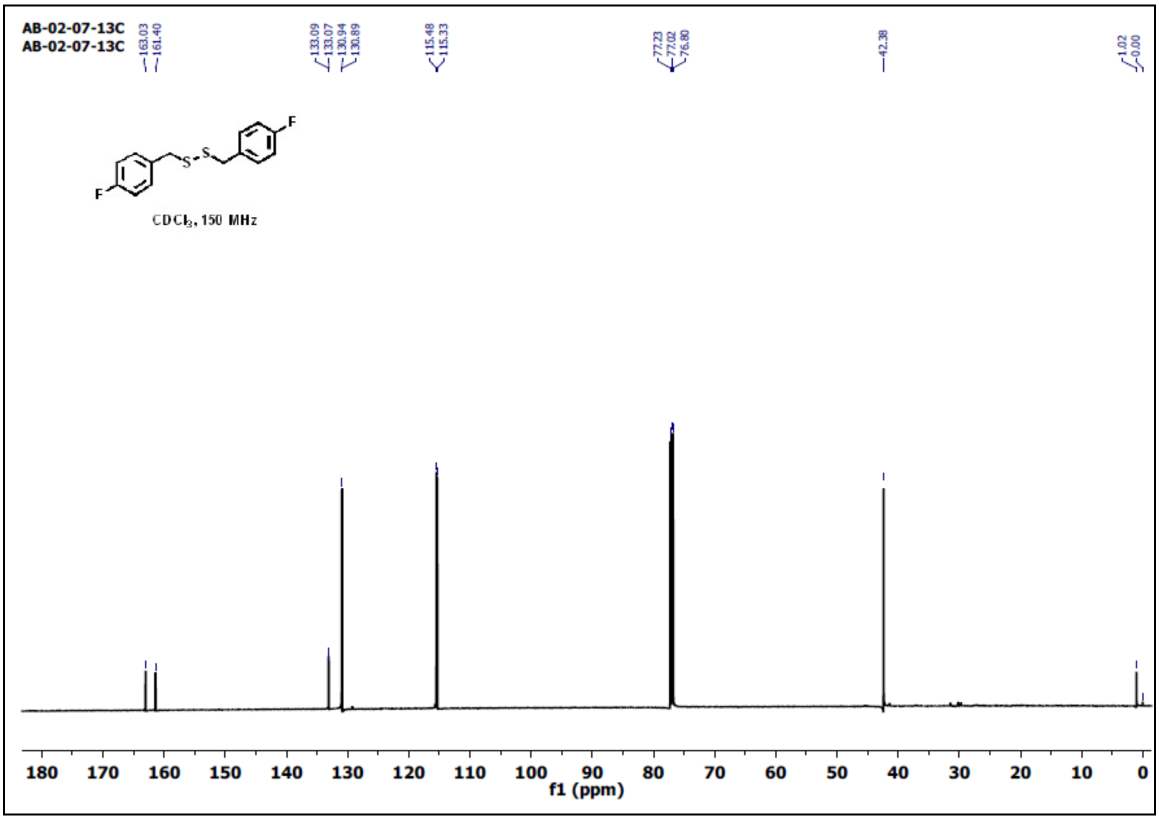

Figure S63: ^{13}C- NMR (CDCl$_3$, 150 MHz, ppm) spectrum of compound **4i**.

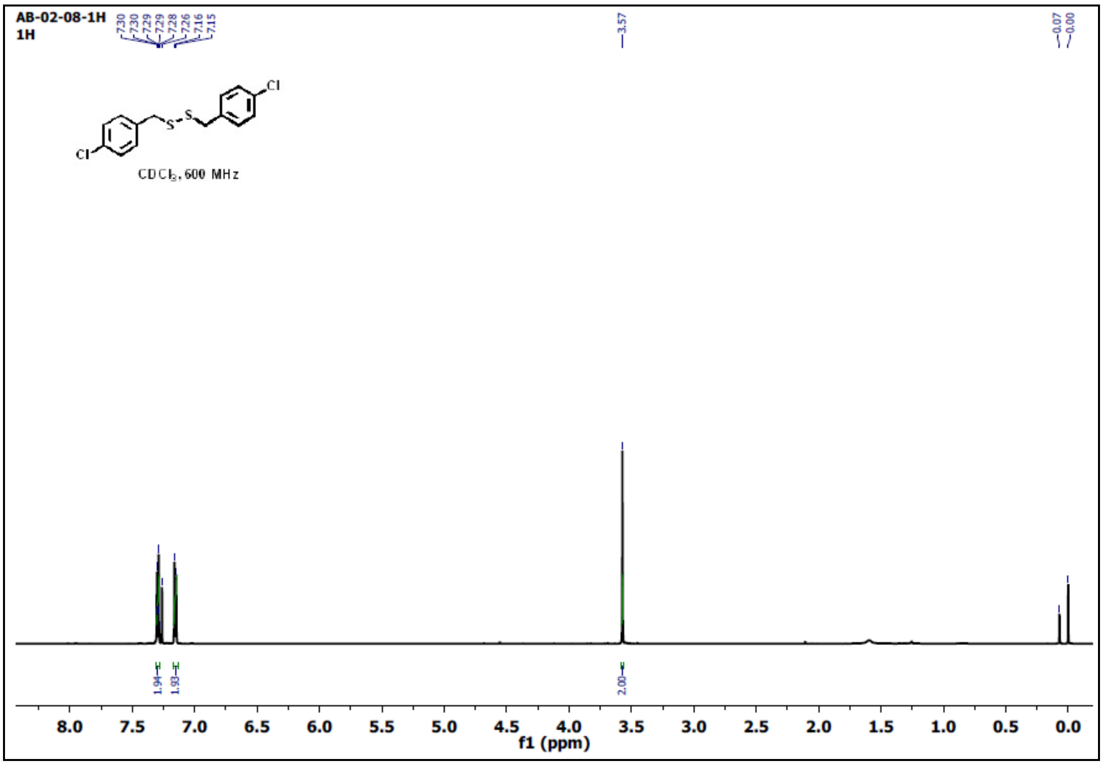

Figure S64: ^{1}H- NMR (CDCl$_3$, 600 MHz, ppm) spectrum of compound **4j**.

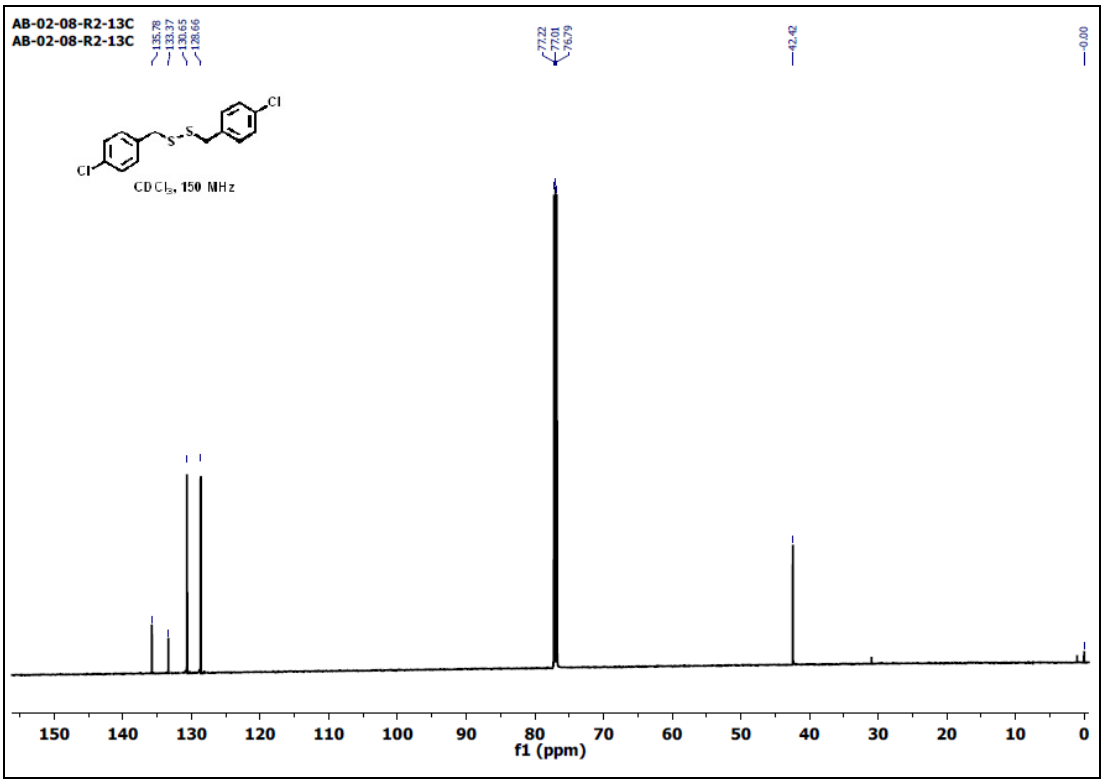

Figure S65: ^{13}C- NMR ($CDCl_3$, 150 MHz, ppm) spectrum of compound **4j**.

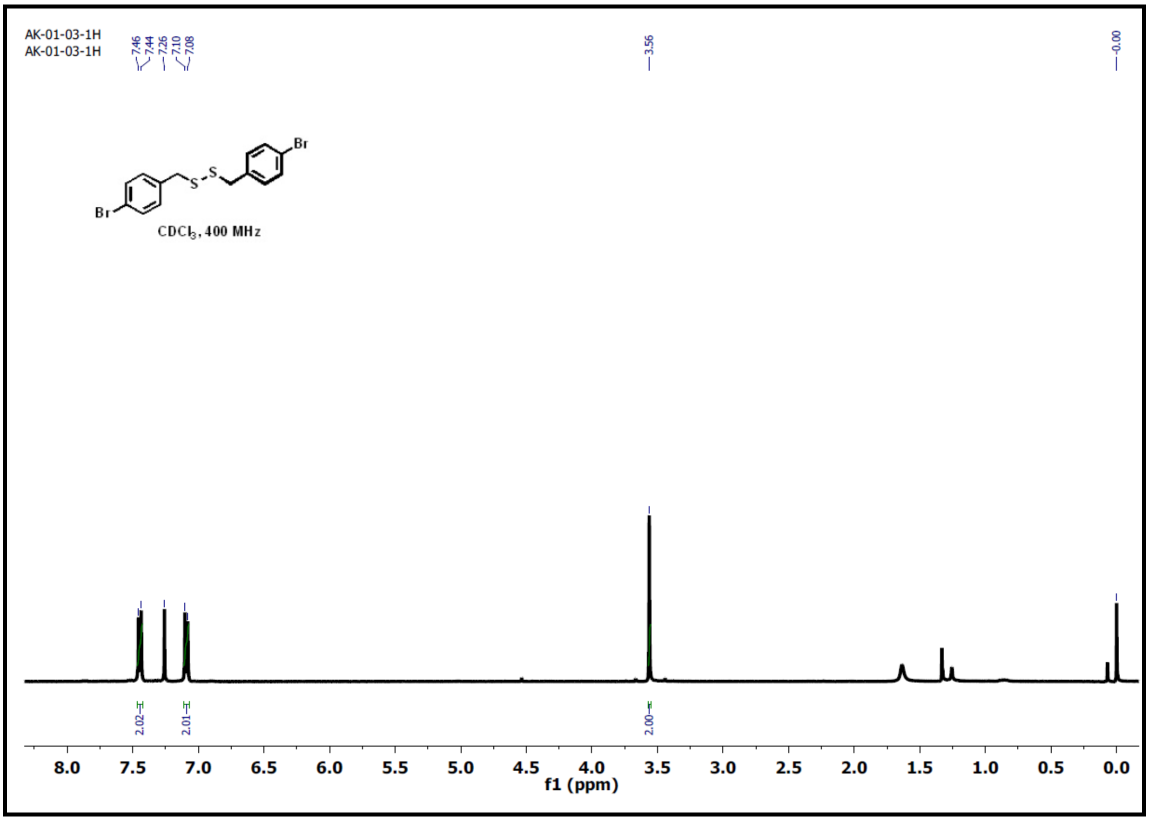

Figure S66: ^{1}H- NMR ($CDCl_3$, 400 MHz, ppm) spectrum of compound **4k**.

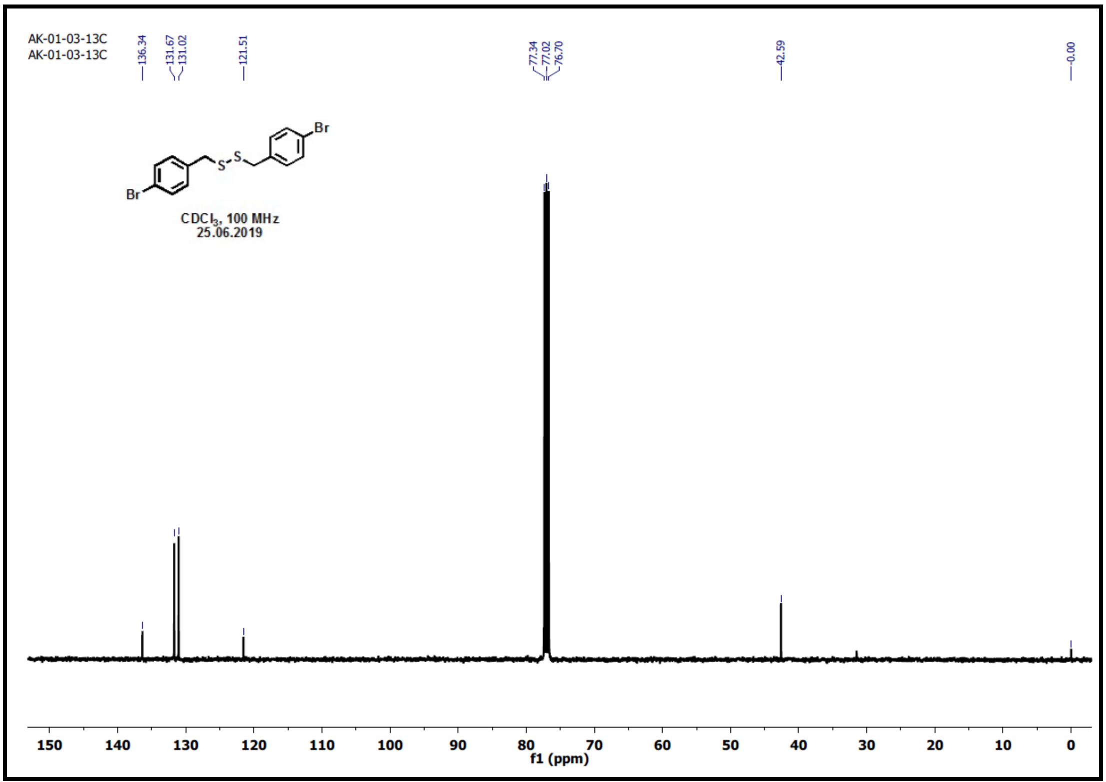

Figure S67: ^{13}C- NMR ($CDCl_3$, 100 MHz, ppm) spectrum of compound **4k**.

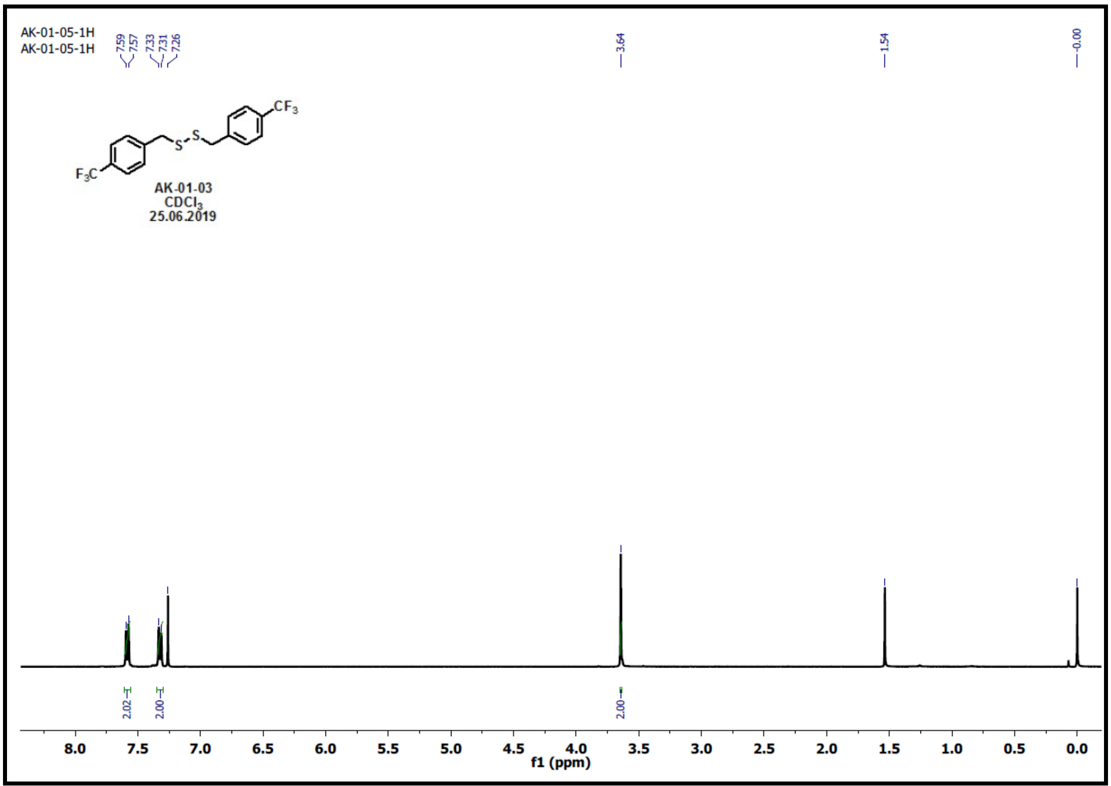

Figure S68: ^{1}H- NMR ($CDCl_3$, 400 MHz, ppm) spectrum of compound **4l**.

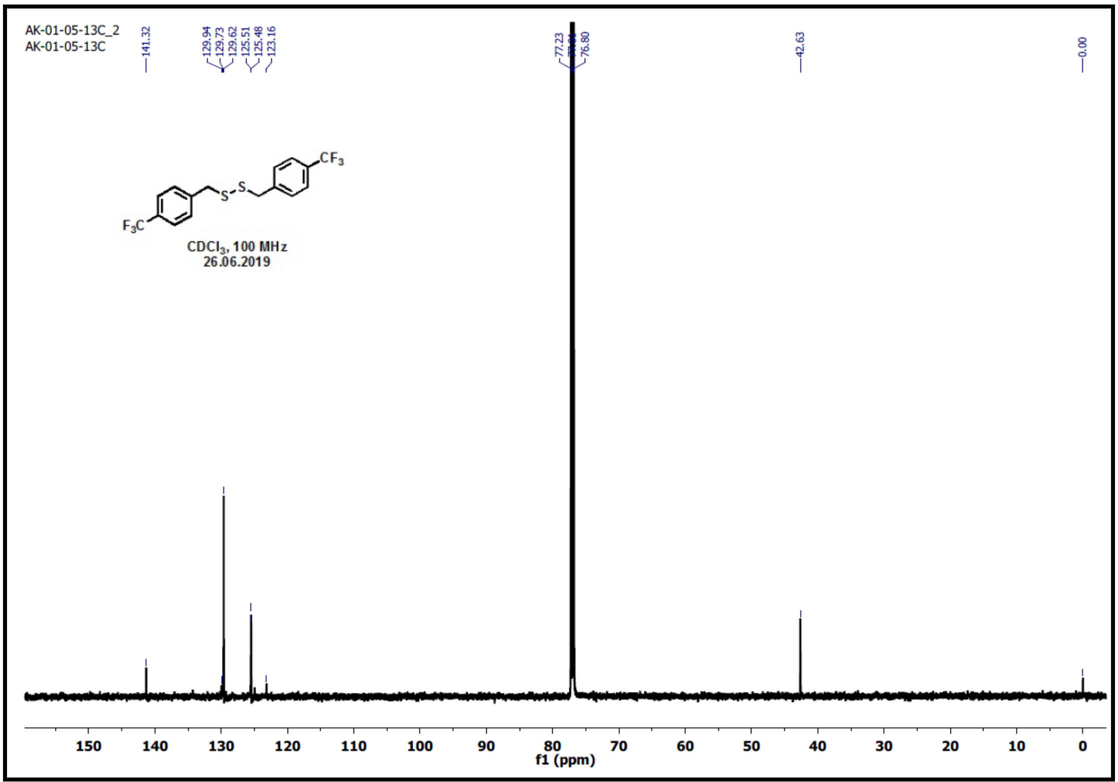

Figure S69: ^{13}C- NMR ($CDCl_3$, 100 MHz, ppm) spectrum of compound **4l**.

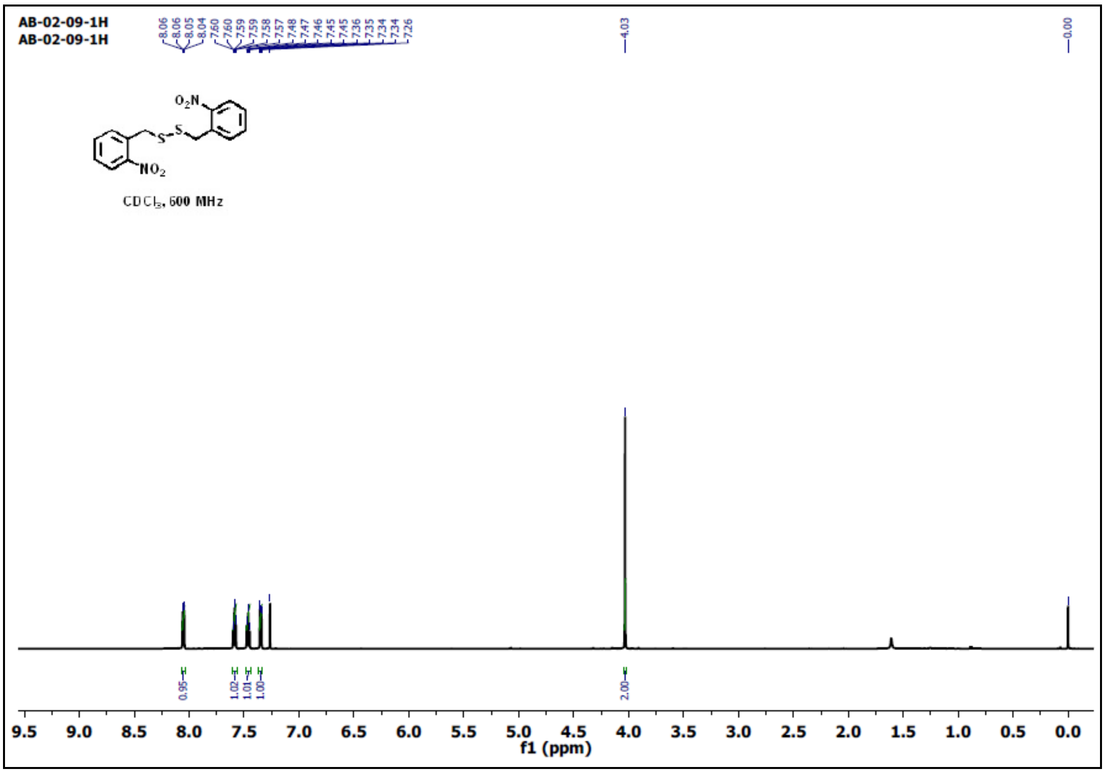

Figure S70: ^{1}H- NMR ($CDCl_3$, 600 MHz, ppm) spectrum of compound **4m.**

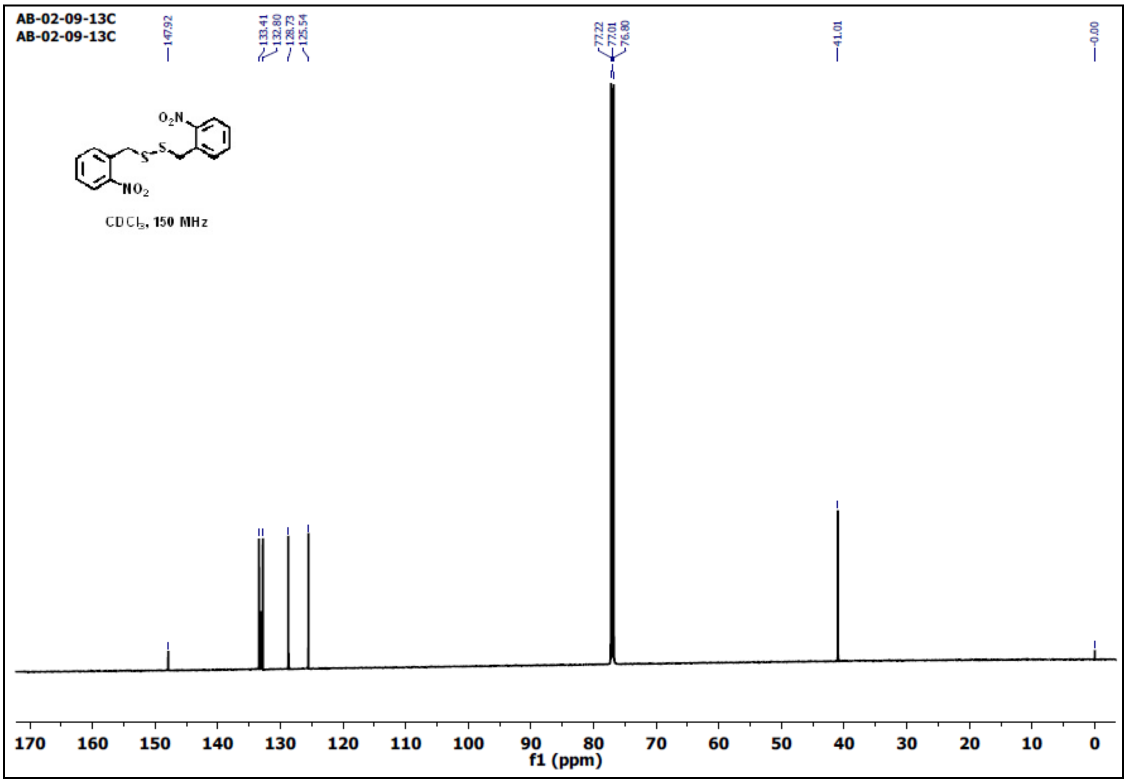

Figure S71: ^{13}C- NMR ($CDCl_3$, 150 MHz, ppm) spectrum of compound **4m**.

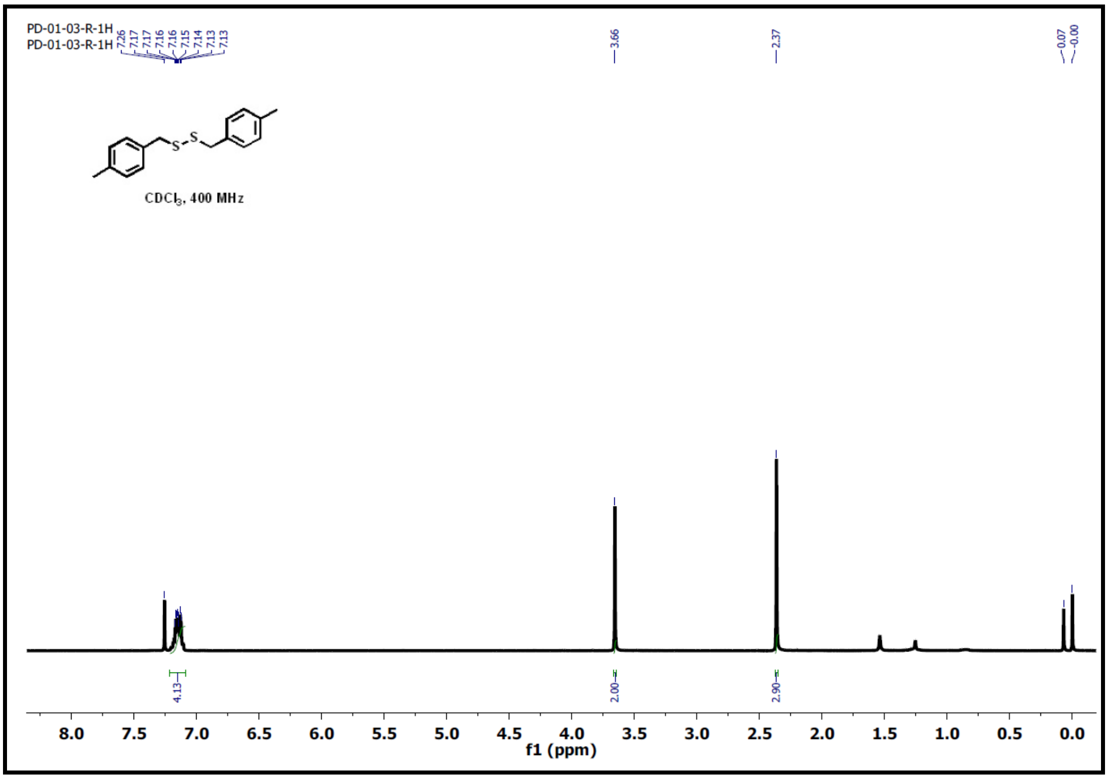

Figure S72: ^{1}H- NMR ($CDCl_3$, 400 MHz, ppm) spectrum of compound **4n**.

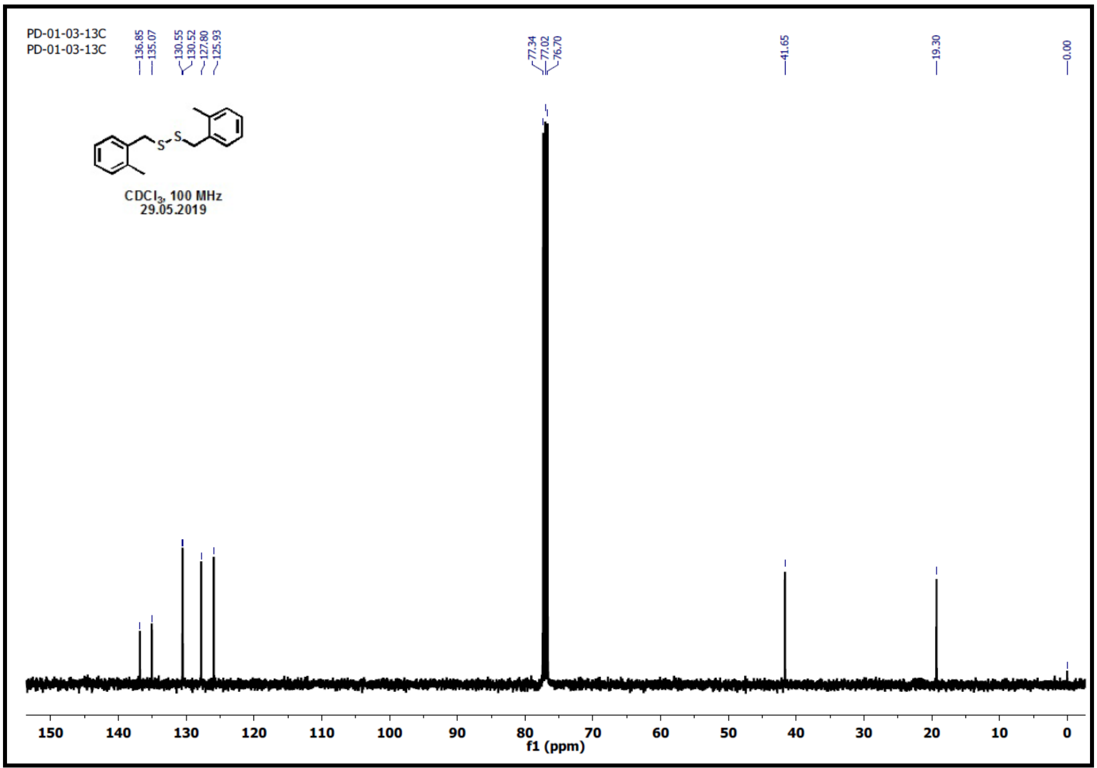

Figure S73: ^{13}C- NMR ($CDCl_3$, 100 MHz, ppm) spectrum of compound **4n**.

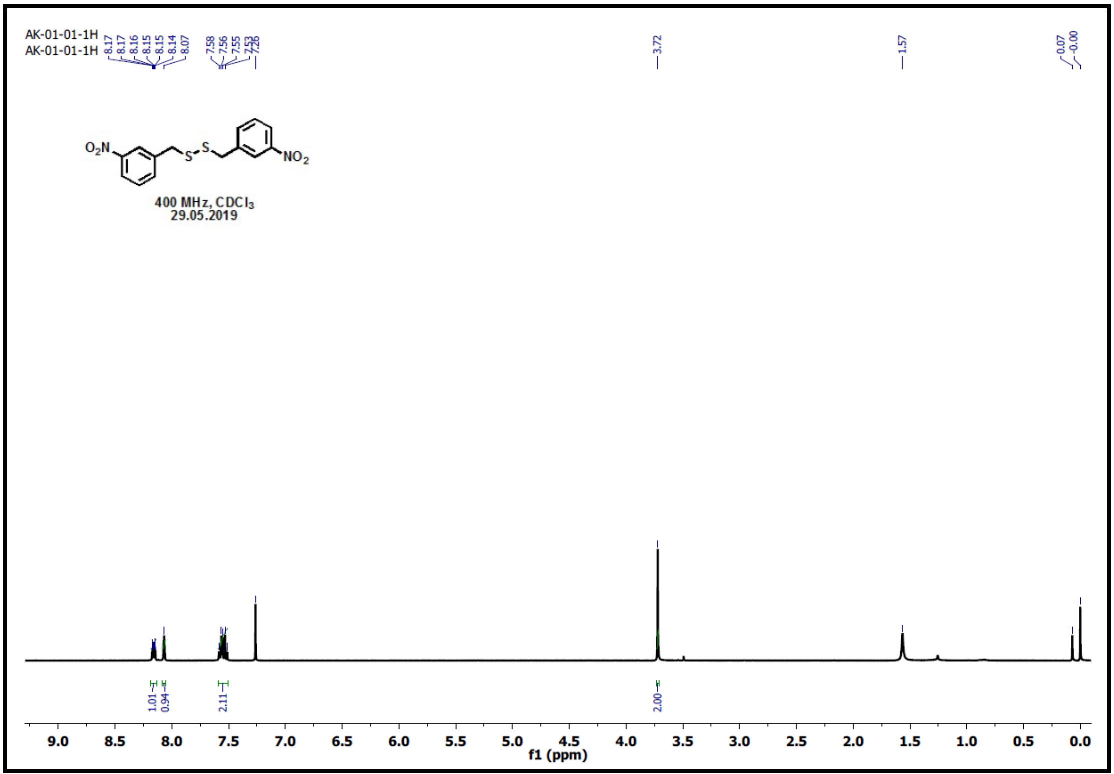

Figure S74: ^{1}H- NMR ($CDCl_3$, 400 MHz, ppm) spectrum of compound **4o**.

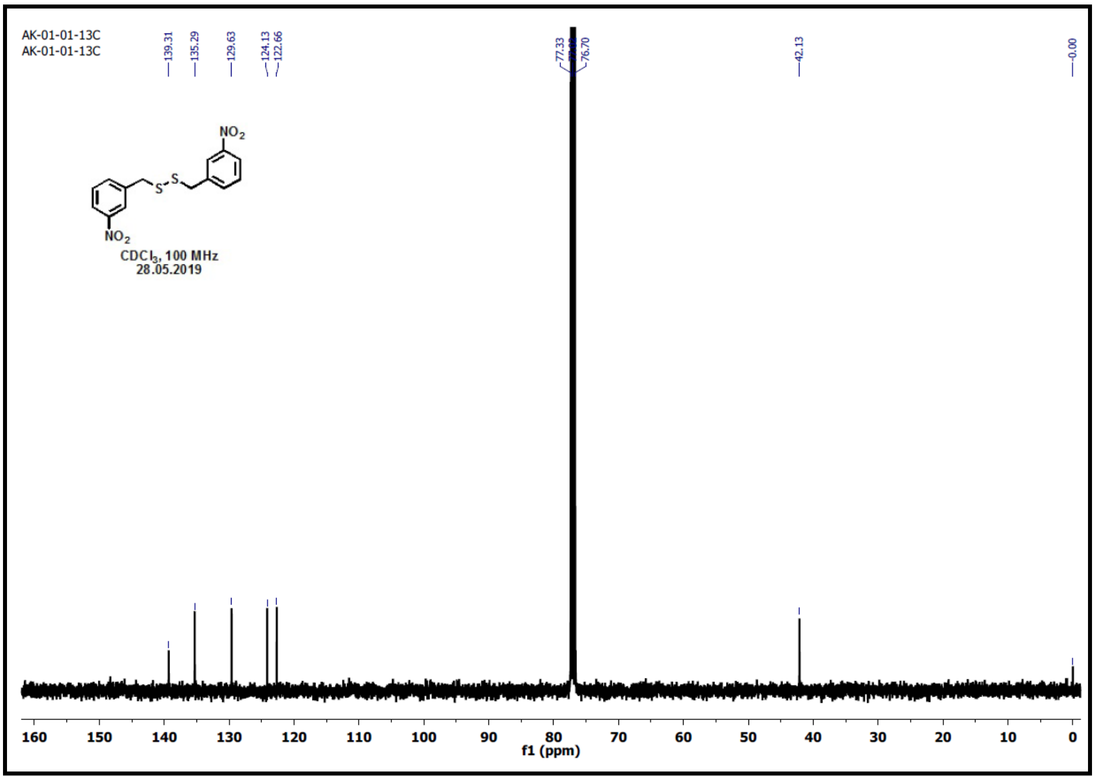

Figure S75: ^{13}C- NMR (CDCl$_3$, 100 MHz, ppm) spectrum of compound **4o**.

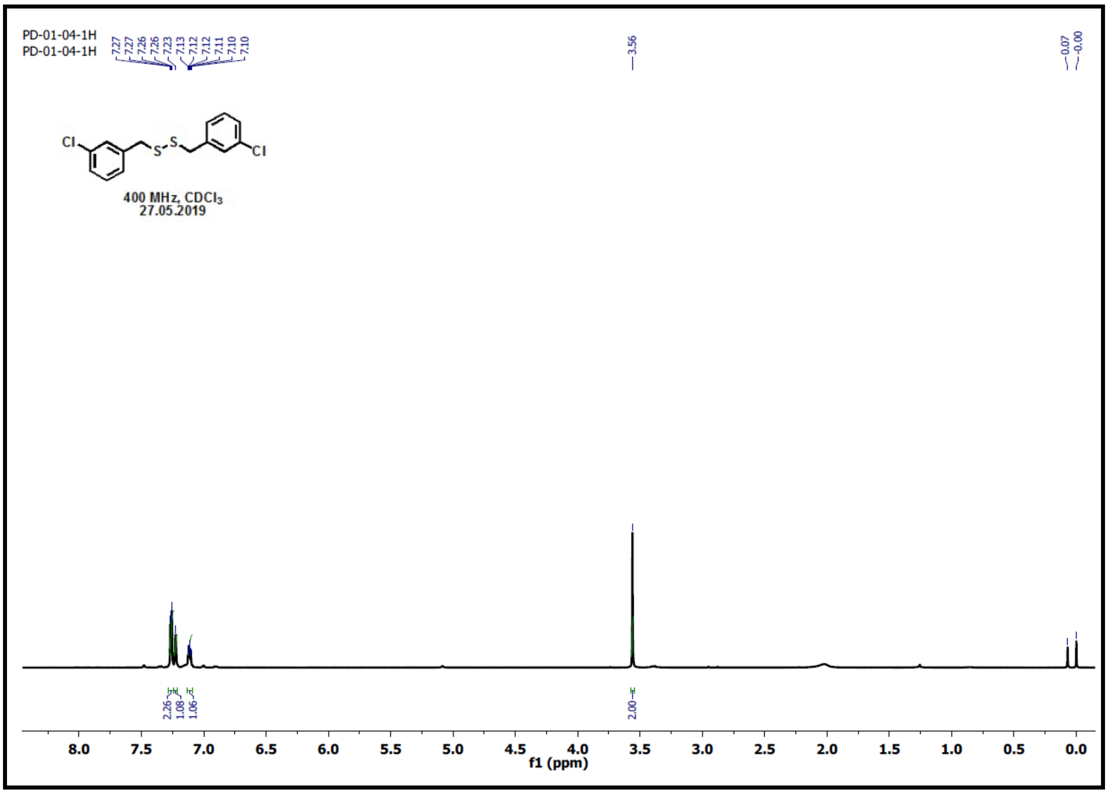

Figure S76: ^{1}H- NMR (CDCl$_3$, 400 MHz, ppm) spectrum of compound **4p**.

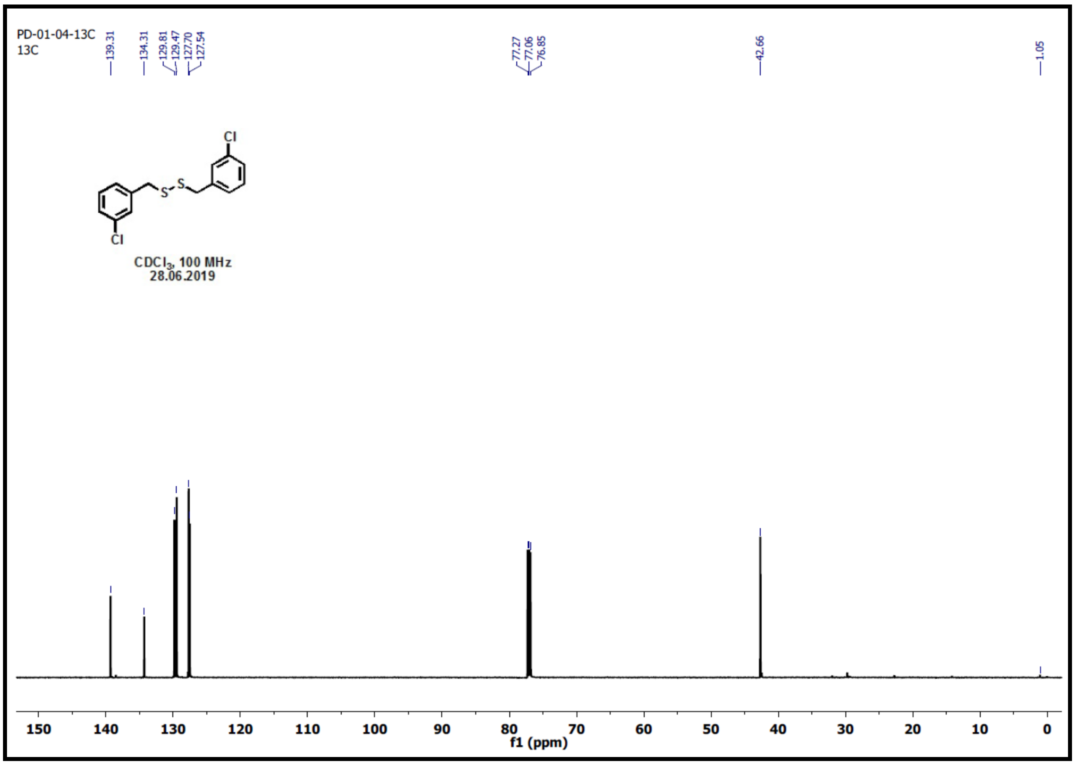

Figure S77: ^{13}C- NMR ($CDCl_3$, 100 MHz, ppm) spectrum of compound **4p**.

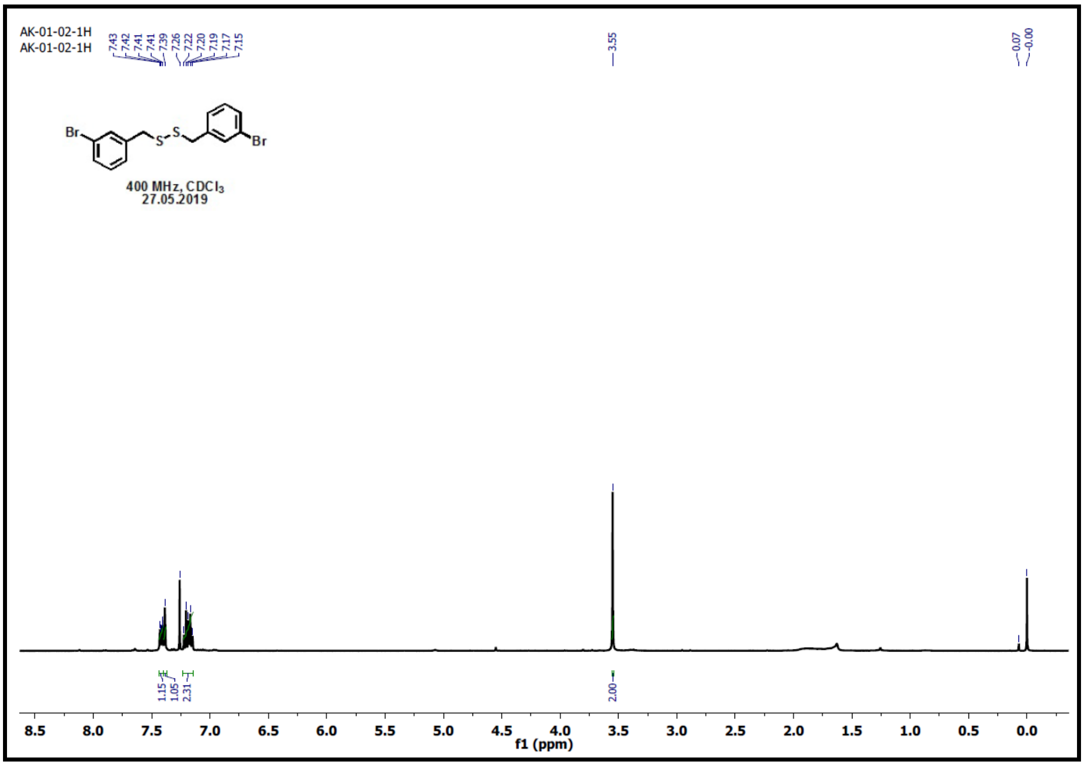

Figure S78: ^{1}H- NMR ($CDCl_3$, 400 MHz, ppm) spectrum of compound **4q**.

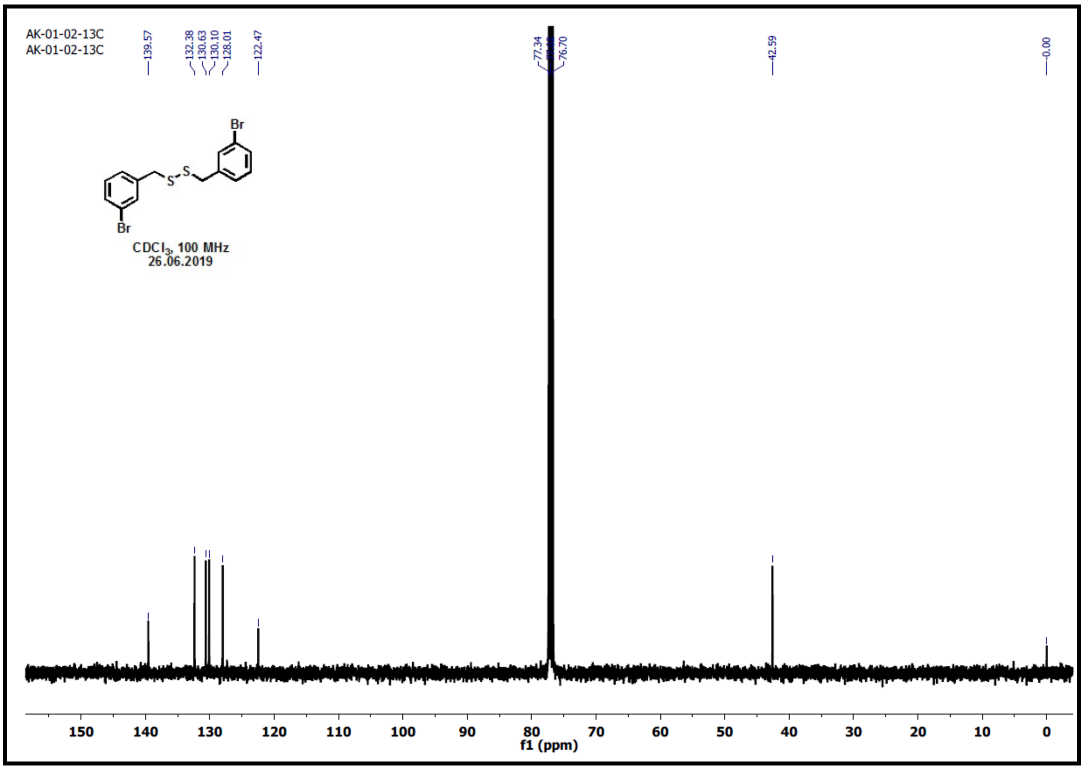

Figure S79: ^{13}C- NMR ($CDCl_3$, 100 MHz, ppm) spectrum of compound **4q**.

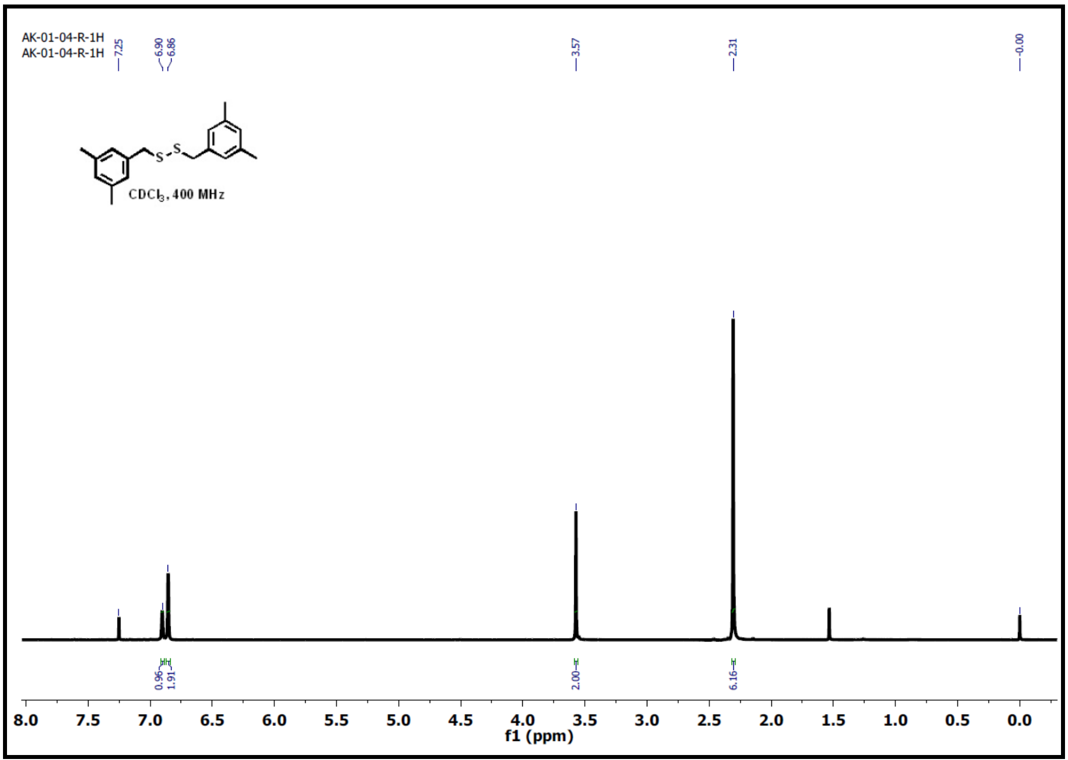

Figure S80: ^{1}H- NMR ($CDCl_3$, 400 MHz, ppm) spectrum of compound **4r**.

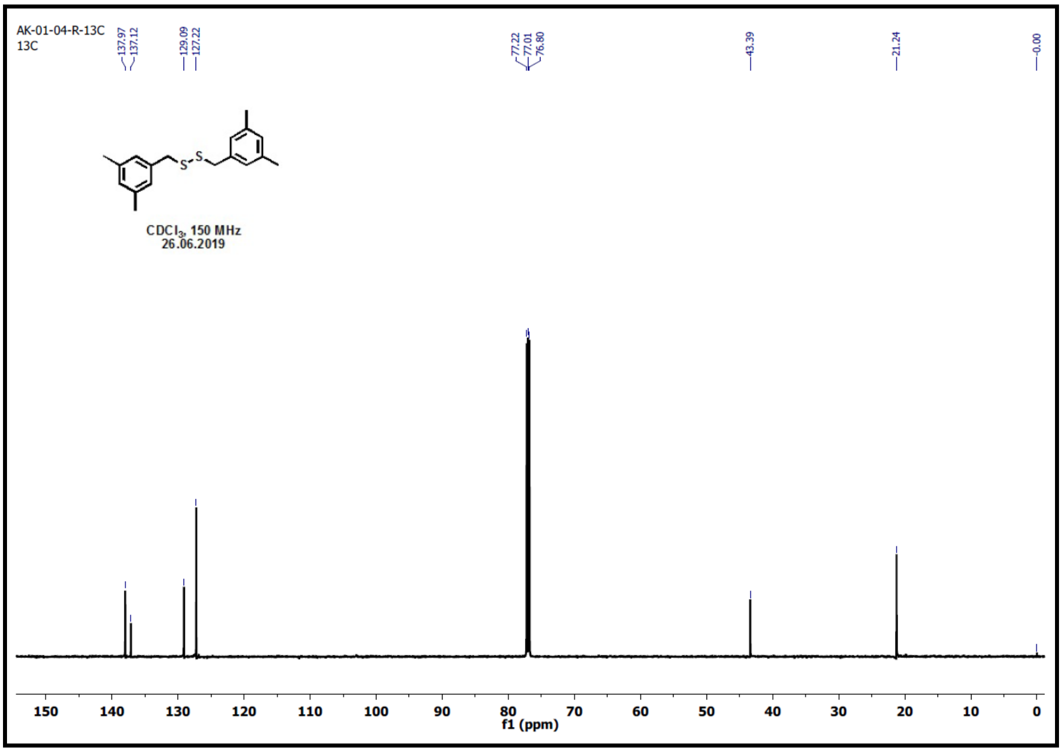

Figure S81: ^{13}C- NMR (CDCl$_3$, 150 MHz, ppm) spectrum of compound **4r**.

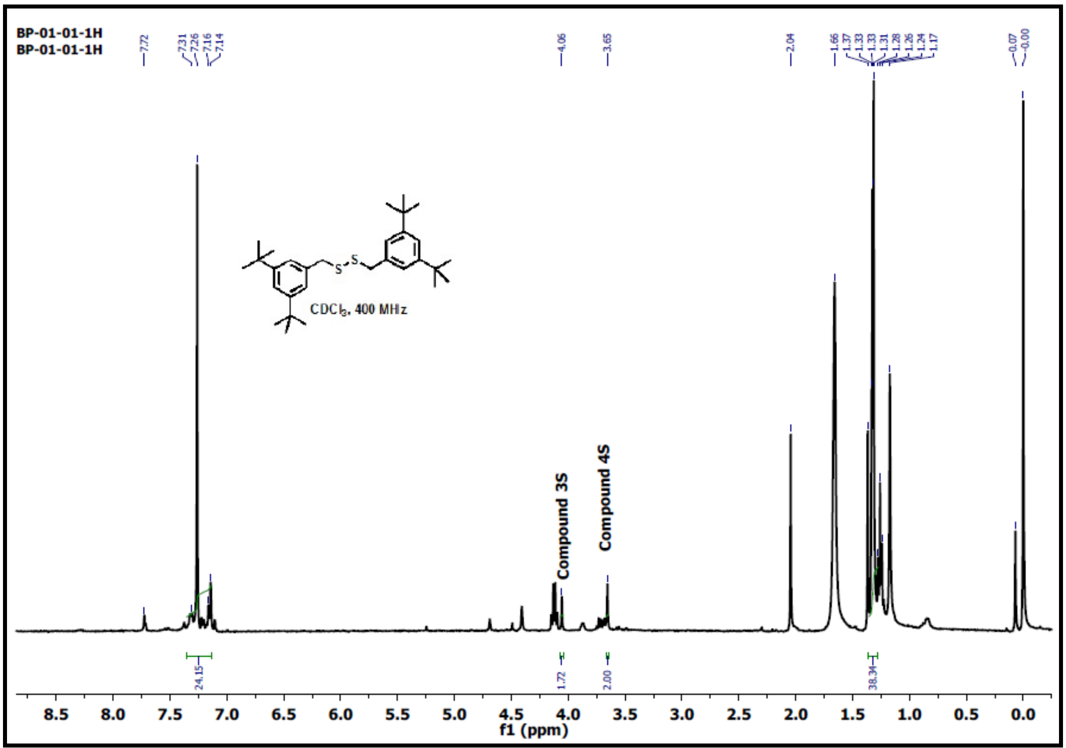

Figure S82: ^{1}H- NMR (CDCl$_3$, 400 MHz, ppm) spectrum of compound **4s**. Here trisulfide **3s** and the desired disulfide **4s** were present along with some higher polysulfides.

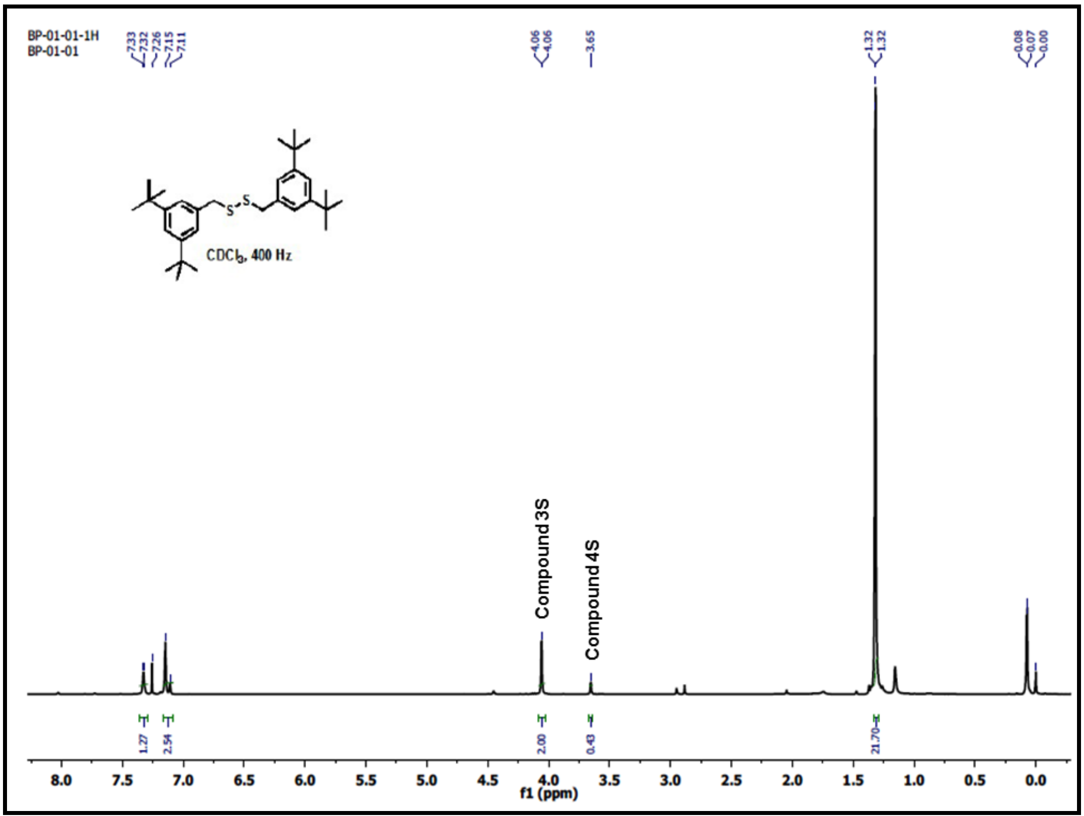

Figure S83: ^{1}H- NMR ($CDCl_3$, 400 MHz, ppm) spectrum of compound **4s** upon the addition of 5 equiv of Na_2SO_3 into the reaction. Here the corresponding trisulfide **3s** became the predominant product after addition of sodium sulfite.

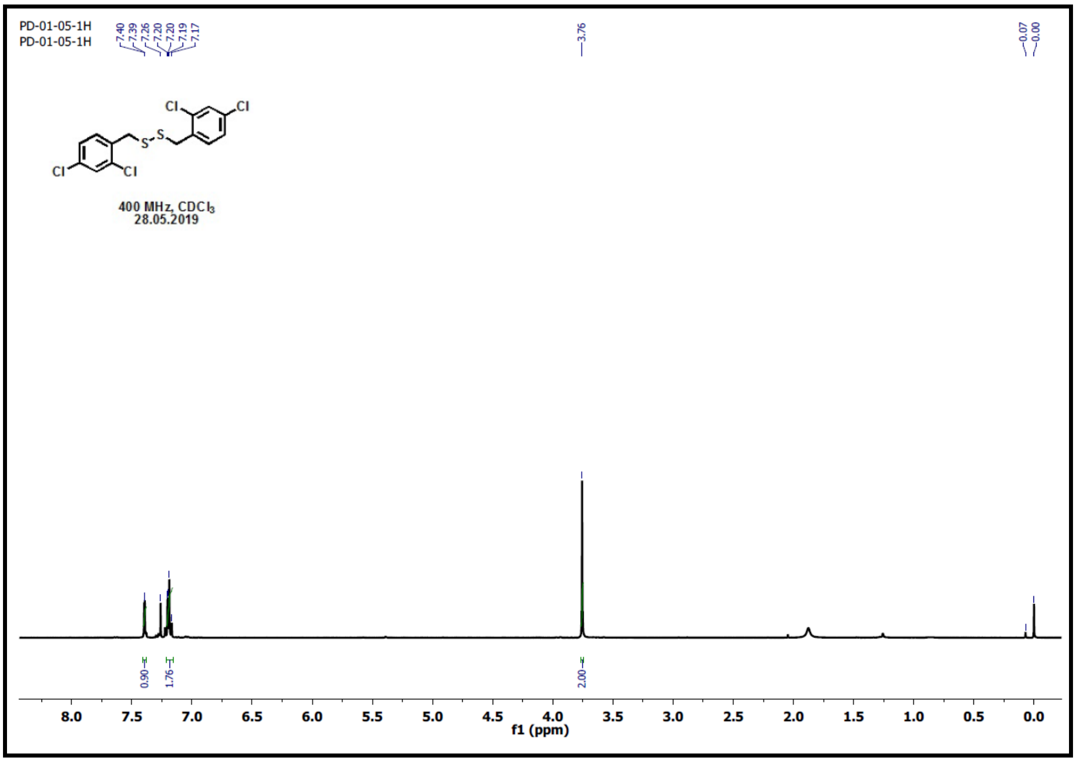

Figure S84: ^{1}H- NMR ($CDCl_3$, 400 MHz, ppm) spectrum of compound **4t**.

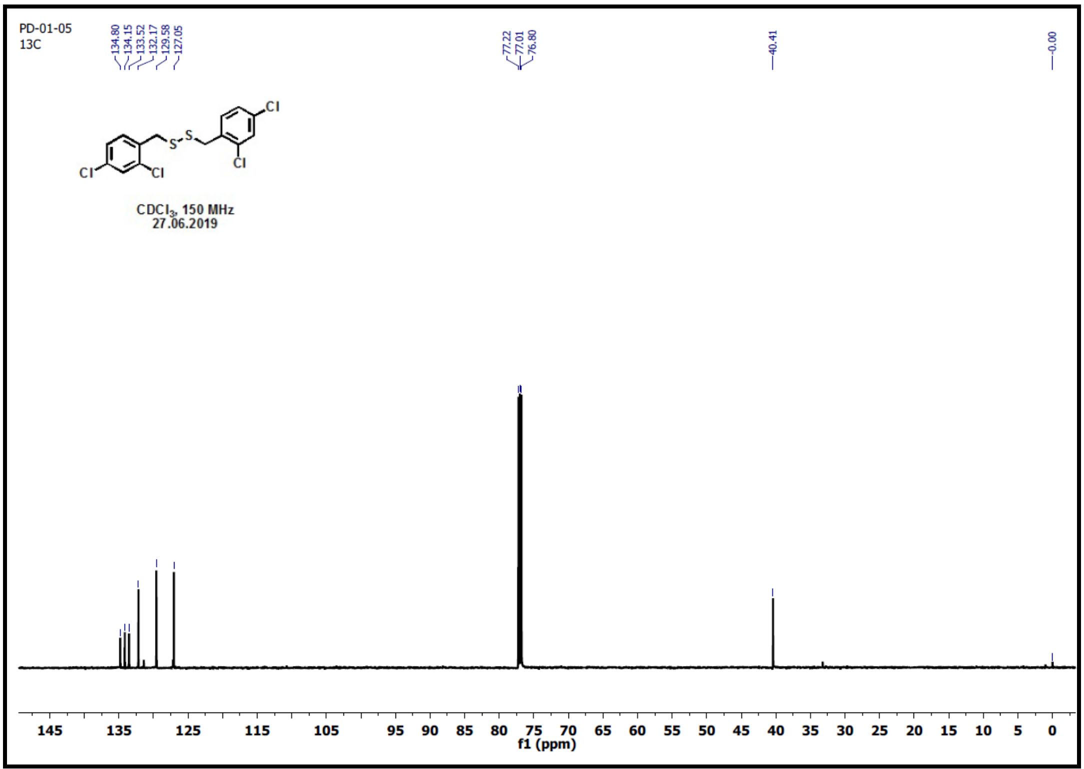

Figure S85: ^{13}C- NMR (CDCl$_3$, 150 MHz, ppm) spectrum of compound **4t**.

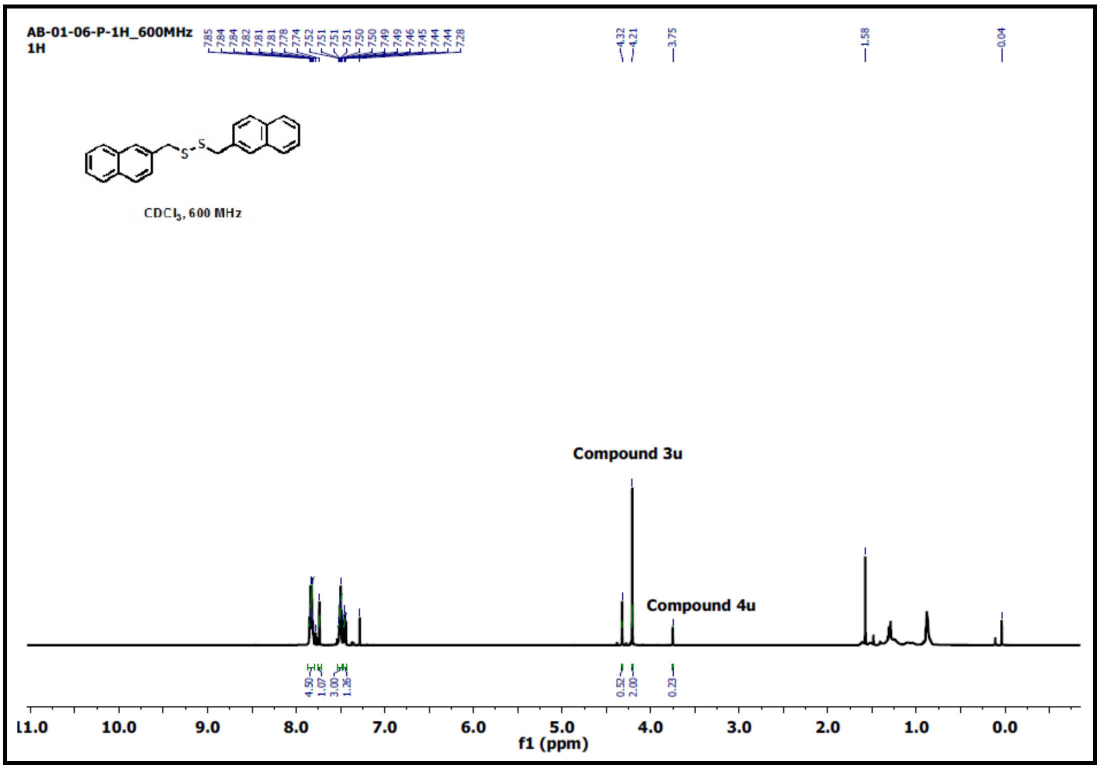

Figure S86: ^{1}H- NMR (CDCl$_3$, 600 MHz, ppm) spectrum of compound **4u**. Here trisulfide **3u** and the desired disulfide **4u** were present along with some higher polysulfides.

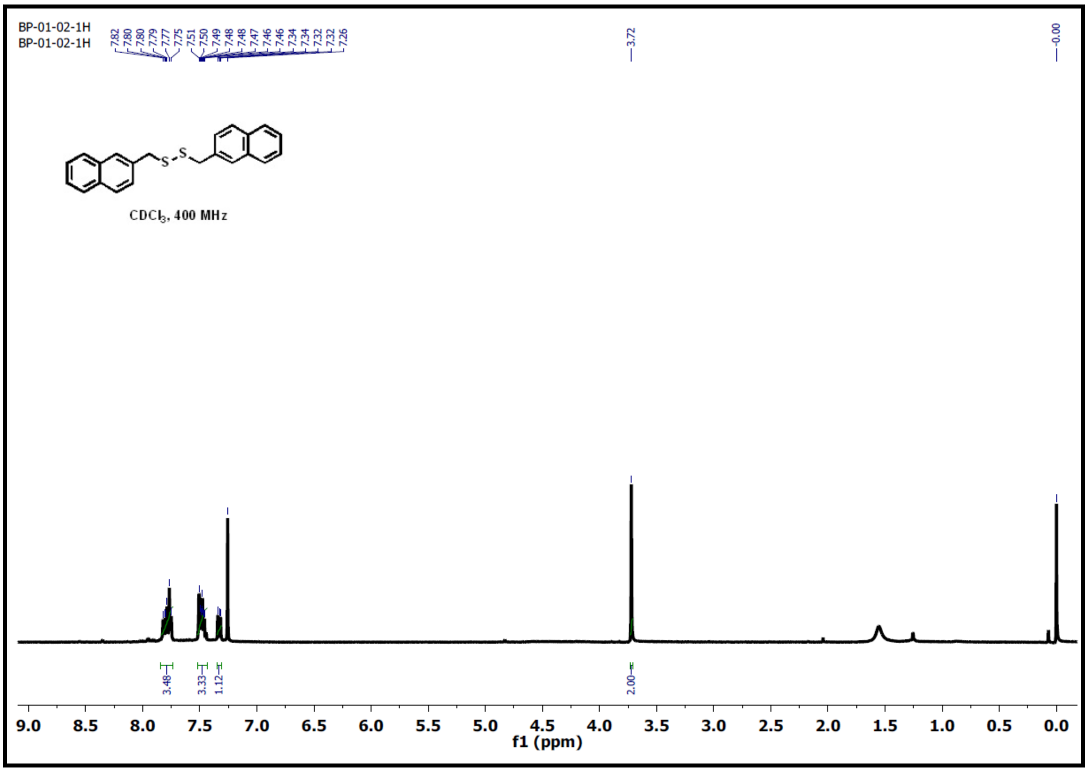

Figure S87: ^{1}H- NMR (CDCl$_3$, 400 MHz, ppm) spectrum of compound **4u** upon the addition of 5 equiv of Na$_2$SO$_3$ into the reaction.

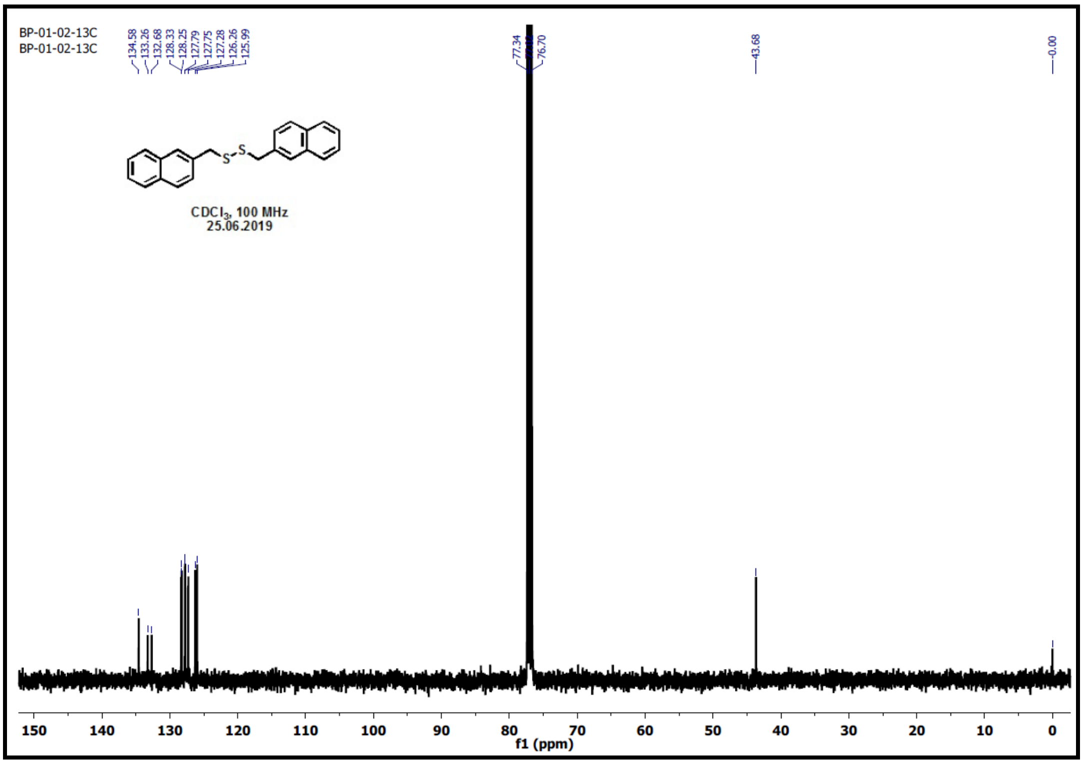

Figure S88: ^{13}C- NMR (CDCl$_3$, 100 MHz, ppm) spectrum of compound **4u** upon the addition of 5 equiv of Na$_2$SO$_3$ into the reaction.

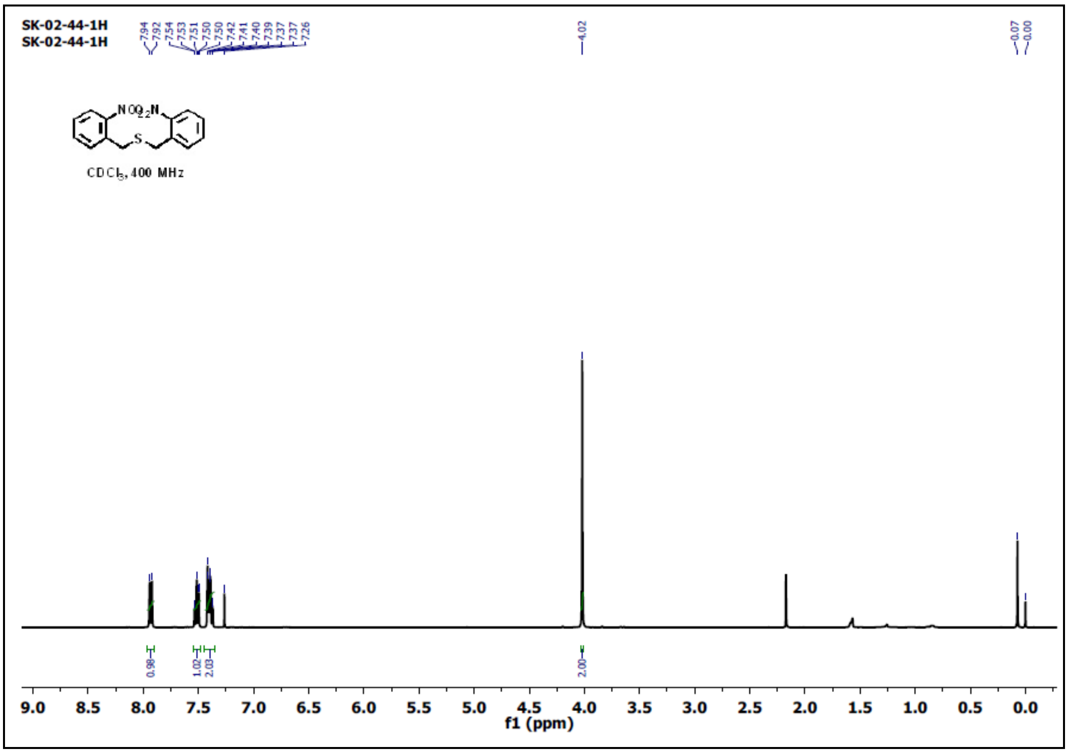

Figure S89: ^{1}H- NMR (CDCl$_3$, 400 MHz, ppm) spectrum of compound **5m**.

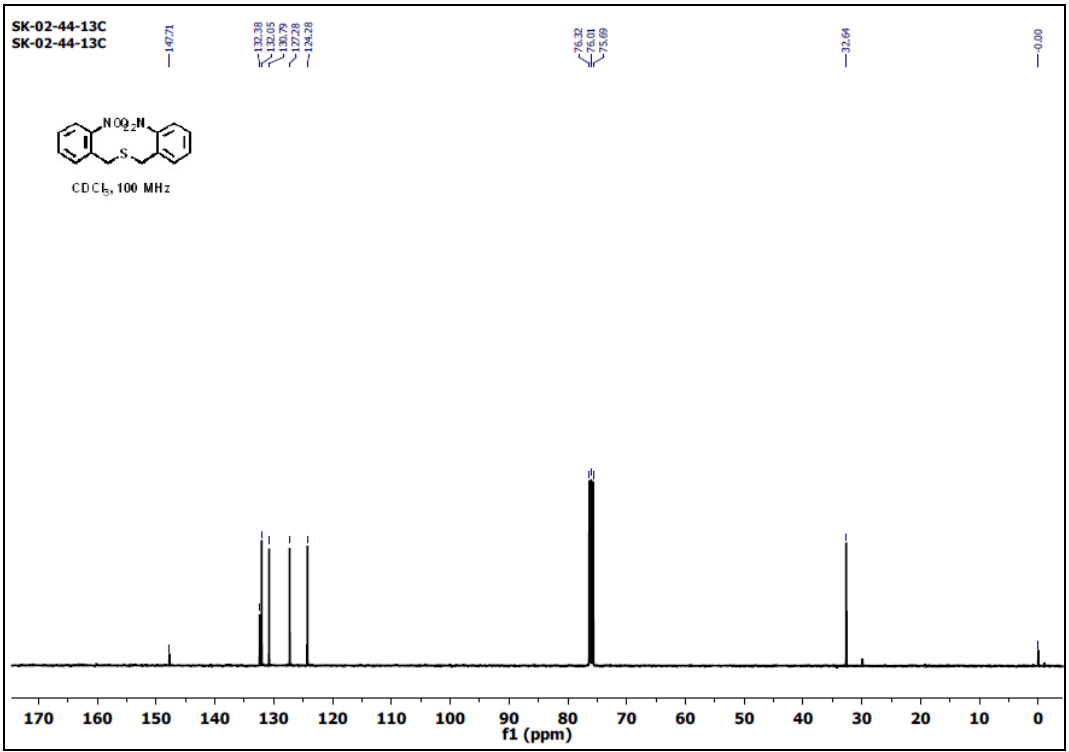

Figure S90: ^{13}C- NMR (CDCl$_3$, 100 MHz, ppm) spectrum of compound **5m**.

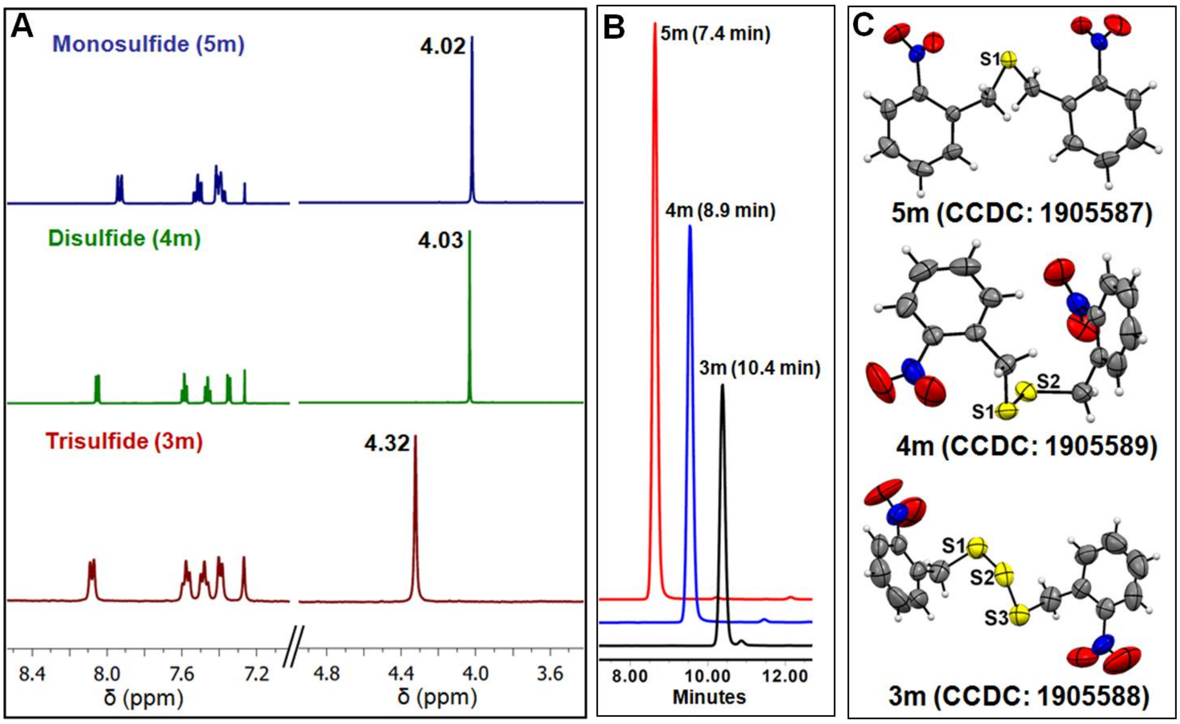

Figure S91: A comparative characterization details of trisulfide (**3m**), disulfide (**4m**) and the corresponding monosulfide (**5m**) using ^{1}H NMR spectra (A), HPLC chromatogram (B) and single crystal X-ray structures (C).

Unsymmetrical trisulfides and disulfides

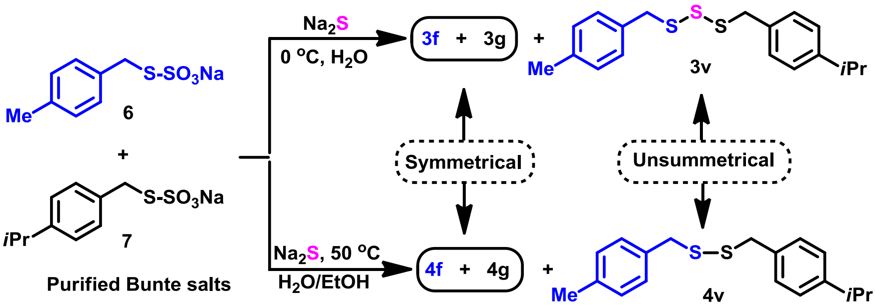

Scheme S1. Schematic representation for the synthesis of mixed trisulfide **3v** and disulfide **4v** during the reaction of Na_2S with two different Bunte salts **6** and **7**. Detection of mixed trisulfide **3v** implies the generation of perthiolate intermediate during the synthesis of trisulfide.

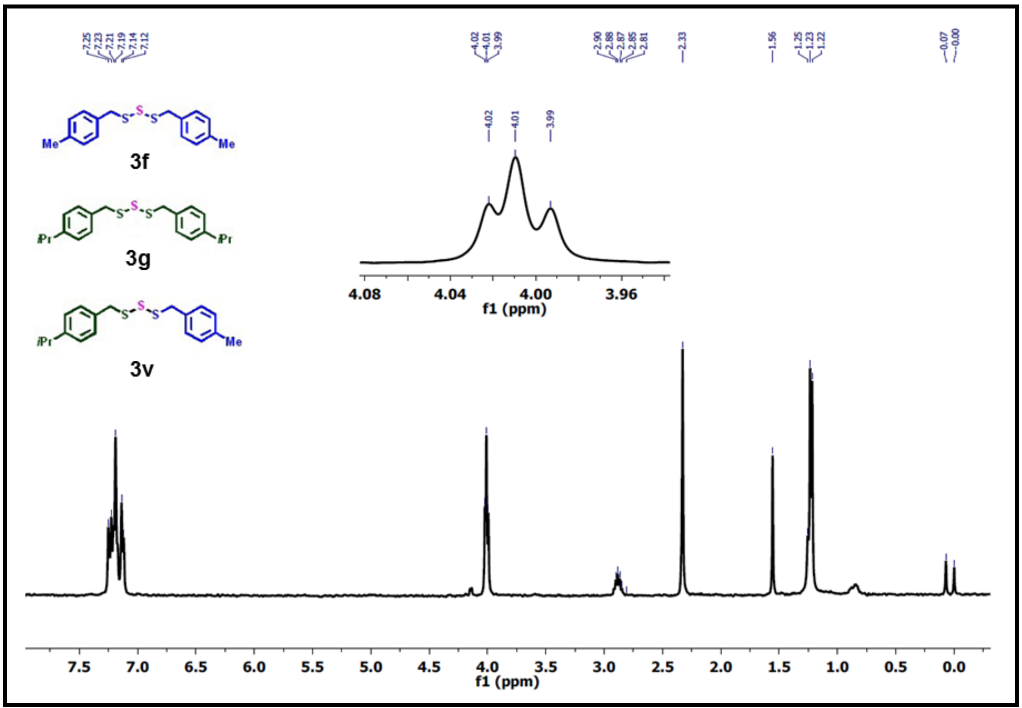

Figure S92: ^{1}H- NMR ($CDCl_3$, 400 MHz, ppm) spectrum of the crude trisulfide mixture containing trisulfides (**3f**, **3g** and **3v**).

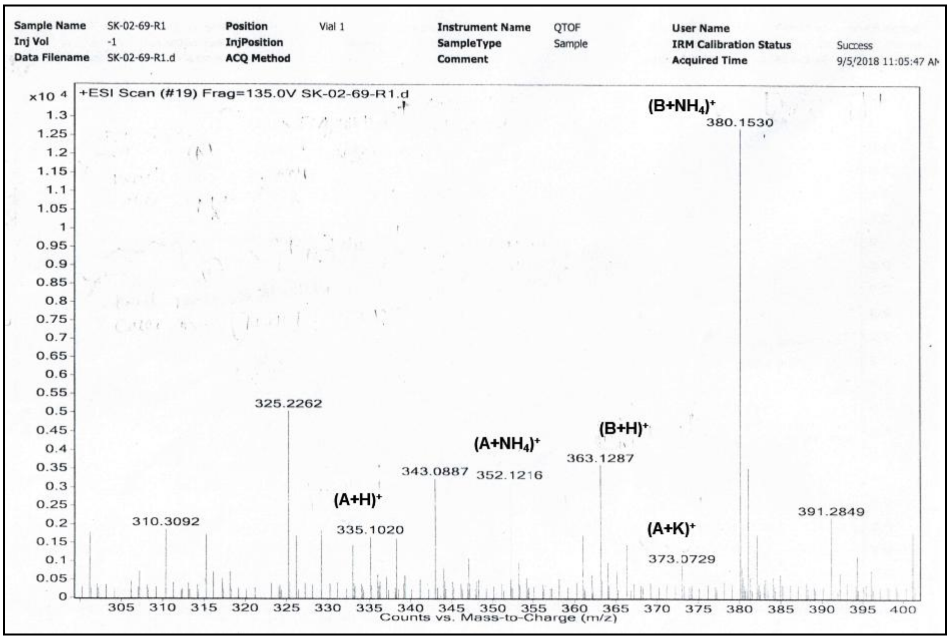

Sample Name	SK-02-69-R1	**Position**	Vial 1	**Instrument Name**	QTOF	**User Name**	
Inj Vol	-1	**InjPosition**		**SampleType**	Sample	**IRM Calibration Status**	Success
Data Filename	SK-02-69-R1.d	**ACQ Method**		**Comment**		**Acquired Time**	9/5/2018 11:05:47 AM

Figure S93: ESI-MS spectrum of crude trisulfide mixture with compounds **3f**, **3g** (B) and **3v** (A). The molecular ion peak for **3f** was not observed during this analysis.

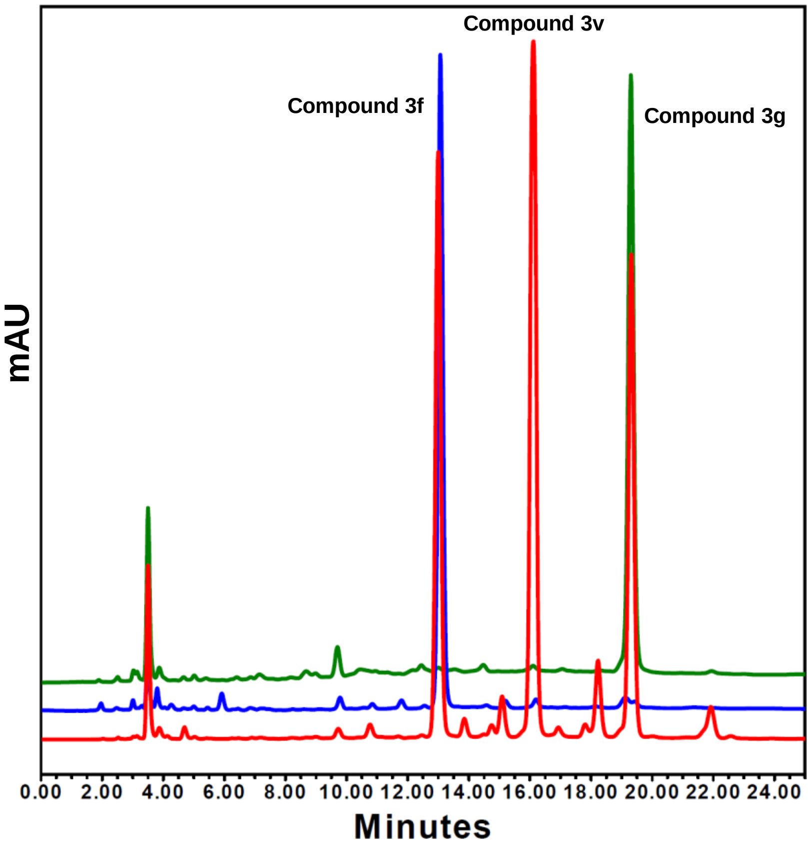

Figure S94: HPLC chromatogram of pure symmetrical trisulfides (**3f** and **3g)** and the crude trisulfide mixture containing unsymmetrical trisulfide **3v**.

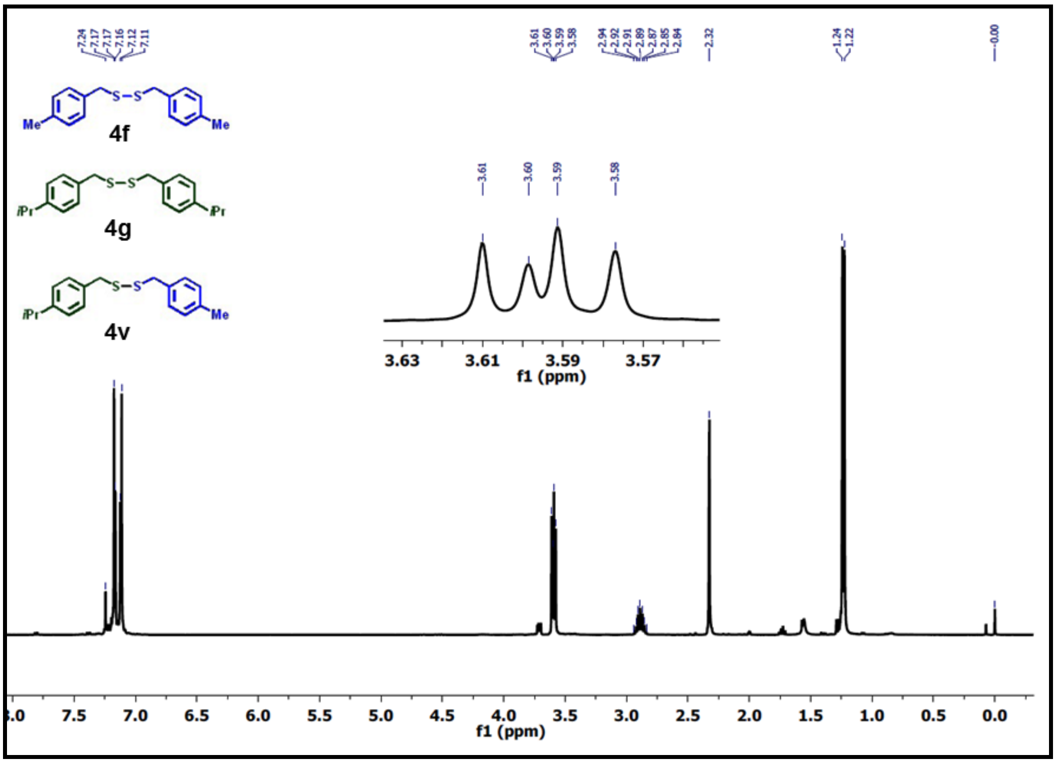

Figure S95: ^{1}H NMR ($CDCl_3$, 400 MHz, ppm) spectrum of the crude disulfide mixture containing (**4f**, **4g** and **4v**).

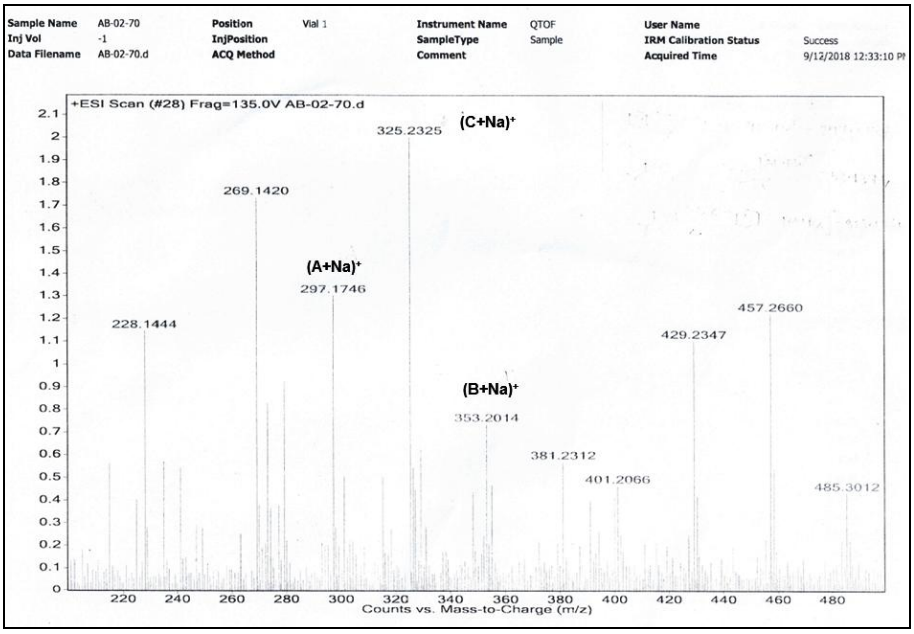

Sample Name AB-02-70
Inj Vol -1
Data Filename AB-02-70.d
Position Vial 1
InjPosition
ACQ Method
Instrument Name QTOF
SampleType Sample
Comment
User Name
IRM Calibration Status Success
Acquired Time 9/12/2018 12:33:10 PM

Figure S96: ESI-MS spectrum of the crude disulfide mixture [**4f** (A), **4g** (B) and **4v** (C)].

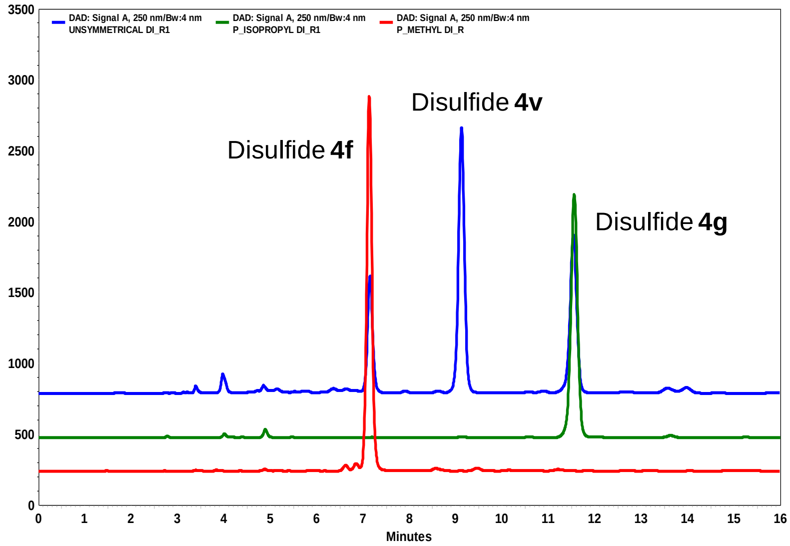

Figure S97: HPLC chromatogram of pure symmetrical disulfides (**4f** and **4g)** and the crude disulfide mixture containing unsymmetrical disulfide **4v**.

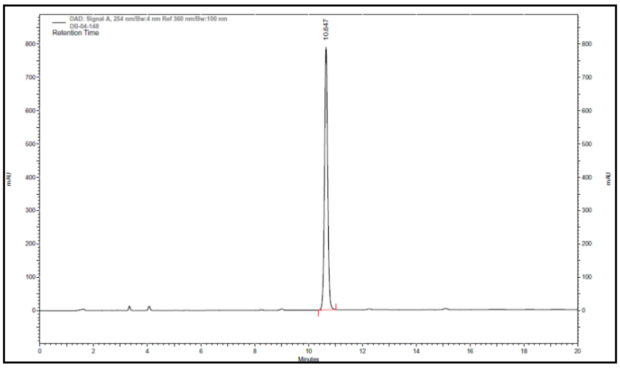

(a)

(b)

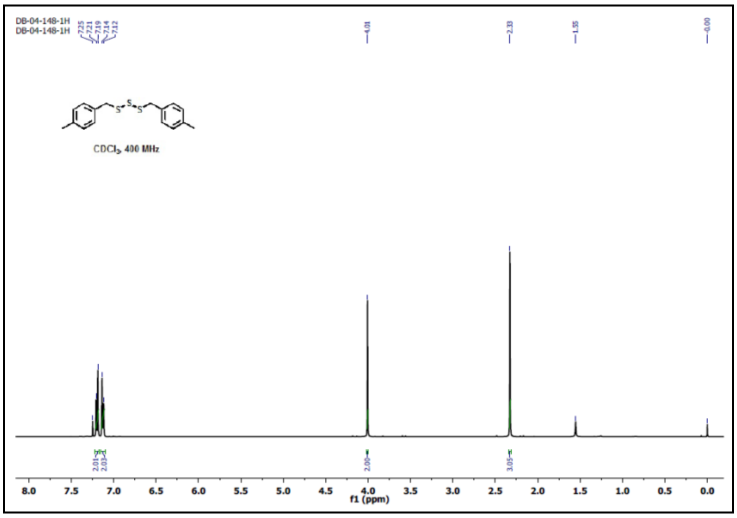

(c)

Figure S98: (a) HPLC chromatogram of compound **3f** yielded from bulk-scale reaction. (b) Synthesized compound **3f** after work-up. (c) ^{1}H-NMR ($CDCl_3$, 400 MHz, ppm) spectrum of compound **3f**.

Effect of Na_2SO_3 towards the formation of disulfide 4a

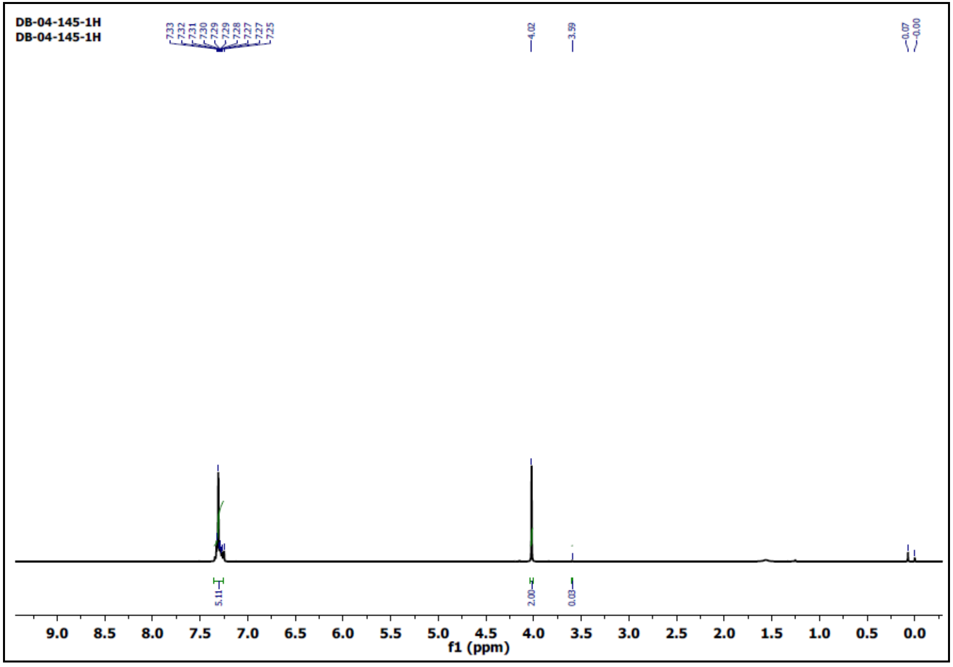

Figure S99: ^{1}H-NMR ($CDCl_3$, 400 MHz, ppm) spectrum of crude product mixture from the reaction of column purified Bunte salt (1.0 equiv) of benzyl bromide with Na_2S (0.5 equiv) **without Na_2SO_3** in water at 0 ºC for 8h. The mixture contained trisulfide **3a** with a very trace amount of disulfide **4a** (99:1).

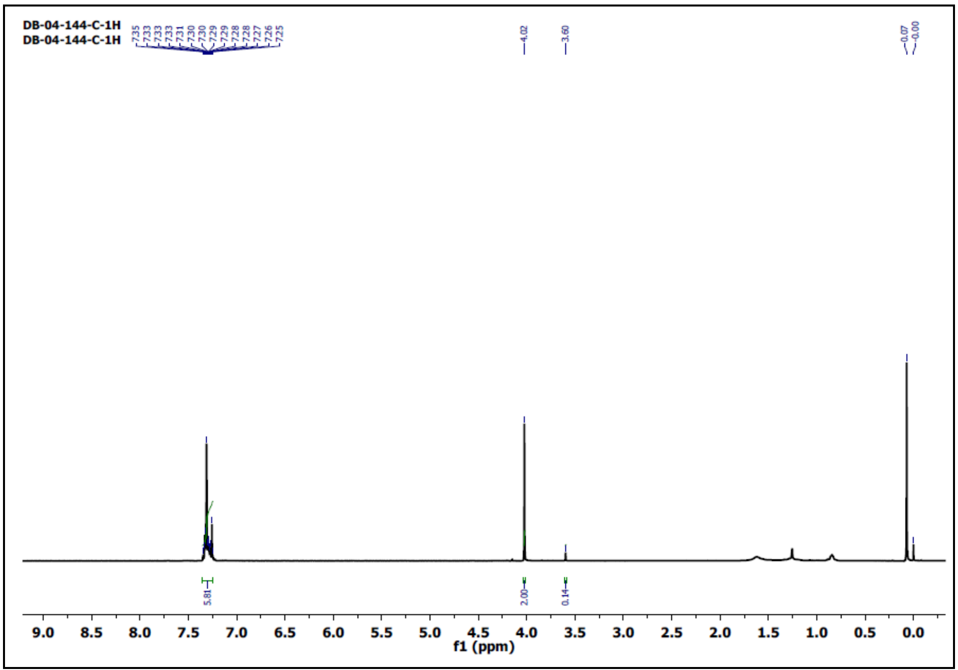

Figure S100: ^{1}H-NMR ($CDCl_3$, 400 MHz, ppm) spectrum of crude product mixture from the reaction of column purified Bunte salt (1.0 equiv) of benzyl bromide with Na_2S (0.5 equiv) and **Na_2SO_3** (5.0 equiv) in water at 0 ºC for 8h. The mixture contained trisulfide **3a** with a slightly increased amount of disulfide **4a** (94:6).

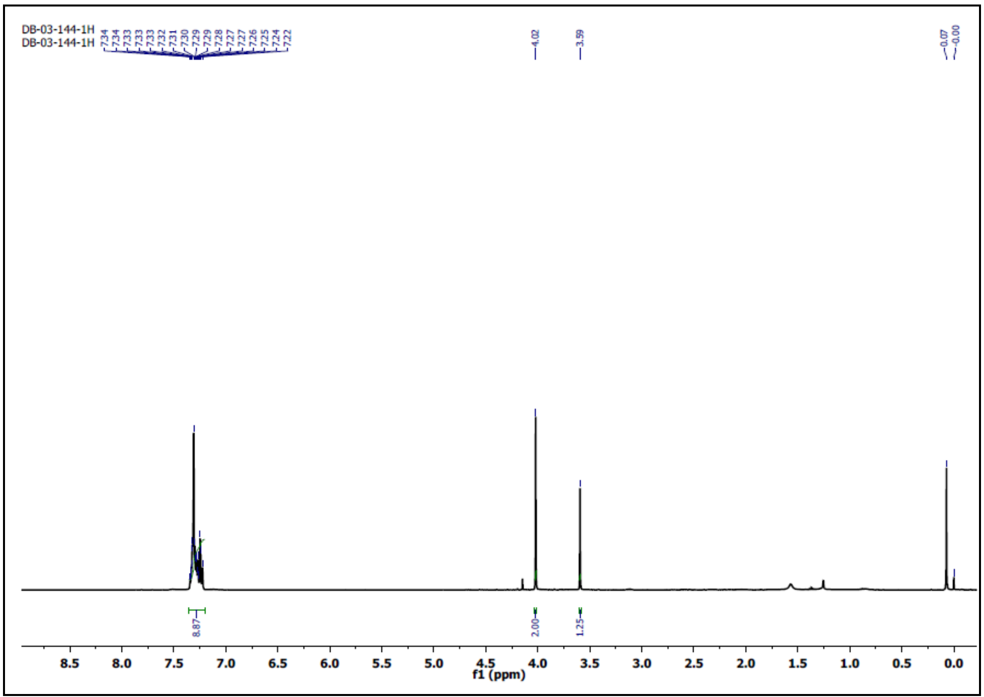

Figure S101: ^{1}H-NMR ($CDCl_3$, 400 MHz, ppm) spectrum of crude product mixture from the reaction of column purified Bunte salt (1.0 equiv) of benzyl bromide with Na_2S (0.5 equiv) **without Na_2SO_3** in water at 50 ºC for 8h. The mixture contained trisulfide **3a** with a significant amount of disulfide **4a** (62:38).

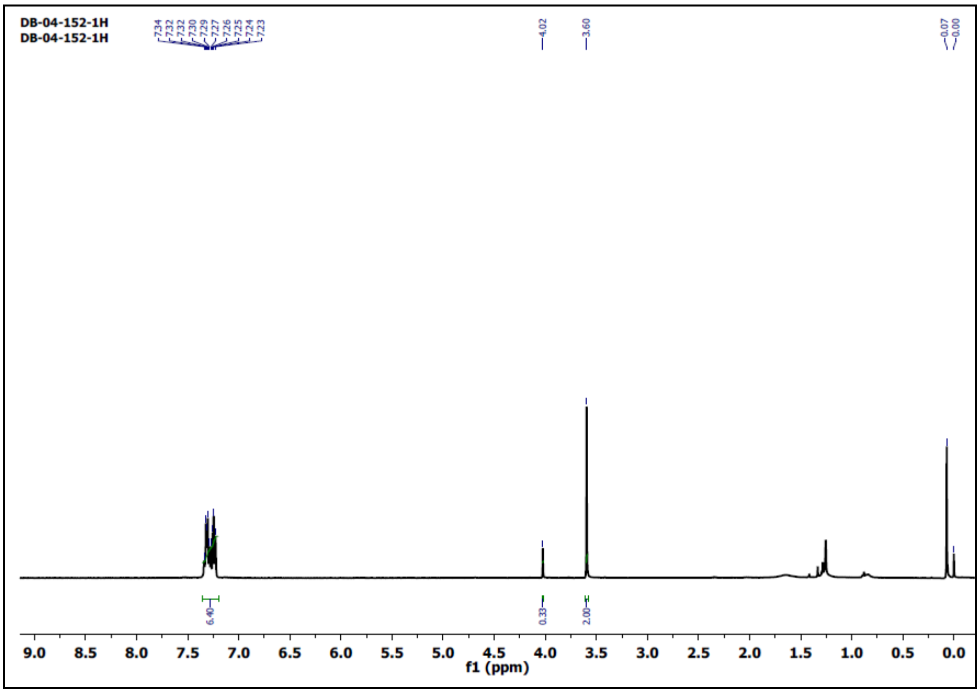

Figure S102: ^{1}H-NMR ($CDCl_3$, 400 MHz, ppm) spectrum of crude product mixture from the reaction of column purified Bunte salt (1.0 equiv) of benzyl bromide with Na_2S (0.5 equiv) and **Na_2SO_3** (5.0 equiv) in water at 50 ºC for 8h. The mixture contained minor amount of trisulfide **3a** and major amount of disulfide **4a** (14:86).

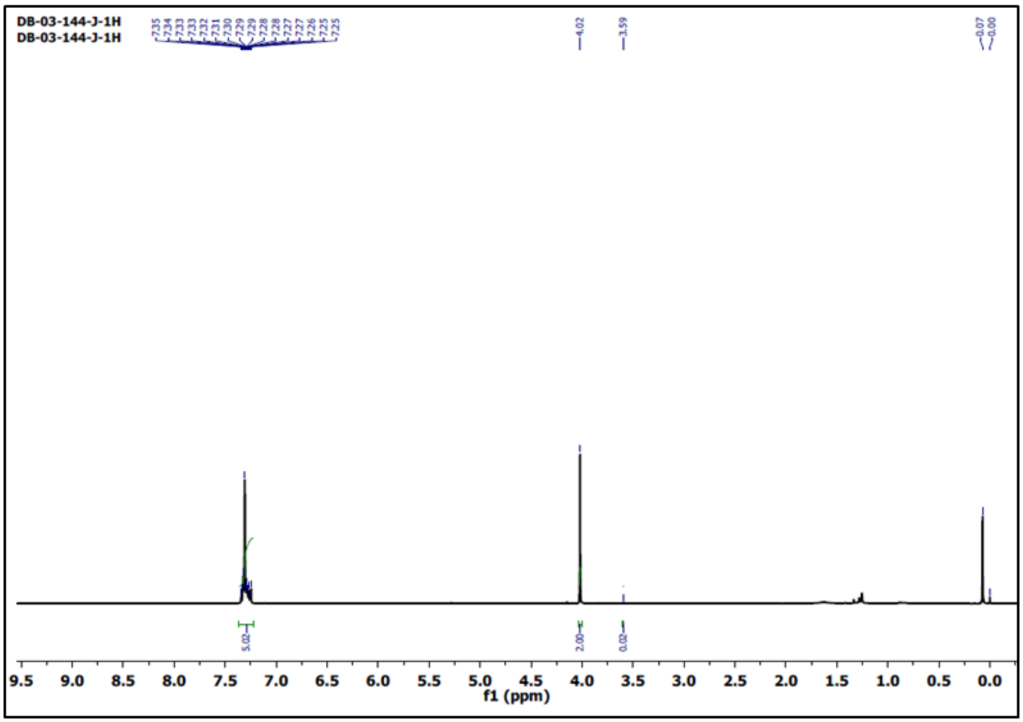

Figure S103: ^{1}H-NMR ($CDCl_3$, 400 MHz, ppm) spectrum of crude product mixture from the reaction of previously synthesized trisulfide **3a** with **Na_2SO_3** (5.0 equiv) in water at 0 ºC for 8h. The disulfide (**4a**) content in the crude product mixture was almost unaltered (99:1).

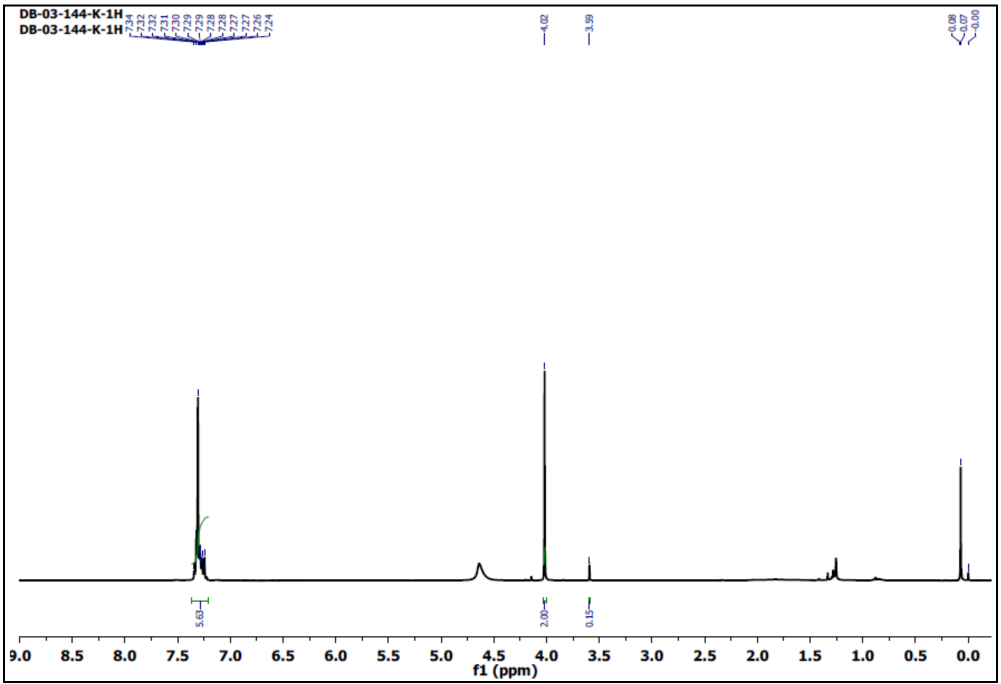

Figure S104: ^{1}H-NMR ($CDCl_3$, 400 MHz, ppm) spectrum of crude product mixture from the reaction of previously synthesized trisulfide **3a** with $\mathbf{Na_2SO_3}$ (5.0 equiv) in water at 50 ºC for 8h. The disulfide content in the crude product mixture was slightly enhanced (93:7).

Cellular morphological study

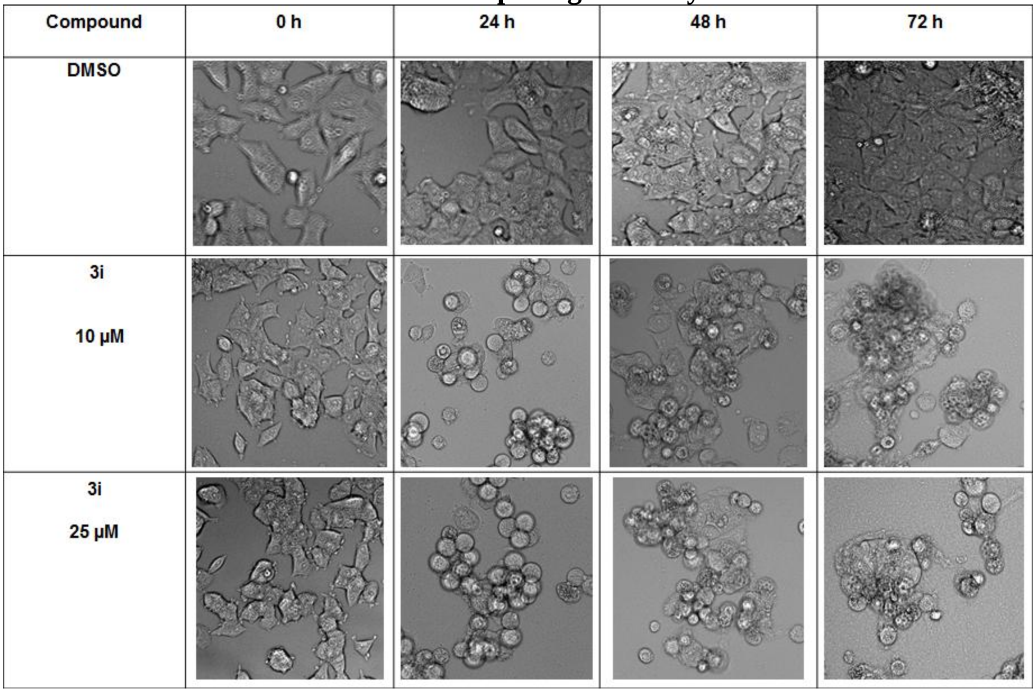

Figure S105: Morphological changes of MCF-7 cells upon the treatment of compound **3i**.

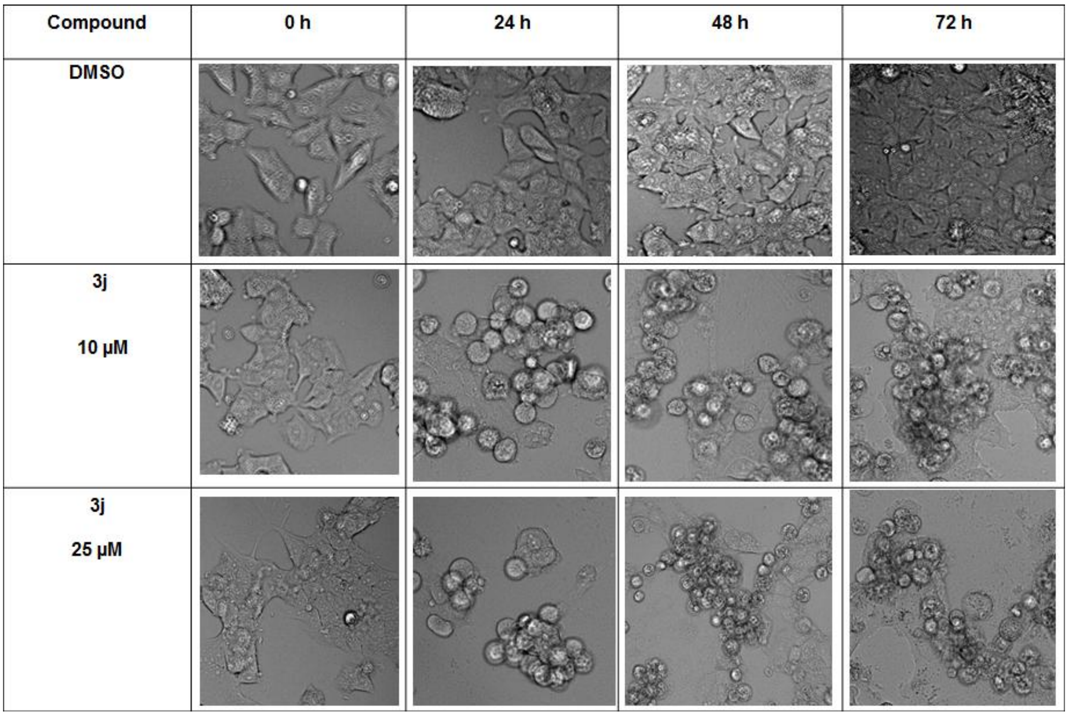

Figure S106: Morphological changes of MCF-7 cells upon the treatment of compound **3j**.

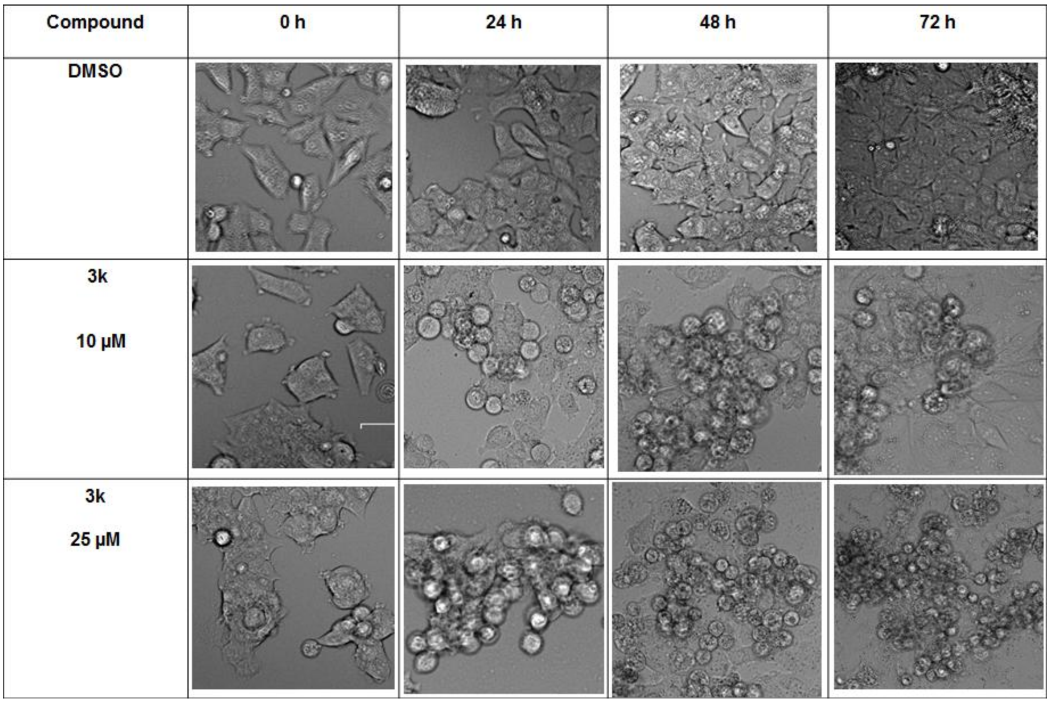

Figure S107: Morphological changes of MCF-7 cells upon the treatment of compound **3k**.

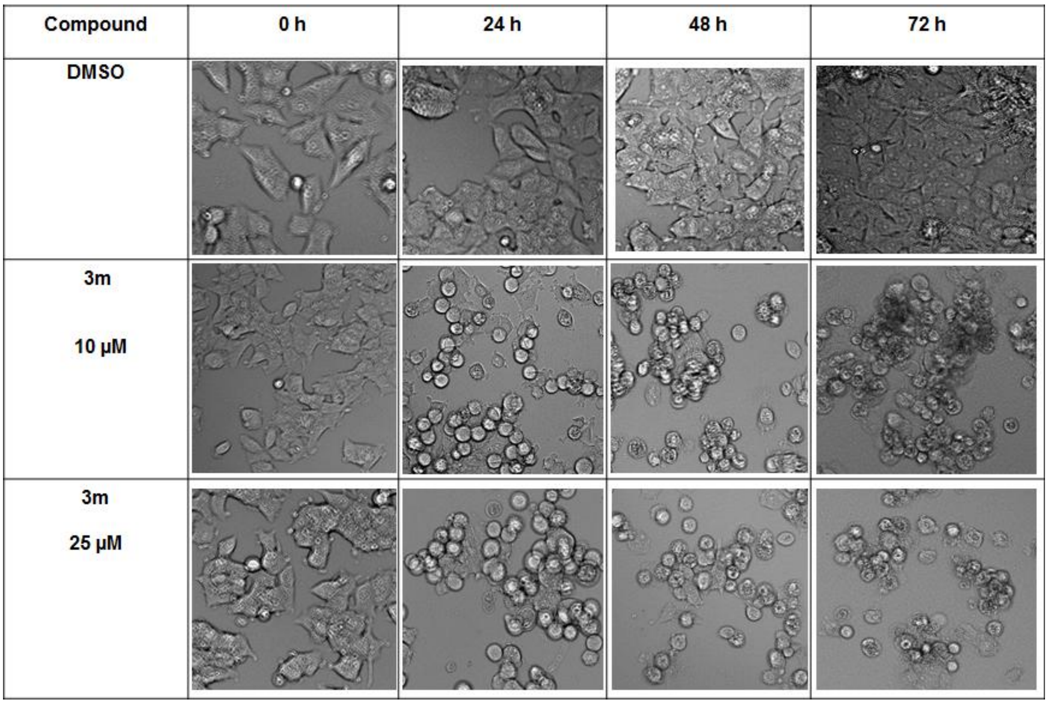

Figure S108: Morphological changes of MCF-7 cells upon the treatment of compound **3m**.

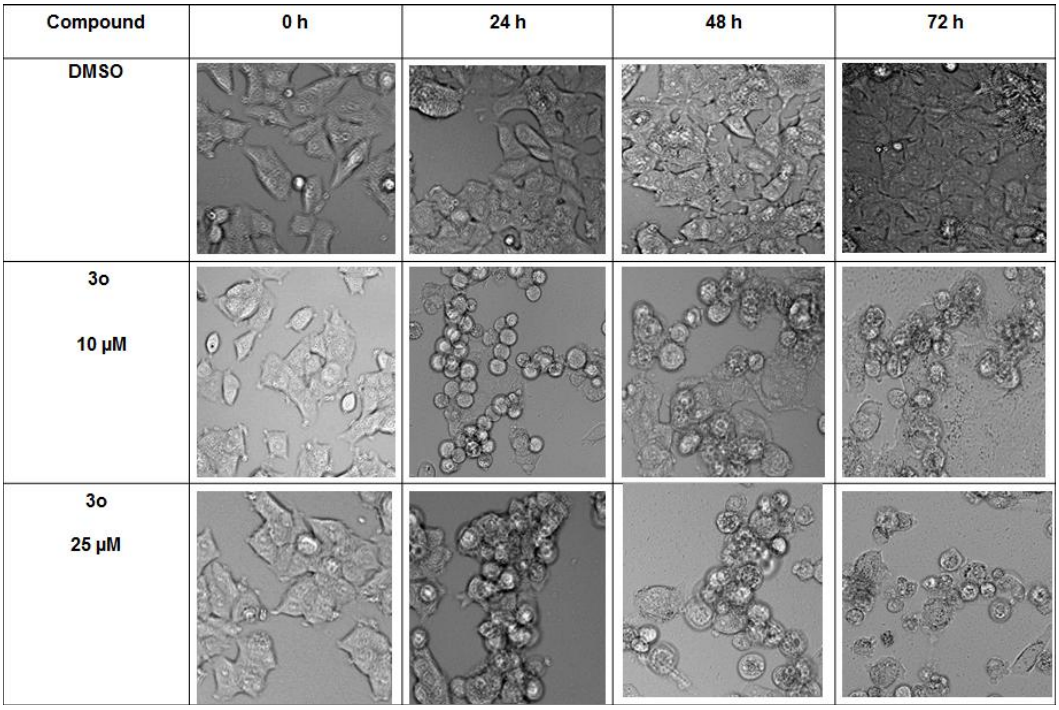

Figure S109: Morphological changes of MCF-7 cells upon the treatment of compound **3o**.

Compound	0 h	24 h	48 h	72 h
DMSO	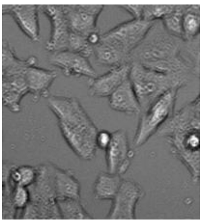	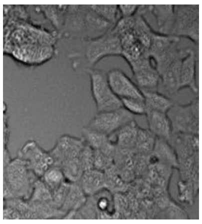	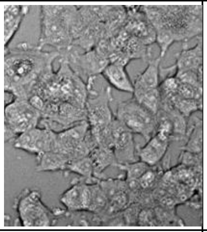	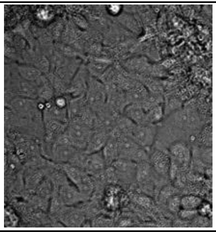
3p 10 µM	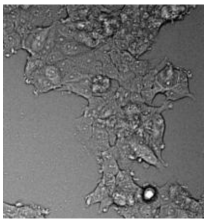	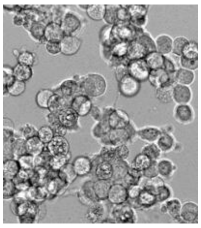	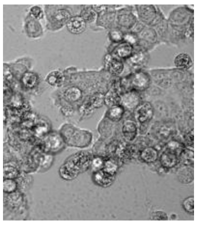	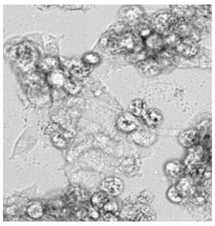
3p 25 µM	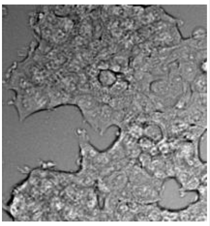	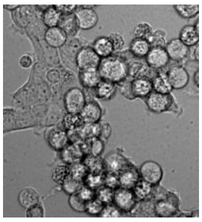	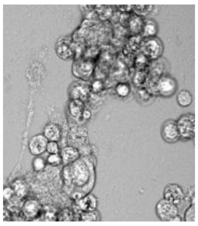	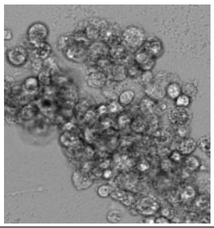

Figure S110: Morphological changes of MCF-7 cells upon the treatment of compound **3p**.

Compound	0 h	24 h	48 h	72 h
DMSO	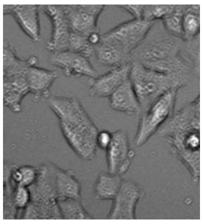	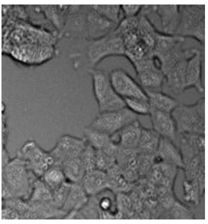	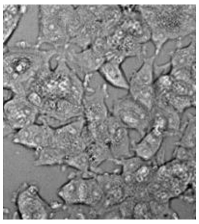	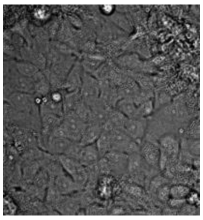
3q 10 µM	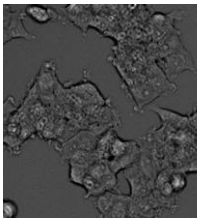	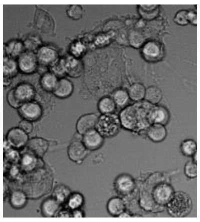	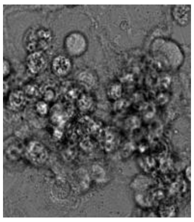	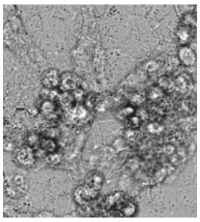
3q 25 µM	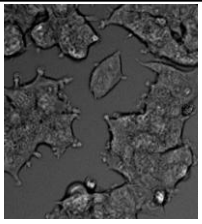	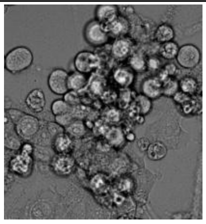	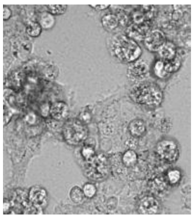	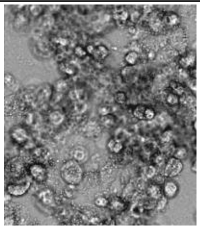

Figure S111: Morphological changes of MCF-7 cells upon the treatment of compound **3q**.

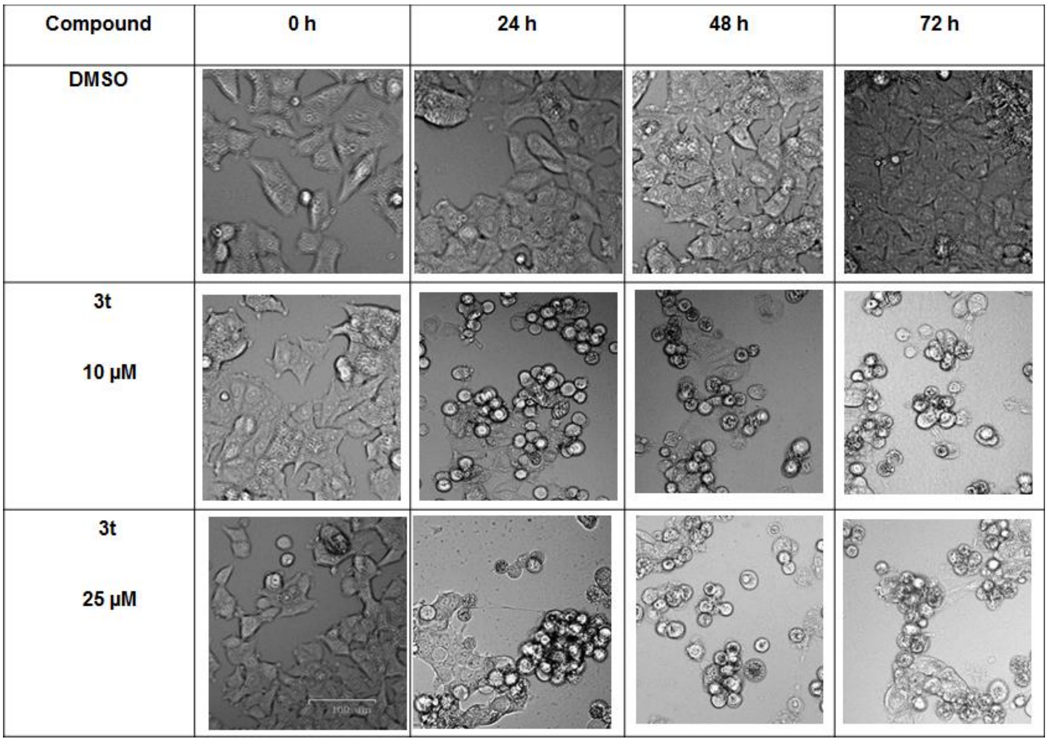

Figure S112: Morphological changes of MCF-7 cells upon the treatment of compound **3t**.

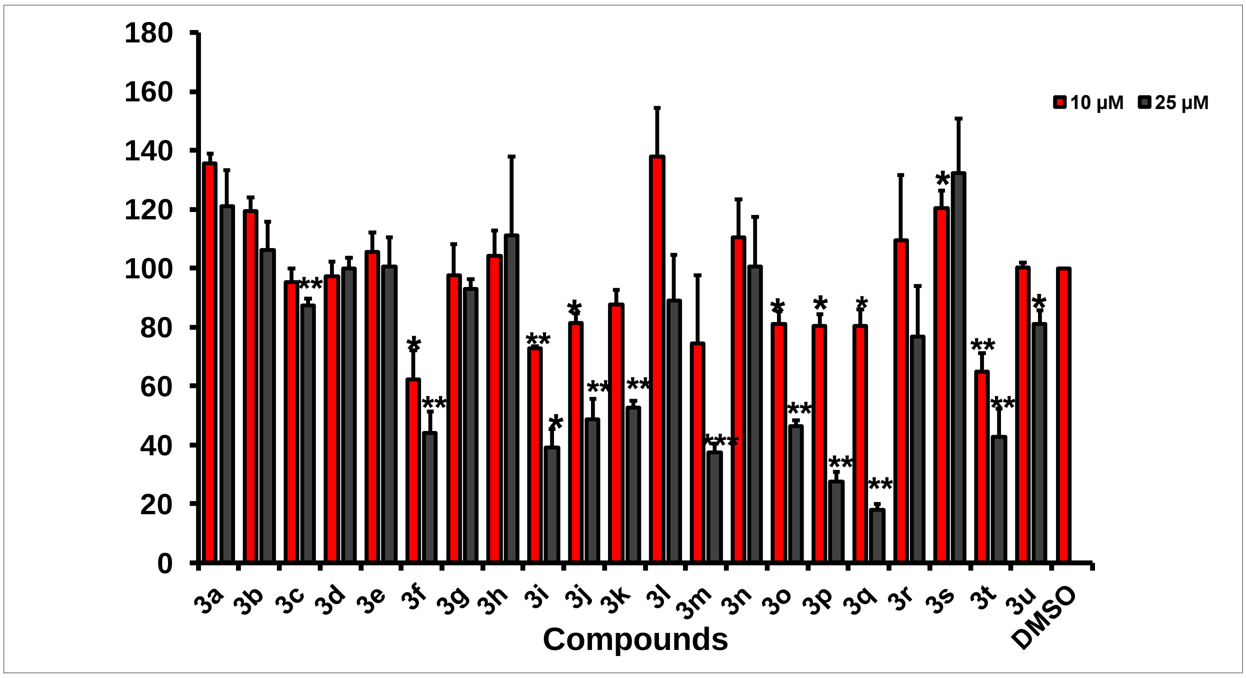

Figure S113: Percentage proliferation of MCF-7 cells in the presence of trisulfides (**3a-3u)** at a concentration of 10 and 25 µM after an incubation of 72h at 37 °C. All data are represented by mean ± SD values and differences between the mean values were assessed by paired t-test. *p<0.05, **p<0.01 indicate the significant difference compared with the control group.

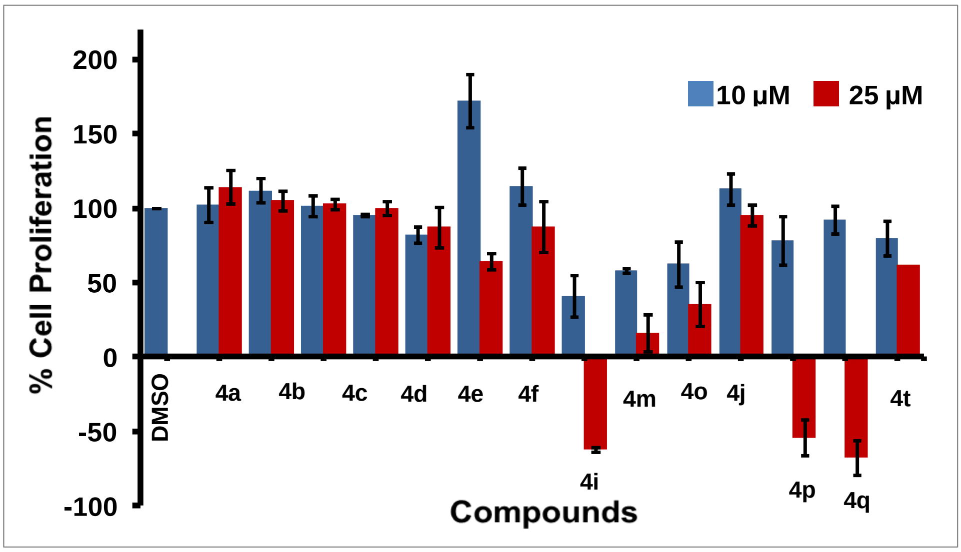

Figure S114: Percentage proliferation of MCF-7 cells in the presence of representative disulfides at a concentration of 10 and 25 µM after an incubation of 72h at 37 °C. We considered 10 µM concentration as a limiting factor for evaluation of their potency in a dose dependency manner.

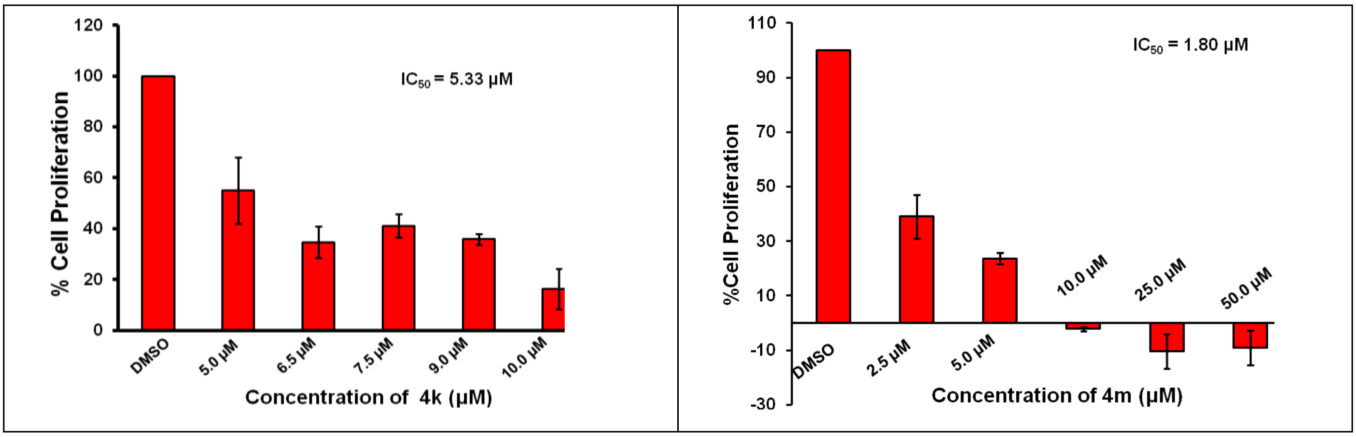

Figure S115: Percentage proliferation of MCF-7 cells in the presence of compounds **4k** and **4m** in a dose-dependent manner after 72h of incubation. Compounds **4k** and **4m** significantly decreased the cellular proliferation at 10 µM concentration and therefore, a dose-dependency was preformed.

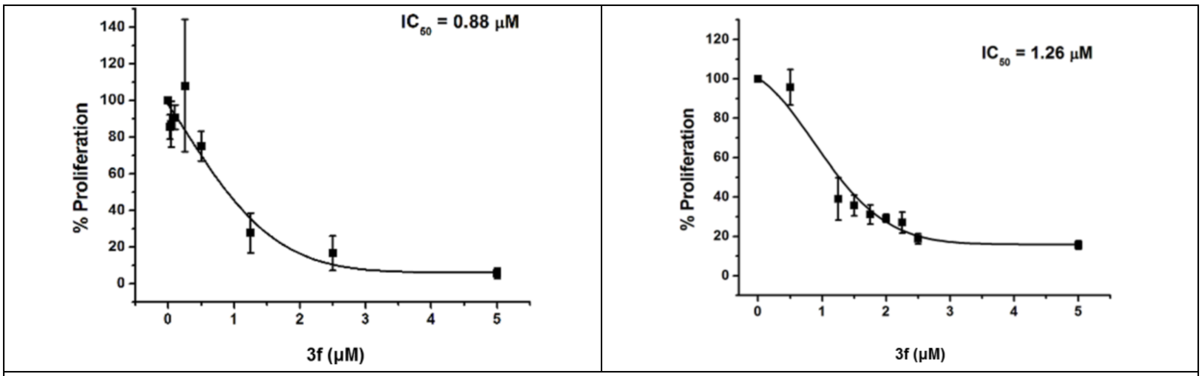

Compound **3f**

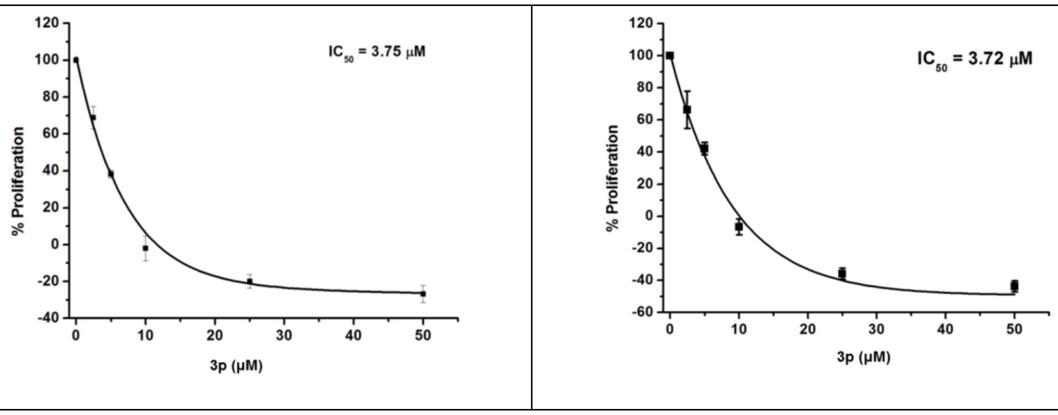

Compound **3p**

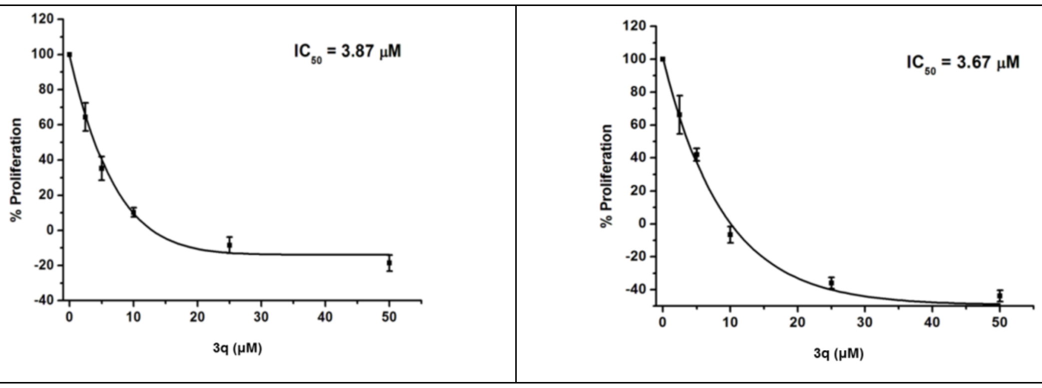

Compound **3q**

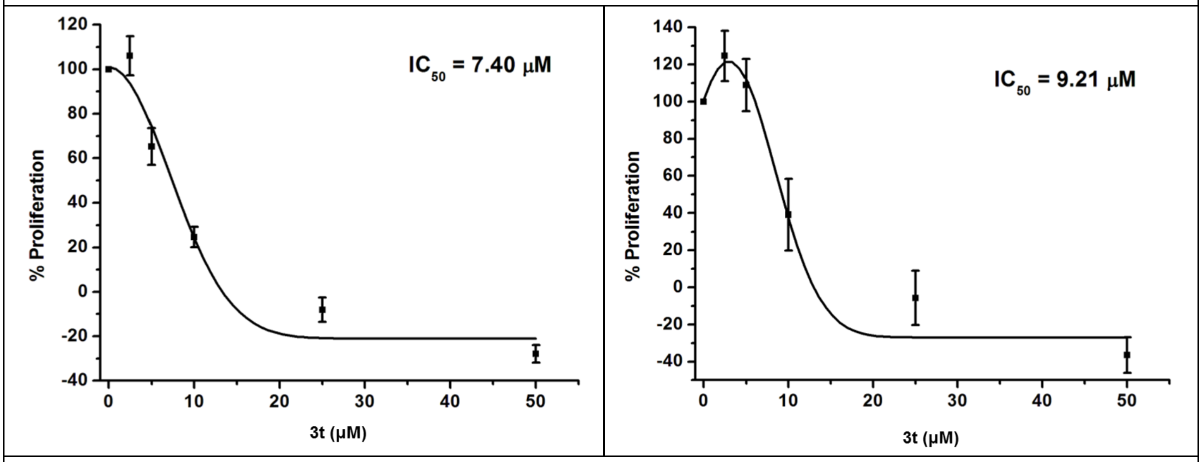

Compound **3t**

Figure S116: Percentage of proliferation of MCF-7 cells in the presence of compounds **3f**, **3p**, **3q** and **3t** in a dose-dependent manner after 72h of incubation.

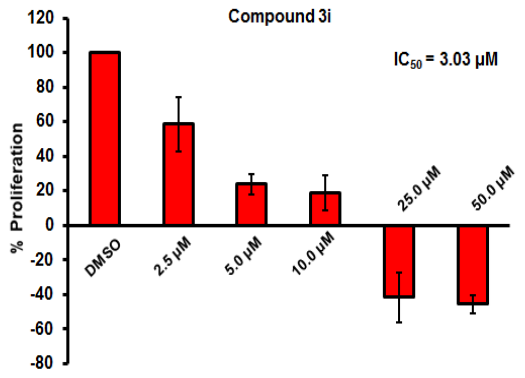

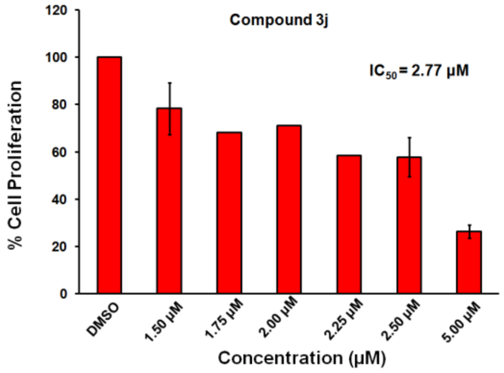

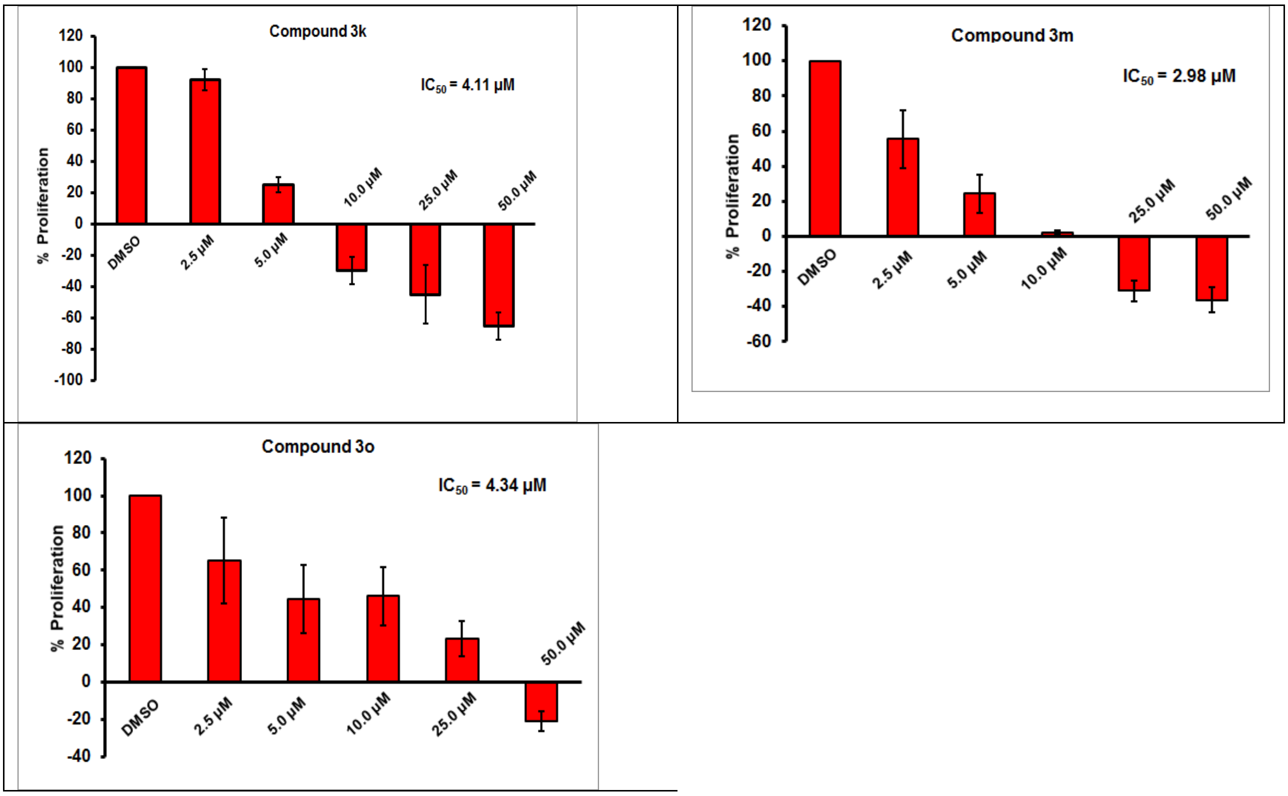

Figure S117: Percentage of proliferation of MCF-7 cells in the presence of compounds **3i**, **3j**, **3k**, **3m, and 3o** in a dose-dependent manner after 72h of incubation.

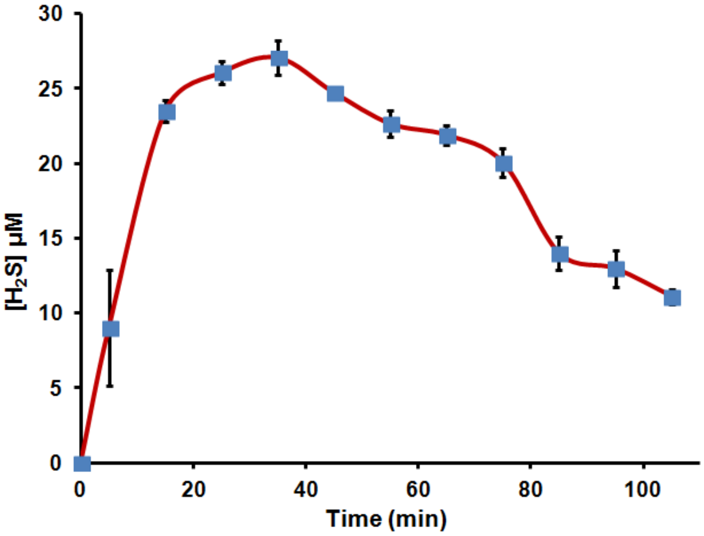

Figure S118: The H_2S release profile of DATS (50 μM) in the presence of GSH (500 μM) using MB assay.

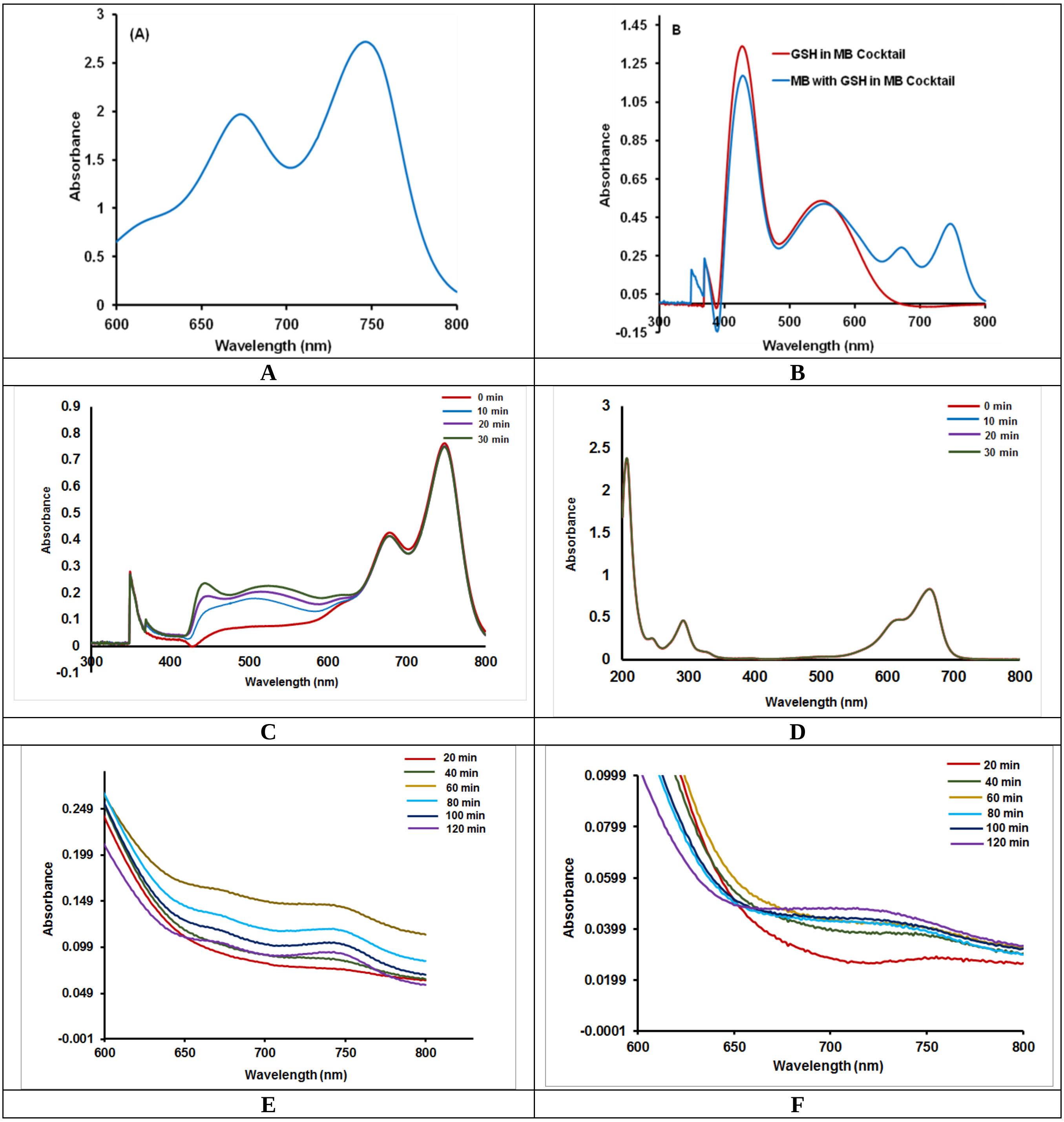

Figure S119. UV-Vis spectral pattern of (A) Pure methylene blue (10.0 µM) in MB-cocktail; (B) Glutathione in MB cocktail (red) and pure MB + GSH in MB cocktail (blue); (C) Pure methylene blue (10.0 µM) and GSH (10 mM) in MB cocktail over time (30 min); (D) Pure methylene blue (10.0 µM) and GSH (10.0 mM) in buffer over time (30 min); (E) UV-Vis spectral pattern of trisulfide **3f** (50.0 µM) in the presence of GSH (500.0 µM) in MB-cocktail showing the characteristic MB spectral pattern; (F) UV-Vis spectral pattern of disulfide **4f** (50.0 µM) in the presence of GSH (500.0 µM) MB-cocktail, which does not show the characteristic MB spectral pattern.

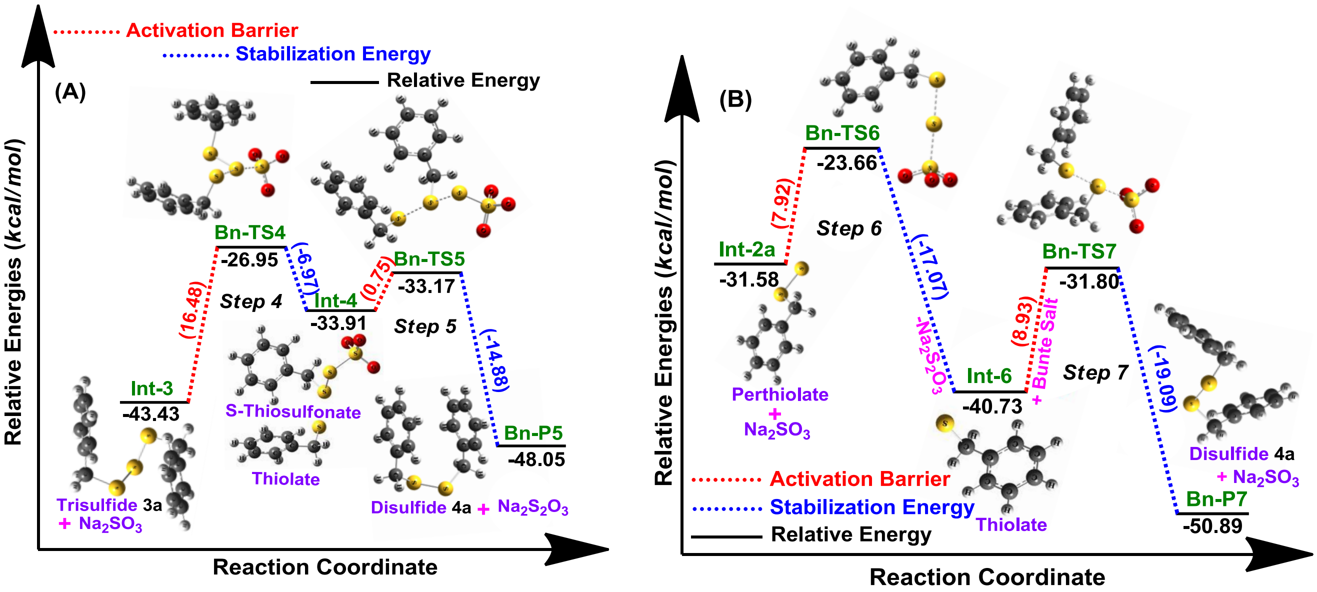

Figure S120. Energy profile diagram for the reaction of trisulfide **3a** (A) and perthiolate intermediate (B) with the co-produced Na_2SO_3 to form disulfide **4a**. Sodium ions are not depicted here for clarity in the representation. All the reported energy values (kcal/mol) were calculated at M06/6-31+G(d) level of DFT in water solvent. See Table S4 and DFT calculation section in ESI for energy values at various levels and further computational details.

Table S4: Energy values at various level of DFT and effect of zero point and free energy correction on the energy profiles of reactions.

Structure	**ΔE(1)**	**ΔZ**	**ΔG**	**ΔE(2)**	**ΔE(3)**	**ΔE(4)**
Bn-R1	0	0	0	0	0	0
Bn-TS1	14.01	13.66	15.09	14.92	13.13	12.30
Int-1	-17.85	-17.10	-14.09	-16.65	-17.46	-22.81
Bn-TS2	-8.96	-9.13	-5.31	-7.74	-6.27	-16.08
Int-2	-37.97	-38.93	-15.37	-36.83	-34.77	-48.74
Bn-TS3	-32.51	-33.53	-7.49	-31.36	-30.78	-44.88
Int-3	-43.43	-44.61	-19.38	-42.25	-44.54	-57.12
Bn-TS4	-26.95	-28.82	-3.39	-25.58	-26.16	-38.69
Int-4	-33.91	-34.61	-10.59	-32.83	-30.94	-44.50
Bn-TS5	-33.17	-34.47	-10.19	-32.02	-30.36	-43.19
Bn-P5	-48.05	-48.06	-22.10	-46.86	-44.86	-58.38
Int-2a	-31.58	-32.79	-30.94	-30.10	-36.28	-41.39
Bn-TS6	-23.66	-24.35	-20.98	-22.28	-24.80	-31.89
Int-6	-40.73	-40.59	-38.12	-39.43	-36.94	-47.62
Bn-TS7	-31.80	-32.48	-28.63	-30.71	-28.13	-41.45
Bn-P7	-50.89	-50.99	-47.06	-49.80	-48.15	-60.75

ΔE(1) = Total Energy at M06/6-31+G(d) level of DFT
ΔZ = Sum of electronic and zero-point Energies at M06/6-31+G(d) level of DFT
ΔG = Sum of electronic and Free Energies at M06/6-31+G(d) level of DFT
ΔE(2) = Total Energy at M06/6-31++G(d,p)//M06/6-31+G(d) level of DFT
ΔE(3) = Total Energy at B3LYP/6-31++G(d,p)//M06/6-31+G(d) level of DFT
ΔE(4) = Total Energy at M06/AUG-cc-pVDZ//M06/6-31+G(d) level of DFT

Effect of water solvent was included in all calculations. See DFT calculation section for details. **ΔE(1)** values were used for making energy profile diagrams (Figure 2 and Figure S120).

Table S5a: Optimized XYX coordinates of Bn-R1 and Bn-TS1.

Bn-R1				**Bn-TS1**			
C	-0.72469	2.926357	-0.76419	C	-3.52462	1.965627	-0.46424
C	-0.42354	1.58803	-0.5246	C	-2.41815	1.162645	-0.71057
C	-1.27668	0.805354	0.259012	C	-1.84269	0.417073	0.325697
C	-2.44473	1.371226	0.777821	C	-2.39276	0.485199	1.611443
C	-2.74229	2.71048	0.544633	C	-3.49395	1.29497	1.859251
C	-1.88188	3.490312	-0.22831	C	-4.06223	2.036583	0.822091
H	-0.04993	3.534261	-1.36544	H	-3.96986	2.541387	-1.27373
H	0.482197	1.131536	-0.92821	H	-1.99362	1.101767	-1.7139
H	-3.11366	0.757531	1.383369	H	-1.93811	-0.09224	2.417404
H	-3.64676	3.147483	0.965113	H	-3.9133	1.350634	2.86228
H	-2.11194	4.539307	-0.40936	H	-4.92626	2.669523	1.017048
O	3.523608	1.050084	-0.8603	O	2.54223	0.585074	-1.60052
S	3.119586	-0.30526	-0.36333	S	2.641162	0.363697	-0.12584
S	2.814429	-0.24426	1.646444	S	1.055061	1.383067	0.732163
O	4.235953	-1.27944	-0.67872	O	3.910553	0.907205	0.440036
O	1.87506	-0.78828	-1.04904	O	2.51219	-1.08552	0.217719
C	-0.92985	-0.60674	0.558139	C	-0.66589	-0.39571	0.077973
H	0.14151	-0.81238	0.479082	H	-0.19977	-0.41247	-0.89933
H	-1.32192	-0.94416	1.521072	H	-0.18974	-0.95154	0.872975
Br	-1.77263	-1.82338	-0.76239	Br	-1.81051	-2.54076	-0.5346

Na	5.780568	0.385449	-1.48753	Na	4.5002	-1.33449	1.523615
Na	2.766418	-2.85119	-1.83162	Na	0.958073	2.218033	-2.23823

Table S5b: Optimized XYX coordinates of Int-1 and Bn-TS2.

Int-1				Bn-TS2			
C	-4.42229	0.950849	-0.56632	C	2.465671	-3.17381	-0.25613
C	-3.13286	0.731238	-1.04915	C	1.404179	-2.4497	-0.79882
C	-2.05233	0.630664	-0.16973	C	1.324317	-1.06357	-0.6354
C	-2.28291	0.763526	1.204461	C	2.343938	-0.40987	0.069295
C	-3.5687	0.980508	1.689289	C	3.402785	-1.13177	0.61449
C	-4.64271	1.074788	0.803276	C	3.466433	-2.51701	0.45592
H	-5.25558	1.023817	-1.26359	H	2.509032	-4.25379	-0.39063
H	-2.95992	0.631832	-2.12152	H	0.62092	-2.96758	-1.35289
H	-1.44123	0.693612	1.896456	H	2.292698	0.674147	0.189203
H	-3.73558	1.074955	2.76125	H	4.186397	-0.6091	1.161914
H	-5.64949	1.243245	1.182193	H	4.295672	-3.07947	0.882605
C	-0.66665	0.394102	-0.68405	C	0.190755	-0.29455	-1.24569
H	-0.12228	-0.31208	-0.03303	H	0.564188	0.467656	-1.94401
H	-0.6786	-0.0076	-1.70406	H	-0.47476	-0.96462	-1.80027
O	2.483635	0.653094	0.640555	O	1.410549	2.776389	-0.24795
S	2.240789	1.2374	-0.70429	S	-0.04492	2.64588	-0.56623
O	3.045199	2.436423	-0.98793	O	-0.89417	3.553432	0.286874
S	0.247731	1.996389	-0.70394	S	-0.87984	0.598525	-0.02868
O	2.290679	0.185769	-1.74938	O	-0.32234	2.948085	-2.02029
S	0.621304	-2.69097	1.31377	S	-2.16377	-1.73454	0.647412
Na	-2.07755	-2.89804	0.914975	Na	-3.63294	-0.15832	-1.06471
Na	2.528649	-1.89827	-0.51499	Na	0.065242	-1.61722	2.21963
Na	1.479695	-0.38454	2.521584	Na	-1.962	4.679813	-1.57243

Table S5c: Optimized XYX coordinates of Int-2 and Bn-TS3.

Int-2				Bn-TS3			
C	0.822982	2.569235	-1.6643	C	0.293585	2.685883	1.358449
C	0.736703	1.809885	-0.50089	C	0.390963	2.113632	0.093816
C	1.463184	2.165153	0.64045	C	-0.75261	1.902075	-0.68447
C	2.293188	3.288729	0.5886	C	-1.99595	2.276524	-0.16487
C	2.38353	4.050558	-0.57548	C	-2.09737	2.84779	1.102083
C	1.647803	3.69384	-1.7049	C	-0.9515	3.055332	1.867943
H	0.244735	2.277202	-2.54169	H	1.19264	2.839636	1.955223
H	0.097674	0.924674	-0.47228	H	1.363652	1.802901	-0.29354
H	2.86816	3.56931	1.472806	H	-2.89425	2.119115	-0.76468
H	3.029214	4.927432	-0.59942	H	-3.07348	3.134838	1.490871
H	1.718964	4.289698	-2.6137	H	-1.02731	3.503018	2.857783
C	1.388163	1.310252	1.863067	C	-0.66193	1.248991	-2.02652
H	1.604846	1.876483	2.778895	H	-1.42532	1.639292	-2.71175
H	0.402389	0.833946	1.962449	H	0.323997	1.38742	-2.48525
S	2.632349	-0.0447	1.697707	S	-0.91734	-0.59315	-1.89165
S	2.246248	-1.25883	3.376518	S	0.807414	-1.42744	-2.70796
C	2.833305	-3.08553	-1.36901	C	-1.08158	-3.17258	1.312712
C	1.580145	-3.26656	-0.78578	C	0.089857	-3.20382	0.556863

C	0.490771	-2.48669	-1.18107
C	0.674417	-1.51984	-2.17572
C	1.925025	-1.336	-2.75699
C	3.008464	-2.11959	-2.35728
H	3.67276	-3.70133	-1.04936
H	1.443926	-4.02081	-0.00922
H	-0.17109	-0.89892	-2.47664
H	2.056995	-0.57861	-3.52894
H	3.985963	-1.97655	-2.81526
C	-0.84891	-2.68863	-0.54493
H	-1.66274	-2.69067	-1.28125
H	-0.8922	-3.64379	-0.00867
O	-2.19236	0.268879	-1.56408
S	-2.79444	-0.33499	-0.34876
O	-3.16153	0.705613	0.646318
S	-1.26407	-1.38873	0.702113
O	-3.8569	-1.31176	-0.64531
Na	-2.78003	2.662612	-0.76163
Na	4.537804	0.175603	4.289813

C	1.09384	-2.2541	0.754335
C	0.910347	-1.27265	1.735196
C	-0.25891	-1.23668	2.488979
C	-1.2616	-2.18514	2.278455
H	-1.8563	-3.91925	1.142513
H	0.223872	-3.97232	-0.20593
H	1.6943	-0.52902	1.893469
H	-0.38989	-0.46326	3.246094
H	-2.17685	-2.15464	2.86828
C	2.345611	-2.29966	-0.06853
H	3.238048	-2.38382	0.566952
H	2.339345	-3.16712	-0.73763
O	3.898707	0.374291	1.639832
S	4.368378	-0.02732	0.258441
O	4.818414	1.236975	-0.46912
S	2.623904	-0.80781	-1.13306
O	5.55109	-0.96787	0.341964
Na	4.378321	2.740174	1.34013
Na	7.099004	0.523591	-0.77349

Table S5d: Optimized XYX coordinates of Int-3 and Bn-TS4.

Int-3

C	0.34121	3.10667	1.904426
C	1.312199	2.249576	2.421831
C	2.373677	1.81423	1.626101
C	2.446993	2.250138	0.297954
C	1.479491	3.102279	-0.22196
C	0.422772	3.534653	0.582049
H	-0.47927	3.440593	2.537954
H	1.246954	1.914355	3.457904
H	3.268219	1.90527	-0.33321
H	1.547899	3.432047	-1.25806
H	-0.32945	4.211368	0.179072
C	3.393076	0.870116	2.176922
H	4.413775	1.153089	1.883738
H	3.353853	0.822442	3.271677
S	3.235091	-0.84891	1.515353
S	1.408817	-1.46344	2.307833
C	3.081673	-3.46394	-1.55528
C	1.919749	-3.37626	-0.78862
C	0.989322	-2.36166	-1.0228
C	1.23247	-1.43425	-2.04339
C	2.38904	-1.5248	-2.8108
C	3.320479	-2.53626	-2.56574
H	3.799762	-4.25963	-1.36118
H	1.73362	-4.10161	0.005028
H	0.500891	-0.64249	-2.23248
H	2.568116	-0.80238	-3.60664
H	4.226437	-2.60306	-3.16666

Bn-TS4

C	-1.93371	-4.11536	-0.47815
C	-1.0141	-3.36032	0.249689
C	-1.44926	-2.38338	1.148375
C	-2.82449	-2.17996	1.310738
C	-3.74421	-2.92952	0.586226
C	-3.29977	-3.90058	-0.31346
H	-1.57953	-4.87366	-1.17517
H	0.056254	-3.52966	0.12183
H	-3.17288	-1.41698	2.009659
H	-4.81128	-2.76056	0.724268
H	-4.01857	-4.48997	-0.88075
C	-0.46632	-1.55304	1.90454
H	-0.79797	-1.37295	2.937066
H	0.524985	-2.022	1.944658
S	-0.26365	0.158179	1.237501
S	0.612213	-0.17052	-0.6071
C	-1.2852	3.98072	0.792092
C	-0.93997	3.302099	-0.37729
C	-1.88745	2.554483	-1.08087
C	-3.20005	2.517491	-0.59413
C	-3.55108	3.193936	0.569308
C	-2.59062	3.924737	1.2729
H	-0.52864	4.552828	1.328385
H	0.084954	3.348843	-0.74942
H	-3.94943	1.937854	-1.13634
H	-4.57815	3.154551	0.930928
H	-2.86334	4.453577	2.185213

C	-0.22635	-2.23226	-0.16487	C	-1.50916	1.79436	-2.31553
H	-1.12197	-1.97734	-0.7507	H	-2.21758	2.007867	-3.12862
H	-0.43152	-3.14765	0.402925	H	-0.51347	2.109114	-2.65941
O	-1.32	0.80685	-2.63723	O	3.022134	-0.34138	1.686844
S	-2.22941	0.558665	-1.40852	S	2.800453	-0.38684	0.198226
O	-2.85093	1.966959	-1.10796	O	3.598746	0.743594	-0.44284
S	-0.1142	-0.82221	1.029582	S	-1.5079	-0.03563	-2.07523
O	-3.42873	-0.28629	-1.90173	O	3.276467	-1.68723	-0.40185
Na	-1.55932	3.13911	-2.67136	Na	4.472042	1.669906	1.583563
Na	-5.05625	1.37998	-1.6094	Na	4.718888	-0.66407	-2.06452

Table S5e: Optimized XYX coordinates of Int-4, Bn-TS4 and Bn-P5.

Int-4				**Bn-TS5**				**Bn-P5**			
C	-0.35006	4.321036	-0.71828	C	-1.09548	4.324267	-0.22595	C	-1.43942	3.038867	0.646218
C	0.224522	3.102121	-1.07743	C	-0.31851	3.281646	-0.73084	C	-0.60455	1.967504	0.348085
C	-0.51592	1.918473	-1.01694	C	-0.83422	1.987153	-0.8289	C	-0.86839	1.145724	-0.75482
C	-1.84692	1.976369	-0.58564	C	-2.14555	1.749897	-0.39794	C	-1.98071	1.421456	-1.5529
C	-2.42182	3.190883	-0.22623	C	-2.92216	2.787681	0.10723	C	-2.81857	2.495359	-1.25502
C	-1.67479	4.36817	-0.29201	C	-2.40099	4.080157	0.192177	C	-2.54961	3.306804	-0.15638
H	0.240916	5.23436	-0.77107	H	-0.67676	5.327444	-0.15714	H	-1.22092	3.673533	1.504472
H	1.261715	3.065253	-1.41354	H	0.706261	3.471175	-1.05511	H	0.272187	1.753392	0.964979
H	-2.43421	1.056906	-0.52217	H	-2.5521	0.736735	-0.44858	H	-2.19405	0.784442	-2.41359
H	-3.45963	3.221249	0.104123	H	-3.94229	2.589236	0.435155	H	-3.68584	2.696441	-1.88311
H	-2.12653	5.318623	-0.01174	H	-3.01123	4.89193	0.585519	H	-3.20391	4.145794	0.077751
C	0.10308	0.618853	-1.4095	C	-0.00427	0.890509	-1.41834	C	0.051573	0.017852	-1.0831
H	-0.58058	-0.00232	-2.00447	H	-0.51105	0.429881	-2.27382	H	-0.11224	-0.36396	-2.09806
H	1.040095	0.757724	-1.96141	H	0.971132	1.261676	-1.75342	H	1.100667	0.337814	-1.00194
S	0.467604	-0.5108	0.013922	S	0.315438	-0.52501	-0.26484	S	-0.01334	-1.43752	0.059512
S	1.896101	0.577674	1.064194	S	1.764406	0.65348	1.055882	S	2.729342	0.262013	1.678188
C	-5.51017	-0.47004	0.449108	C	-5.37356	-1.20921	0.286114	C	-5.58926	-0.17917	-0.5413
C	-4.68921	-1.53063	0.077241	C	-4.34131	-1.99009	-0.2241	C	-4.73504	-1.27637	-0.51755
C	-3.41882	-1.69465	0.644342	C	-3.09768	-2.05008	0.417072	C	-3.76754	-1.40606	0.485167
C	-3.00192	-0.77082	1.607456	C	-2.92026	-1.31336	1.591162	C	-3.6752	-0.41552	1.465758
C	-3.82052	0.293117	1.985916	C	-3.95182	-0.52967	2.108354	C	-4.52646	0.687835	1.441097
C	-5.07672	0.450574	1.405498	C	-5.18119	-0.47218	1.456427	C	-5.48588	0.807421	0.439842
H	-6.49497	-0.36099	-0.00467	H	-6.33394	-1.17677	-0.2275	H	-6.34127	-0.09293	-1.3246
H	-5.03029	-2.24635	-0.67349	H	-4.49087	-2.56191	-1.14184	H	-4.817	-2.04893	-1.28458
H	-2.01342	-0.88335	2.056055	H	-1.95682	-1.35131	2.101603	H	-2.92777	-0.51244	2.254931
H	-3.46943	1.006749	2.731403	H	-3.79142	0.041218	3.022561	H	-4.43507	1.457772	2.206417
H	-5.71591	1.28384	1.695235	H	-5.98759	0.141163	1.856496	H	-6.15073	1.67004	0.420344
C	-2.52958	-2.82132	0.214815	C	-1.98614	-2.87452	-0.15618	C	-2.8685	-2.59704	0.517063
H	-1.72534	-2.95386	0.953117	H	-1.19553	-3.01852	0.594927	H	-2.39853	-2.72827	1.499257
H	-3.10531	-3.75788	0.190714	H	-2.35456	-3.87138	-0.4353	H	-3.423	-3.51866	0.29038
O	3.520757	0.598682	-1.38858	O	3.413644	0.977751	-1.33962	O	3.04605	1.685506	-0.83949
S	3.713678	0.117052	-0.01	S	3.536172	0.293751	-0.03554	S	3.813387	0.731845	0.005252
O	3.929933	-1.34845	0.086937	O	3.674524	-1.19173	-0.19208	O	4.069005	-0.56192	-0.74469
S	-1.78329	-2.54762	-1.46115	S	-1.23602	-2.12377	-1.66471	S	-1.52028	-2.63977	-0.75061
O	4.717573	0.870981	0.784141	O	4.625667	0.817833	0.830339	O	5.14518	1.296717	0.406629
Na	0.870723	-3.5214	-1.27922	Na	2.197534	-2.36146	-1.66551	Na	3.202675	-2.42927	0.381876

Na	5.923314	-1.16982	1.61652	Na	5.67187	-1.43984	1.25247	Na	6.475063	-0.4225	-0.61484

Table S5f: Optimized XYX coordinates of Int-2a and Bn-TS6.

Int-2a				Bn-TS6			
C	-0.48748	-0.05043	-0.05675	C	1.101423	1.105082	-0.6571
C	0.690913	-0.47933	0.549224	C	1.269375	-0.27566	-0.62384
C	1.819765	0.345296	0.578358	C	1.82678	-0.90787	0.495898
C	1.748451	1.606566	-0.02263	C	2.19404	-0.11802	1.590395
C	0.572393	2.038606	-0.63058	C	2.031091	1.267408	1.56004
C	-0.54953	1.210695	-0.64797	C	1.487198	1.884132	0.435708
H	-1.36059	-0.70143	-0.06556	H	0.664527	1.577767	-1.53604
H	0.74106	-1.4667	1.010935	H	0.974384	-0.88266	-1.48199
H	2.626957	2.254027	-0.00759	H	2.612871	-0.59898	2.475107
H	0.530241	3.025503	-1.08925	H	2.326086	1.8653	2.421712
H	-1.4705	1.548494	-1.12057	H	1.357453	2.965142	0.411041
C	3.094305	-0.13419	1.193793	C	2.043448	-2.38837	0.50024
H	3.676278	0.690684	1.627667	H	2.186308	-2.75314	1.526843
H	2.911936	-0.88205	1.976964	H	1.17017	-2.90461	0.077689
O	10.27353	-3.36442	2.158401	O	7.772956	-2.86025	3.210539
S	9.160346	-2.7038	3.00871	S	7.114656	-1.64189	2.56067
O	8.221531	-3.84096	3.482399	O	6.602971	-0.70993	3.661436
S	4.123909	-0.92874	-0.11843	S	3.507311	-2.90785	-0.50103
O	9.903256	-2.26006	4.318485	O	8.264189	-0.87047	1.862212
S	5.83961	-1.5337	0.946654	S	5.32956	-2.28821	1.015738
Na	6.653886	1.088675	0.232277	Na	4.753237	-0.16635	-0.78924
Na	8.761056	-3.7114	5.75887	Na	8.097469	1.059563	3.204266
Na	12.05204	-2.9208	3.623937	Na	9.934008	-2.48064	2.314903

Table S5g: Optimized XYX coordinates of Int-6, Bn-TS7 and Bn-P7.

Int-6				Bn-TS7				Bn-P7			
C	13.80873	-3.0361	1.541253	C	-0.87667	2.873728	-1.82362	C	-3.63899	2.300091	-0.27277
C	13.32932	-1.84169	1.007496	C	-1.17952	1.915338	-0.86117	C	-2.55239	2.255951	0.599725
C	14.08148	-1.13325	0.067344	C	-0.95716	2.175578	0.496877	C	-1.25782	2.055018	0.113708
C	15.32286	-1.63717	-0.33193	C	-0.44587	3.421934	0.86498	C	-1.06054	1.917575	-1.26633
C	15.80265	-2.83101	0.198513	C	-0.14071	4.384196	-0.09747	C	-2.14412	1.971286	-2.13772
C	15.04592	-3.53361	1.136778	C	-0.34917	4.110248	-1.44672	C	-3.43696	2.157537	-1.64425
H	13.21239	-3.58037	2.271927	H	-1.05022	2.654943	-2.87689	H	-4.6439	2.452252	0.119117
H	12.36111	-1.45025	1.32579	H	-1.57828	0.941629	-1.15879	H	-2.70905	2.37324	1.673538
H	15.91376	-1.0767	-1.05803	H	-0.27787	3.640504	1.920351	H	-0.04372	1.752906	-1.63605
H	16.76858	-3.21795	-0.12283	H	0.264081	5.347969	0.209033	H	-1.98229	1.866229	-3.21022
H	15.42034	-4.46846	1.55083	H	-0.10606	4.856346	-2.20188	H	-4.28387	2.196663	-2.32791
C	13.57827	0.162134	-0.48316	C	-1.26535	1.143689	1.539133	C	-0.09621	1.970421	1.046812
H	13.92976	0.329674	-1.50845	H	-1.04705	1.526119	2.543097	H	0.819581	2.4063	0.620793
H	12.48249	0.202362	-0.49705	H	-2.32559	0.856485	1.518344	H	-0.30669	2.441112	2.015008
O	16.36734	1.693711	-1.37867	O	-2.50717	-1.2425	-1.04463	O	3.095343	2.226685	0.284863
S	15.29661	2.618244	-0.94338	S	-2.34313	-1.53961	0.44596	S	3.463408	1.380219	-0.96061
O	15.82606	3.773008	-0.18064	O	-3.64243	-1.09705	1.121228	O	3.823615	-0.02578	-0.36122
S	14.14352	1.60241	0.534238	S	-0.33192	-0.4448	1.352692	S	0.479008	0.247798	1.379935
O	14.36748	2.981141	-2.03547	O	-2.1099	-3.01401	0.65864	O	2.147526	1.127942	-1.73772
S	11.46952	5.030288	-0.08946	S	1.728332	0.490823	2.166614	S	-0.96759	-0.56339	2.623136

C	10.29517	4.0439	0.95611	C	2.460788	1.158783	0.605299	C	-2.25421	-1.2794	1.492182
C	9.710063	2.879048	0.220199	C	2.850859	0.100996	-0.38028	C	-1.71789	-2.10203	0.367634
C	8.690489	3.071464	-0.72187	C	3.985945	-0.68926	-0.16425	C	-1.0708	-3.3196	0.604138
C	10.17043	1.57571	0.437494	C	2.095837	-0.11693	-1.53622	C	-1.86079	-1.65866	-0.94896
C	8.159457	2.001373	-1.4351	C	4.356318	-1.67283	-1.07588	C	-0.58111	-4.07851	-0.45408
H	8.316875	4.082251	-0.89601	H	4.58123	-0.52688	0.736268	H	-0.95056	-3.67105	1.630185
C	9.641494	0.498677	-0.27575	C	2.462108	-1.10307	-2.45202	C	-1.37595	-2.41882	-2.01292
H	10.95368	1.406894	1.180883	H	1.212534	0.497302	-1.72084	H	-2.35907	-0.70659	-1.14201
C	8.636749	0.707439	-1.21748	C	3.592477	-1.88476	-2.22475	C	-0.73456	-3.63107	-1.76793
H	7.366233	2.174057	-2.16172	H	5.245253	-2.27517	-0.89203	H	-0.08432	-5.0272	-0.25579
H	10.00857	-0.51071	-0.08729	H	1.862767	-1.25846	-3.34841	H	-1.50015	-2.06004	-3.03402
H	8.221789	-0.13238	-1.77276	H	3.880615	-2.65399	-2.93985	H	-0.35541	-4.22771	-2.59618
H	10.82327	3.685434	1.851038	H	1.745477	1.861702	0.158079	H	-2.85343	-1.88226	2.189491
H	9.488972	4.708809	1.297535	H	3.3426	1.734936	0.918208	H	-2.88423	-0.46424	1.118308
Na	12.00567	3.171574	-2.16294	Na	1.576878	2.594807	4.221995	Na	3.66283	0.609338	1.894392
Na	18.17706	3.120271	-0.04792	Na	-4.55288	-0.04811	-0.80547	Na	1.943363	-1.14967	-1.22795

References

[1] Z. Wu, D. Liang, X. Tang, *Anal Chem* **2016**, *88*, 9213-9218.

[2] H. Distler, *Angew Chem Int Ed* **1967**, *6*, 544-553.

[3] A. Baker, M. Graz, R. Saunders, G. J. S. Evans, S. Kaul, T. Wirth, *J Flow Chem* **2013**, *3*, 118-121.

[4] F. K. Ren, X. Y. He, L. Deng, B. H. Li, D. S. Shin, Z. B. Li, *B Korean Chem Soc* **2009**, *30*, 687-690.

[5] V. Panduranga, G. Prabhu, Basavaprabhu, N. R. Panguluri, V. V. Sureshbabu, *Synthesis-Stuttgart* **2016**, *48*, 1711-1718.

[6] W. He, Y. Ding, J. Z. Tu, C. Q. Que, Z. H. Yang, J. X. Xu, *Org Biomol Chem* **2018**, *16*, 1659-1666.

[7] K. M. Khan, M. Taha, F. Rahim, M. Ali, W. Jamil, S. Perveen, M. I. Choudhary, *Lett Org Chem* **2010**, *7*, 415-419.

[8] (a) A. Altomare, C. Giacovazzo, A. G. G. Moliterni, *Acta Crystallogr A* **1994**, *50*, 585-588; (b) A. Altomare, G. Cascarano, G. Giacovazzo, A. Guagliardi, M. C. Burla, G. Polidori, M. Camalli, *J Appl Crystallogr* **1994**, *27*, 435-435.

[9] G. M. Sheldrick, *Acta Crystallogr A* **2008**, *64*, 112-122.

[10] J. K. F. a. M. Popowsky, *Anal Chem* **1949**, *21*, 732-734.

[11] M. J. Frisch, G. W. Trucks, H. B. Schlegel, G. E. Scuseria, M. A. Robb, J. R. Cheeseman, G. Scalmani, V. Barone, B. Mennucci, G. A. Petersson, H. Nakatsuji, M. Caricato, X. Li, H. P. Hratchian, A. F. Izmaylov, J. Bloino, G. Zheng, J. L. Sonnenberg, M. Hada, M. Ehara, K. Toyota, R. Fukuda, J. Hasegawa, M. Ishida, T. Nakajima, Y. Honda, O. Kitao, H. Nakai, T. Vreven, J. J. A. Montgomery, J. E. Peralta, F. Ogliaro, M. Bearpark, J. J. Heyd, E. Brothers, K. N. Kudin, V. N. Staroverov, T. Keith, R. Kobayashi, J. Normand, K. Raghavachari, A. Rendell, J. C. Burant, S. S. Iyengar, J. Tomasi, M. Cossi, N. Rega, J. M. Millam, M. Klene, J. E. Knox, J. B. Cross, V. Bakken, C. Adamo, J. Jaramillo, R. Gomperts, R. E. Stratmann, O. Yazyev, A. J. Austin, R. Cammi, C. Pomelli, J. W. Ochterski, R. L. Martin, K. Morokuma, V. G. Zakrzewski, G. A. Voth, P. Salvador, J. J. Dannenberg, S. Dapprich, A. D. Daniels, O. Farkas, J. B. Foresman, J. V. Ortiz, J. Cioslowski, D. J. Fox, *Gaussian, Inc., Wallingford CT, 2013* **2013**.

[12] S. Miertus, E. Scrocco, J. Tomasi, *Chem Phys* **1981**, *55*, 117-129.

[13] K. Fukui, *Acc Chem Res* **1981**, *14*, 363-368.